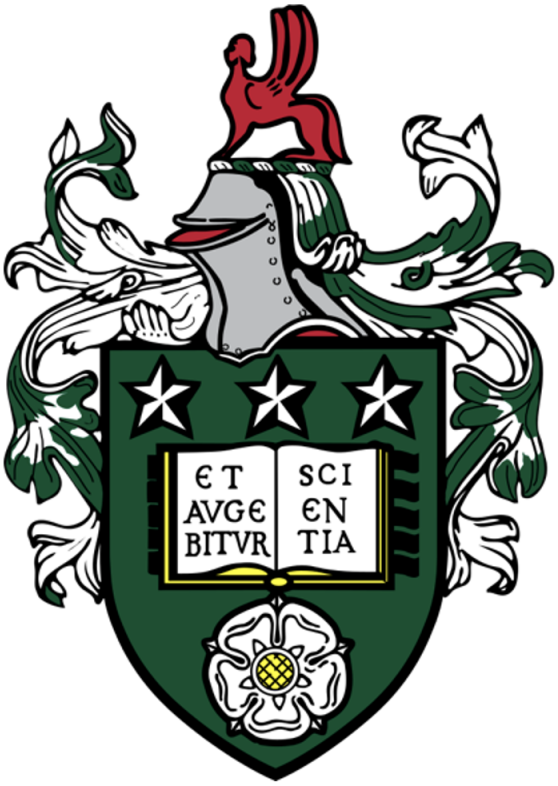

Development and optimisation of functionalised, photoactive gelatin fibres by rotation-assisted wet spinning; for intended use in biomedical applications

Tierney McArdle

Submitted in accordance with the degree requirements of MSc. (Research)

The University of Leeds

School of Design

November 2023

Author's Declaration

I confirm that the work submitted is my own and that appropriate credit has been given where reference had been made to the work of others.

Illustrations

Unless otherwise stated, all illustrated figures presented in this paper are the original work of the author and do not require references or attribution. The candidate confirms that appropriate credit has been given within this thesis where figures have been adapted from the work of others.

Acknowledgements

I am thankful to my academic supervisors, Dr Giuseppe Tronci and Dr Muhammad Tausif, aswell as Dr Joseph Houghton, Dr Samuel Moorcroft, and Dr Charlie Brooker for their support throughout this research project. Furthermore, I wish to express my appreciation to Dr Mark Taylor for his continuous support throughout my time at the University of Leeds.

I am grateful to the support from the Bristol Composites Institute during the period of overlap while completing the write up for this MSc thesis and starting my PhD. That was a very stressful time.

Thank you to my Parents (Debbie and Paul), Siblings, Grandparents, Nanny, extended family, and close friends for supporting me throughout my time at University. I would not be where I am without your love and support. A special shout out to Archie Donald who asked to be mentioned. You are one of the most important people in my life. When I grow up I want to be just like your mum. Yeah Croydon. Finally, a special thanks to my wee dog Frankie- who I love more than words can express.

Abstract

Despite advances in surgical techniques, conventional tendon grafting and artificial reconstructive methods for repairing ruptured tendons, injured of this nature continue to face significant limitations related to high re-rupture rates and lengthy recovery periods. The high incidence of re-rupture after surgical grafting highlights the limitations of current techniques to restore the native tendon structure and bio-mechanical properties critical for withstanding physiological loading when compared to pre-injured strength. Artificial tendon reconstruction made from synthetic woven textiles is becoming more widely used, however these also pose limitations in that woven structures do not possess intrinsic stretch or elasticity, which limits their ability to mechanically mimic biological tissues such as tendon and muscle.

While limited in literature, functionalised gelatin (F-gelatin) has shown to possess good bio-compatibility and bio-stability within the bio-material field. The manufacture of continuous filament fibres through wet spinning (WS) enables gelatin-based materials to be incorporated into textiles that possess tuneable qualities when compared to synthetic polyesters, hydrogels, woven structures, and electrospun meshes [409] . Despite this, the production of gelatin-based fibres poses several challenges such as poor reproducibility, bio-degradation *in vivo*, and insufficient fibre qualities such as brittleness and limited durability.

The research presentedbuilds on prior findings by Rickman et al. [307], with the interest of reducing fibre production time to address the feasibility of scaled-up WS production of gelatin-based filament fibres for use in artificial tendon reconstruction. To address these challenges, chemical and photoactive crosslinking of the native porcine gelatin has been used to enhance the polymer's stability in environments mimetic of those *in vivo*.

This study largely focuses on the optimisation of a lab-scale WS set up, as well as fibre optimisation through a series of fibre drawing and Ultraviolet (UV) light -curing trials so to determine the most successful combination (identified through stress and strain properties). Findings showed good spinnability of F-gelatin when the polymer dope (containing polymer and 50 mM acetic acid) was held at 65°C and spun into a very cold alcohol-based coagulation solution held at 2°C. The difference in temperature between the dope and coagulation solutions was found to increase the rate of phase transition from liquid to solid, resulting in the quicker formation of WS fibres. It was also found that spinning reproducibility was improved under cool ambient temperatures.

In conclusion, this research emphasises that 4-Vinylbenzyl Chloride (4VBC) fictionalisation of porcine gelatin-based materials, in conjunction with UV crosslinking offers a promising direction for producing bio-compatible WS fibres relevant to tendon reconstructive materials. This research therefore looks to lay foundations for (a) the scaled-up production of functionalised gelatin (F-gelatin) fibres, so to determine the feasibility of mass production; as well as (b) to produce gelatin fibres that possess improved mechanical qualities that demonstrate the potential to be manufactured into a structured textile (such as knitting). This research also argues in brief the benefits of incorporating knitted structures into bio-mimetic textiles (such as artificial tendons), so to better imitate biological tissues.

Contents

List of Figures

List of Tables

List of Equations

3.1 TNBS Absorbency

$$\frac{Moles(lys)}{Gelatin} = \frac{2 * Abs * 0.02}{1.46 * 10^4 * p * m} \tag{1}$$

3.2 TNBS molar lysine content

$$F = (1 - \frac{Gel_F}{Gel_N}) * 10 \tag{2}$$

3.3 Swelling index (percentage increase)

$$SI = 100 * \frac{x_s - x_d}{x_d} \tag{3}$$

3.4 Stress value

$$\sigma = \frac{F}{A} \tag{4}$$

3.5 Strain value

$$\epsilon = \frac{\Delta l}{l_0} \tag{5}$$

3.6 Stress/strain

$$E = \frac{\sigma}{\epsilon} \tag{6}$$

Abbreviations

	AA	Amino Acid
	ACL	Anterior cruciate ligament
	AcOH	Acetic acid
	AT	Achilles Tendon
	ATR	Artificial Tendon Reconstruction
	CBE	Circular Bio-economies
	CS	Centrifugal spinning
	CWS	Conventional wet spinning
	DI	De-ionised [water]
	DP	Decimal point\s
	DS	Dry spinning
[]	ECM	Extracellular Matrix
	EtOH	Ethanol
	F-gelatin	Functionalised gelatin
	G	Gauge [needle]
	Gel-4VBC	4-Vinylbenzyl Chloride- functionalised gelatin
	Gel-MA	Methacrylic acid- functionalised gelatin
	GMA	Glycidyl methacrylate
	GS	Gel spinning
	H-bond/s	Hydrogen bonds
	HCl	Hydrochloric acid
	IPA	2-Propanol (Isopropyl alcohol)
	I2959	2-Hydroxy-4-(2-hydroxyethoxy)-2-methylpropiophenone (Irgacure 2959)

LK	Leeds-Keio [polyester]
L0	Original length
M	Molar
MA	Methacrylic acid
MMP	Matrix metalloproteases
MW	Molecular weight/s
NaCl	Sodium chloride
NaHCO	Sodium bicarbonate
NHS	National Health Service (UK)
PBS	Phosphate buffered saline
PEG	Polyethylene Glycol
PEG 400	Polyethylene Glycol 400
PEG 8000	Polyethylene Glycol 8000
PSG	Porcine skin gelatin
RT	Room Temperature
RWS	Rotary wet spinning
[]	
SEM	Scanning electron microscopy
SI	Swelling Index
TE	Tissue engineering
TEA	Triethylamine
TNBS	2,4,6-Trinitrobenzene sulfonic acid
TR	Tissue Regeneration
TS	Tensile Strength
T1C	Type 1 Collagen
T3C	Type 1 Collagen
UTS	Ultimate tensile strength
UV	Ultraviolet (light)
WS	Wet spinning
wt.%	Weight percentage [solute]
w/v	Weight value [solute]
3DP	Three-dimensional printing
4VBC	4-Vinylbenzyl Chloride

Chapter 1

Introduction

1.1 Research Context

Tendon rupture is a prevalent issue within the National Health Service (NHS) and other healthcare providers [138][407][397], occurring most frequently to tendons around large joints; e.g. the Patella and quadriceps at the knee joint, the rotator cuff at the shoulder joint, bicep long/short heads between the elbow and shoulder, and the AT of the ankle joint) [92]. This is likely due to the high repetitive stress and long-term overuse sustained by these joints during everyday activities [410]. While injuries of this type are common, treatment is often long-term and regularly involves surgery [40], post-operative rehabilitation [353], and follow-up appointments [382][433]. Complications such as re-rupture, infection, and loss of mechanical function are common and are factors in prolonging the recovery process, and reducing overall quality of life.

Much of the current literature reports that the most affected demographic is that of working-class adult males [281][331]; however, this prevalence may be skewed by gender bias in population-based studies [314] on injury prevalence or a lack of willing to report injuries within sport-based demographics [109]. It is for these factors (among others) that the exact impact of tendon rupture is unknown, however is assumed to be greater than the current literature suggests.

Looking specifically at the AT, injury and rupture result in functional impairment, pain,

and swelling, which significantly impacts a patient's day-to-day, and overall quality of life. In long-term cases, the inability to engage in physical activities can have long-term consequences, affecting strength, endurance, gait patterns, and causing ongoing discomfort in the affected joint.

As will be discussed further in **Section 2.5.**, high frequency rates of complications and re-rupture [275][413] have generated interest in the development of Artificial Tendon Reconstruction (ATR) in recent decades. Much of this new development have come in the form of synthetic or biological grafts to repair or reinforce damaged tendon tissue [52][120][335]. Commonly woven textile structures composed of synthetic polyester fibres [417][418][419][420][421], these devices are usually surgically fixed into place through conventional operative techniques such as stitching or multi-strand sutures [363]. For biological grafts and artificial reconstructions alike, this bio-synthetic interface remains at a significantly at higher risk of repeat tears often due to the differences in material/mechanical properties throughout the tendon's entirety (spanning from bone-to-tendon-to-muscle). While woven textiles can provide excellent joint and tendon support through its rigid structure, the author hypothesises that these materials are limited through the inability to mimic local collagenous tissue.

Woven textiles have certain limitations when used in biomimetic materials and structures, particularly in applications requiring advanced nature-inspired materials. Plain weave structures; where weft yarns pass over and under the warp yarns; exhibiting isotropic properties along the direction of fibres. This property means that fabrics of this class present consistent mechanical characteristics in both the weft and warp directions. However, many biological structures, such as skin, bone, and tendons, are composed of materials with anisotropic properties; whereby they exhibit varying mechanical attributes in different directions. Restoring ruptured tendons at the myotendinous junction (MTJ) poses significant obstacles due to the intricate interdigitation of native tendon and muscle tissues, creating a highly complex interfacial region. The author suggests that by introducing a third equally dissimilar material (a woven structure) into the interfacial region, a significant disconnect between native tissue and artificial implant is created, preventing a cohesive healing pattern. For this reason, the author presents the hypothesis

that woven textiles may be inadequate in the bio-receptive replication of such anisotropic features found in natural materials, in that the inherent isotropy of woven textiles restricts their capacity to fully mimic the directionally dependent mechanical properties observed in numerous biological systems. This discrepancy between the isotropic nature of woven fabrics and the anisotropic behaviour of many natural materials can pose challenges when attempting to develop biologically similar structures that share the complex mechanical attributes of their biological counterparts. Overcoming this limitation may require exploring alternative textile architectures or material compositions that can better approximate the anisotropic characteristics present in the structures that inspire biomimetic design.

The author therefore argues the potential benefits of biomimetic knitted structures in the artificial reconstruction of tendons at the tendon-muscle/bio-synthetic interface; while setting the foundations for biocompatible F-gelatin fibres that might possess adequate mechanical properties to withstand the rigorous knitting process.

Gelatin-based materials have been at the heart of biomaterial and tissue engineering (TE) research for decades. A protein found in abundance in humans, mammals, and sea-life alike, the material offers excellent biocompatibility, bio-receptibility, and processability, gelatin has proven a successful in a range of medical-related applications, such as wound dressings, TE, drug delivery systems, and serving as a scaffold for regenerating damaged or lost tissue. Despite its many applications, denatured collagen requires a degree of chemical processing to enhance its mechanical properties, while ensuring its thermal and wet stability when used in *in vivo* applications. F-gelatin refers to a chemically modified (or crosslinked) gelatin containing specific functional groups, which improve mechanical performance, while allowing the material to be processed into various states such as hydrogels, fibres, or membranes/films. Crosslinking offers a range of advantages for biomaterials and biomedical applications. The introduction of a robust network of covalent bonds improves the mechanical/ structural integrity and durability of the material. As will be discussed in further detail, crosslinking also improves the compatibility and integration of the material with other substances, in addition to improving the bio-receptibility; enabling implanted biomaterials to properly integrate

and interact with the surrounding biological environment, cells, and tissues [107]. This can promote desirable cellular responses, adhesion, and integration within the target biological environment. Finally, crosslinking can introduce pH or temperature-responsive properties, allowing the material to adapt to specific physiological conditions or trigger targeted release mechanisms. This versatility (via crosslinking) expands the potential applications of biomaterials, such as native gelatin, which would be otherwise limited by its poor mechanical properties and rapid degradation *in vivo*.

Traditional crosslinking methods have exhibited limitations such as restricted mechanical strength and cytotoxicity [272]. Recent advancements in this field focus on developing functionalised collagen materials, particularly for high-strength hydrogel production. A novel approach involves grafting photo-active moieties onto the collagen backbone, and subsequent UV-light irradiation initiates the synthesis of a covalently crosslinked network, resulting in a mechanically robust hydrogel. This UV-irradiation technique is appealing as it eliminates the need for incorporating cytotoxic materials during the precipitation stages preceding the spinning process [423]. Consequently, this approach offers the potential for excellent mechanical properties and biocompatibility in the resulting collagen hydrogels. The compatibility of this approach with the wet-spinning process for collagen-based materials is therefore of considerable interest. WS involves the extrusion of a spinning solution into a compatible non-solvent, leading to coagulation and solidification through diffusional exchange. Within this research project, f-gelatin fibres are crosslinked with both 4VBC and a photo-initiator to enhance mechanical strength, reduce susceptibility to potential enzymic degradation, and improve thermal and wet stability, through formation of covalent inter-molecular and intramolecular bonds between collagen molecules [150].

1.2 Research Statement

In this study, an assessment of existing methodologies concerning gelatin-based wet-spun biomaterials has been conducted, with a specific focus on (a) identifying openings in the present understanding of gelatin as a functional biomaterial, and (b) further investigate the feasibility of producing UV-cured, 4VBC-functionalised gelatin (Gel-4VBC)

through optimised WS methodology. This research is primarily focused on laboratory-based investigations to develop optimised methodologies at the lab scale. Moreover, the research endeavours to align with advancements in textile production techniques by undertaking optimisation procedures aimed at enhancing the characteristics and structure of the fibres. Through this comprehensive approach, the study aims to address the current gaps in knowledge, explore the feasibility of scaled-up production, and enhance the overall quality of gelatin-based biomaterial fibres.

1.3 Aims and Objectives

To date, there is very limited published literature on the WS of functionalised gelatin, and even less on the specific use of gel-4VBC as a dope polymer. The aim of this research is to address the current gap in literature through the process optimisation and development of wet spun, photoactive, and crosslinked gelatin fibres. The objectives to be met through this body of research are as follows :

1. Evaluate current approaches to gelatin-based wet-spun biomaterials and highlight gaps in current knowledge.
2. Determine the feasibility of the optimised f-gelatin as a bioresceptive material.
3. Determine the feasibility of manufacturing UV-cured Gel-4VBC filament fibres through WS methodologies at a laboratory-scale.
4. Looking towards textile manufacturing techniques, carry out fibre optimisation processes with a view to improve fibre properties and morphology.
5. Provide recommendations for further work in this field.

Chapter 2

Literature Review

2.1 Biological Materials: Collagen and Gelatin

Collagen is a naturally occurring hierarchical matrix polymer, found abundantly in tendon, ligament, skin, blood vessels, organs, etc. The primary function of collagen is to provide rigidity and mechanical support to the Extracellular Matrix (ECM) of connective tissues; accounting for roughly a third of protein content in animals [336]. 28 variations of collagen have been identified, each comprised of 46 polypeptide chains [306]; however, 90% of total human collagen content has been found to be Type 1 Collagen (T1C) with types 2, 3 (T3C) and 4 making up the majority of the remaining 10%.

Collagen is a structural protein that plays a crucial role in maintaining the integrity of various tissues and organs in the body; aiding in homeostatic regulation, mechanical strength, and the capacity to carry out chemical reactions with adjacent biomolecules [336]. Stabilised by a ladder of recurrent interstrand hydrogen bonds between the N-H groups of glycine residues and carbonyl groups of adjacent amino acid (AA) residues; these inter-chain bonds are responsible for its high mechanical strength and resistance to degradation [171]. Disruption to these bonds by the partial hydrolysis of collagen, resulting in the breakdown of the triple helical structure, produces gelatin, where the triple-helix structure of native collagen is transformed into a random coil or disordered structure in gelatin (**Figure 2.1**). This is typically achieved through prolonged heating or treatment with acids or enzymes [244].

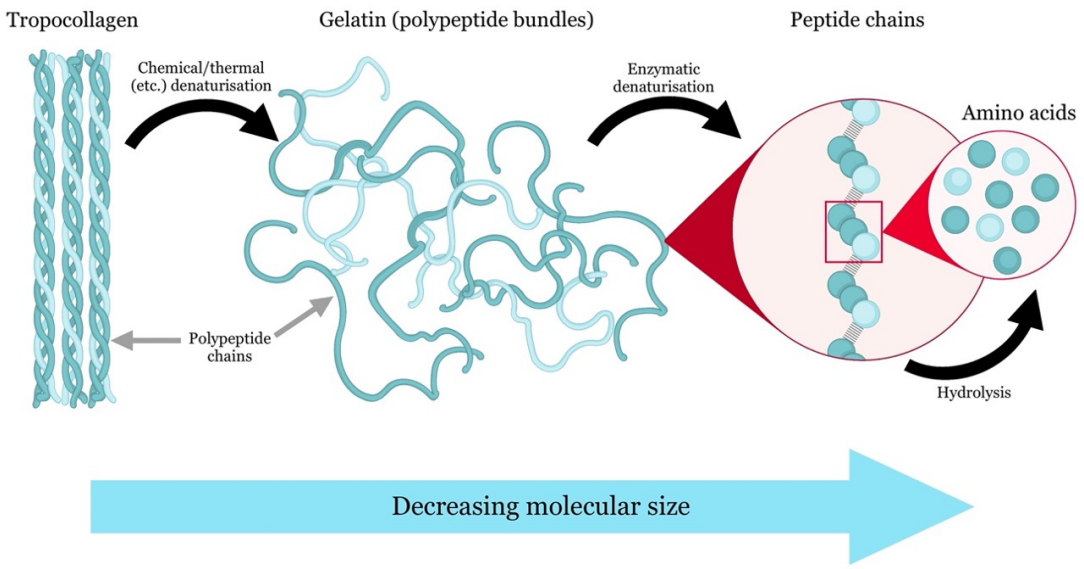

Figure 2.1: *Schematic illustration depicting the irreversible denaturisation of collagen to produce gelatin.*

2.1.1 Polypeptide Structure

The collagen monomer is composed of three protein polypeptide alpha chains, assembled in a tightly packed, left-hand-polyproline helical arrangement (polyproline II-type configuration), which coil around each other forming a 'loose right-handed superhelix' [327]. These polypeptide chains are build-up of a repeating tri-amino acid motif, commonly noted as Gly-X-Y. "Gly" referring to the repeating Glycine molecule which is present every third amino acid (AA) in the chain; is smaller in size than other AAs present in the chain [327] facilitating the close packing of the triple helix. This residue sits close to the 'superhelical central axis' [327], and plays a key role in the arrangement of crosslinks between adjacent collagen monomers, further contributing to the integral strength and stability of the polypeptide chain. The succeeding "X" and "Y" components represent any configuration of AAs; of the 17 AAs found in collagen [327][412]. The most commonly appearing are proline, hydroxyproline, arginine, and lysine (**Figure 2.2**).

During initial synthesis in the endoplasmic reticulum, α-chains self-assemble, forming a triple helical structure called procollagen. During maturation of the procollagen (**Figure 2.3d**), N- and C-terminal propeptides are cleaved in a process referred to as exocytosis,

leading to the formation of tropocollagen (mature monomer) [349]. The hierarchical structure of collagen is illustrated in **Figure 2.3**. Tropocollagen forms the foundational unit for collagen-based tissues, boasting dimensions of approximately 1.5 nm in diameter and 300 nm in length. Stacking in clusters of five, these monomers adopt a staggered arrangement with a 67 nm overlap (termed D-periodicity, where "D" is 67 nm) [350]. Strong covalent bonds hold the regularly spaced gap and overlap segments together, contributing to the overall structural integrity. The inter-monomer gap (0.54D in length) is essential for maintaining flexibility and elasticity within the fibril, enabling stretching and deformation without fracturing. Collagen fibrils aggregate to form larger fibres, supported by ECM proteins like glycosaminoglycans, proteoglycans, and lysyl oxidases that facilitate fibril crosslinking.

2.1.2 Extracellular Matrix

The ECM is the non-cellular, hydrous polymer network in a connective tissue (**Figure 2.4**), which acts as a cellular scaffold, providing structural stability, while supporting cell differentiation and self-regulatory stability [355], regulates tissue development [313], and wound healing [243] [323] [304] [60]. The matrix is largely comprised of water, proteoglycans (long-chain polysaccharides, such as biglycan and perlecan, filling the interstitial space) [312][355], and interwoven fibrous proteins (collagen, elastin, fibronectin laminins and other glycoproteins) [243][313][369][355]. It is uniquely tailored to specific tissue structures throughout the body [173], and dictates tissue-specific

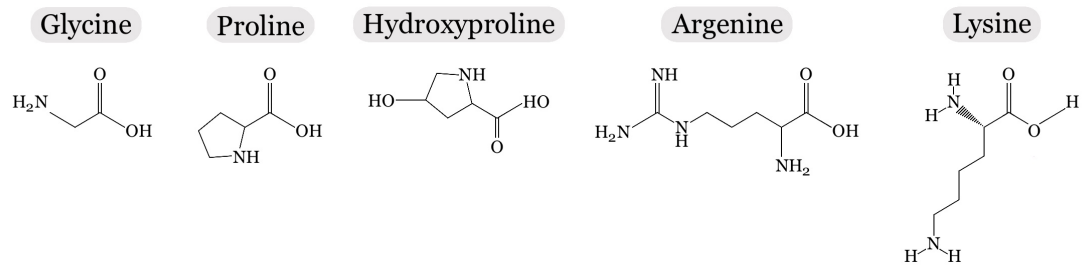

Figure 2.2: *Chemical structures of the four most commonly appearing amino acids present in collagen polypeptide chains. From left to right; Glycine, Proline, Hydroxyproline, Arginine and Lysine.*

mechanical properties such as tensile properties and elasticity, cell adhesion and chemotaxis. Within the ECM, collagen makes up roughly 30% of the fibrous protein mass [112], and is the primary structural support of the entire matrix [313][112].

Proteoglycans are comprised of glycosaminoglycans which are covalently bonded to protein molecules (such as collagen fibres) within a tissue's ECM [157][322][112]. This double bonding of neighbouring fibres increases the stiffness and rigidity of the ECM structure, reducing the likelihood of stress-induced tears in tissues, while increasing tensile strength of the overall structure. This enables the structure to withstand high

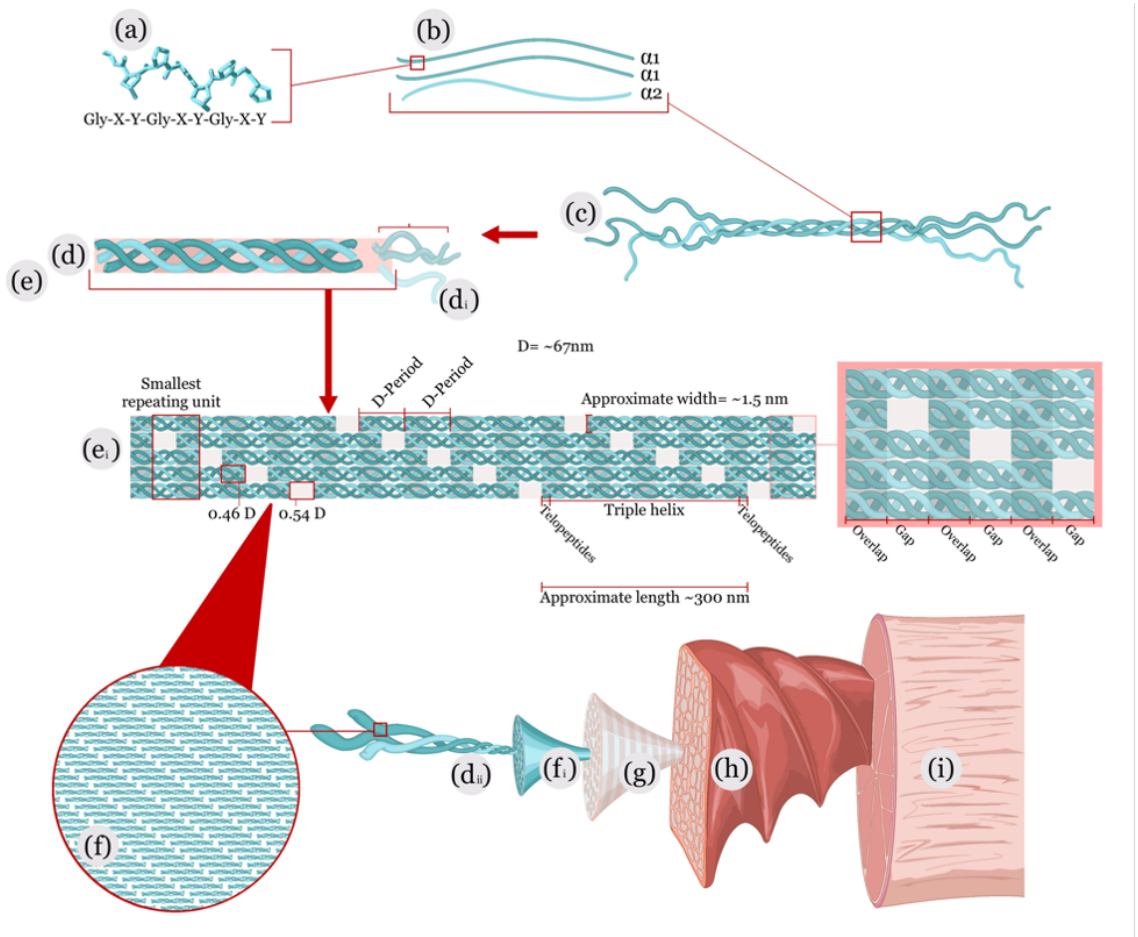

Figure 2.3: *Hierarchal structure of collagen: (a) proteinogenic amino acid chain; (b) polypeptide chains; (c) Procollagen peptidase; (d) Tropocollagen and its (di) cleaved chain ends; (e) Rows of monomers staggered in axial periodicity, forming larger microfibrils. (ei) and (eii) depict the "gap" and "overlap" segments; (eiii) smallest repeating unit of a collagen fibril; (f, fi) packing of monomers into a microfibril and larger fibril-structure, which packs into (h) fascicles.*

levels of stretching and structural deformation: an important quality in native materials such as skin, bone, cartilage, and tendon/ligament [186][44]. On a molecular level, this crosslinking of fibres decreases susceptibility to enzymic degradation [220][135] and protein break-down [135], aiding in the long-term structural integrity.

2.1.3 Collagen Denaturisation

Collagen can undergo denaturation when subjected to various processes, including heating and other methods such as electrical, enzymatic, or chemical treatments. This denaturation process transforms the native collagen structure into gelatin (**Figure 2.1**). It is a chemical process which has a significant impact on the structure and function of biological proteins and tissues. Break-down of the triple helix results in a loss of inherent strength, structure, and overall performance. This is largely due to the breaking of

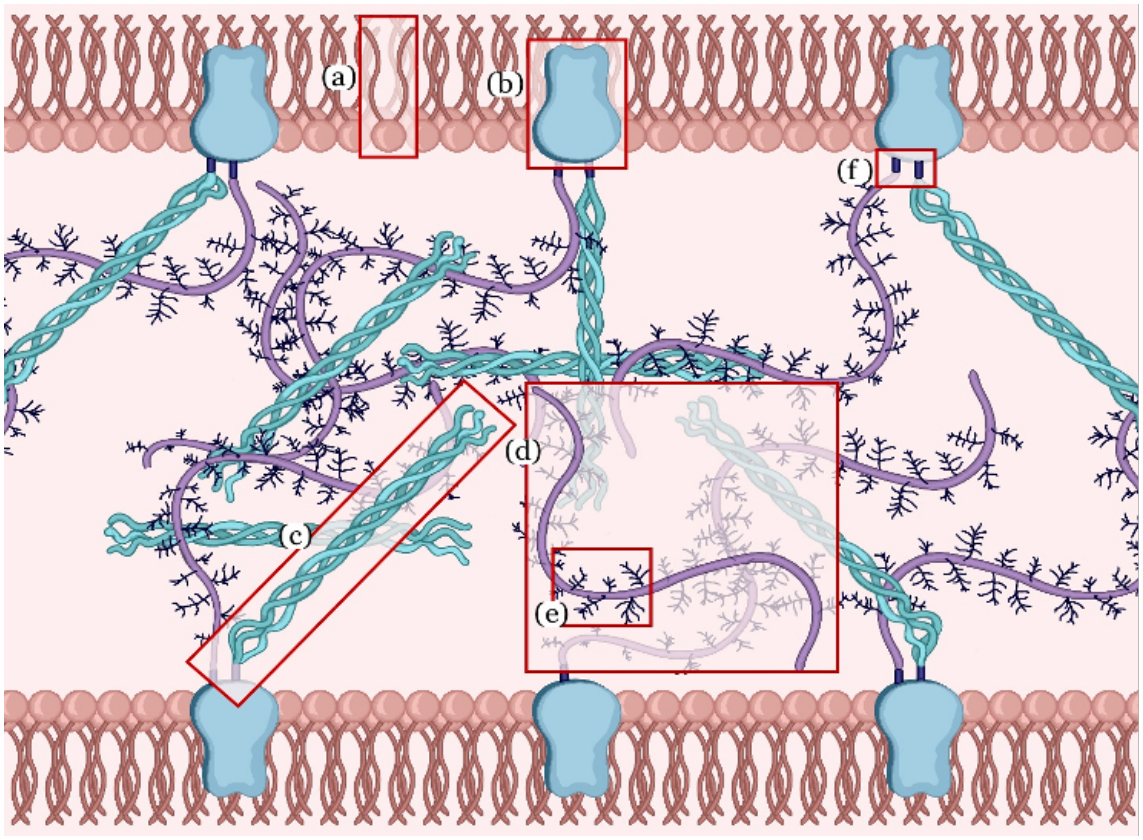

Figure 2.4: *The ECM network (generalised) between cells. Main components are highlighted as (a) the cell/plasma membrane, (b) integrin, (c) collagen fibres, (d) proteoglycan complex comprised of a long polysaccharide chain with (e) linked carbohydrate and protein branches and (f) fibronectin.*

intra-molecular bonds leading to a disarrangement of the helix. During denaturisation, polypeptide α-chains un-coil from each other; the effect of this is diminished mechanical properties, such as strength, flexibility, and deformation resistance. Denaturisation through heating results in the disruption of hydrogen bonds between α-chains. This process is commonly used in common practices such as cooking meat, where collagen within the ECM (connective tissue) denatures, resulting in a tender, more digestible protein when consumed [50][293]. Mukherjee and Rosolen [254], noted that in aqueous conditions, temperatures above 37°C (internal temperature of a healthy human) are enough to initiate denaturisation, which is essentially the reason why human skin starts to develop wrinkles overtime as an individual gets older.

Mechanical stresses such as compression or tensile strain can also lead to the denaturation of collagen. Structures like tendons, ligaments, and other ECM components are particularly susceptible to this type of denaturation following traumatic injuries [208]. This denaturation process is also a contributing factor to the formation of wrinkles as humans age. Over time, collagen fibres can be exposed to external stressors from movement and activity, UV radiation, blue light from screens, and environmental pollution, can further contribute to structural denaturation [282]. Furthermore, enzymatic degradation by proteases' can disrupt the triple-helix structure of collagen by cleaving the individual α-chains and the bonds that interconnect them. During wound healing, this enzymatic degradation of the ECM can delay the healing process by causing the breakdown of the ECM [326][233]. The molecular alignment of the polypeptide chains utilises charge-charge and hydrophobic interactions [336], contributes to gelatin's mechanical strength and proteolytic resistance [219][62][332].

2.1.4 Charge-Charge and Hydrophobic Interactions

Charge-charge interactions, also known as electrostatic interactions, play a crucial role in the structure, folding, and binding of proteins. Microscopically, these interactions occur between charged groups, such as the positively charged amino groups and negatively charged carboxyl groups of amino acid residues [448][231]. The strength of these interactions is inversely proportional to the distance between the charges and directly proportional to the product of their magnitudes [224], which contribute significantly to

the stability of protein structures and the specificity of protein-protein interactions.

Hydrophobic interactions, on the other hand, arise from the tendency of non-polar (hydrophobic) groups to minimise their exposure to water molecules [76]. In proteins, these interactions occur between non-polar amino acid side chains, such as those of alanine, valine, leucine, and isoleucine [180][276]. The hydrophobic effect drives the folding of proteins into compact structures, where non-polar residues are buried in the interior, away from the aqueous environment [356]. Hydrophobic interactions also play a crucial role in protein-protein interactions, to facilitate the binding of hydrophobic surfaces and contributing to the overall binding affinity.

Both charge-charge interactions and hydrophobic interactions play a crucial role in the denaturation of collagen to produce gelatin. The triple-helical structure of collagen, which is stabilised by both electrostatic interactions between charged amino acid residues, form salt bridges and hydrogen bonds, as well as hydrophobic interactions that drive the tight packing of the three polypeptide chains [343][300][201]. During the denaturation process, these interactions must be disrupted to unravel the collagen triple helix into individual random coil polypeptide chains, forming gelatin. Specifically, the electrostatic interactions are weakened by changing the pH or ionic strength of the solution, destabilising the collagen structure. The disruption of both charge-charge and hydrophobic interactions is essential for the unfolding and disordering of the polypeptide chains, converting the highly organised collagen structure into the disordered, random coil conformation characteristic of gelatin.

2.2 Gelatin as a Biomaterial

Gelatin is commonly used in both pharmaceutical and biomedical applications as the material exhibits good biocompatibility and bio-receptibility [431][56][218]. As a collagen derivative, it mimics the ECM of human tissues, making it highly effective in the construction of wound dressings and TE [315][258][176]. Native gelatin is limited by its hydrophilic qualities, meaning that chemical crosslinking is often necessary to make it stable *in vivo*.

2.2.1 Current Limitations

The physicochemical properties of gelatin limit its application as a biomaterial due to poor mechanical strength without chemical crosslinking [127][259], temperature and water sensitivity [214][218], susceptibility to enzymatic degradation [220][135], biodegradability [259], inconsistent properties and poor reproducibility [329], limited crosslinking options [59][99], and limited control over rate of degradation [218].

Gelatin-based substances possess significantly weaker mechanical properties, tensile strength, and deformation resistance, than its collagen counterpart, which limits its applications as a raw material. Gelatin is also more hydrophilic than collagen due to the differences in their molecular structures as a result of structural denaturisation. The high hydrophilicity of gelatin molecules is owed to the abundance of hydrophilic functional groups (amine, hydroxyl, etc.) within the peptide backbone [123][360]. These groups have a strong affinity for water molecules, leading to the absorption and retention of water by the gelatin structure; often resulting in swelling, structural softening, and loss of structural integrity. The high swelling ratio of gelatin gel structures (the ratio of gel mass to the total mass including absorbed water post-hydration) can affect dimensional stability and mechanical properties, this can be problematic in applications requiring precise control over the material's morphology and size [408][399]. Following hydrolysis (the disruption to hydrogen bonds in the triple helix), and the unravelling of collagen's triple helix, a larger number of peptide bonds become exposed, making them more vulnerable to enzymatic degradation. This limits its long-term stability *in vivo* as an implantable biomaterial, with potential losses in structural integrity over time, especially in load-bearing applications (such as regenerating complex tissues or organs) [36][218].

Gelatin-based materials can vary in properties depending on their source (animal or plant-derived), extraction methods, processing conditions, and crosslinking techniques, which can cause challenges in producing consistent material performance. Studies have shown that increasing the bloom strength of gelatin results in higher compressive strength and storage modulus (elastic modulus) of the Gelatin-crosslinked with Methacrylic acid (MA) [15][442]. Methacrylic acid-functionalised gelatin (Gel-MA) hydrogels made from porcine gelatin with a bloom strength of 300 had a compressive strength of 40

kPa, compared to 18 kPa for those made with a bloom strength of 175, suggests an improved structural integrity and resistance to external forces, which corresponds to higher molecular weight and longer collagen chains in the gelatin [129][41]. In addition, a recent study by He et al. [137] revealed that food-grade porcine gelatin had superior gel strength, emulsification and water holding capacity in comparison to gelatin derived from sea-life such as the Big Head Carp, Coregonus Peled and other Carp scales. Overall conclusions form He et al. [137] indicate that gelatin from aquatic animals (primarily cold-water fish) has inferior gelation and mechanical properties in comparison to mammal sources, attributable to lesser AA quantities. A reason for this disparity in collagen properties was noted by Coppola et al. [74], who owed this to the reduced degree of crosslinking in marine animal collagen in comparison to terrestrial animals such as bovine. Additionally, sea-life-derived gelatin possesses a lower proportion of proline and hydroxyproline; which plays a crucial role in stabilising the triple-helical structure of collagen, [91], resulting in a lower proportion of triple-helical structures and a higher proportion of β-turn/β-shift structures; affecting the gelling ability and mechanical strength of the gelatin [91].

2.2.2 Applications of Functionalised Gelatin

The use of gelatin-based materials is often seen as attractive due to its low-cost (in comparison to pure collagen), and biocompatibility due to its natural presence in human tissues [124][27][87]. Chemical crosslinking of gelatin has been shown to improve the chemical and mechanical performance of gelatin, making it appropriate for use in *in vivo* medical devices. While there are many advantages, appropriate crosslinking methods are often limited and can affect the biocompatibility and degradation profile of the material. Some successful chemical crosslinkers include sugars (e.g. fructose) [383], dextran dialdehyde [97], diepoxy-containing compounds [357], aldehyde compounds [303][234][383], genipin [357][435][205], diisocyanates and isocyanates [20], carbodiimidesn [436], and polycarboxylic acids [229].

Previous literature has investigated the successful crosslinking of bridging monomers to collagen and gelatin-based material. These include glycidyl methacrylate (GMA) [90][154][237], MA [316] [78] [334], and 4VBC [34][307]. Chemical crosslinking us-

ing bridging monomers such as these, create a physical connection between polymer chains via covalent bonds that attach one part of the collagen structure at one reactive site and to a different region of the collagen at another site [443]. Native polymers that possess many polar water-binding sites (e.g. gelatin), are highly soluble in water, which affects the mechanical strength of resulting fibres once the raw polymer is processed into fibres (spinning methods to be discussed further in **Section 2.3**.). Zeugolis et al. [443] conducted a review into different crosslinking materials used in the formation of collagen filament fibres; finding that the addition of bridge monomers (crosslinking) into the polymer can significantly alter collegen/gelatin's tensile strength, resistance to temperature, and sensitivity to water/moisture. Tronci et al. [378][380] investigated the effects of crosslinking collagen-based hydrogels with MA, GMA and 4VBC bridging monomers (**Figure 2.5**); noting a positive correlation between material rigidity, compressive modulus, and swelling index.

It has also been noted that hydrogels crosslinked with 4VBC exhibited a higher swelling capacity and compressive modulus than both MA and GMA. One reason for this may be due to the molecular structure of the monomers. 4VBC, an aromatic compound, is highly stable, with higher melting and boiling points (compared to aliphatic compounds of similar molecular weight) [167][194][3]. Additionally, 4VBC's distribution of π electrons between adjacently-stacked benzene rings provides further stabilisation to the chemical (and therefore overall) structure [3]. In contrast, GMA, an aliphatic compound, composed of straight, branched, or open-chain structures (therefore lacking the hexagonal benzene rings of aromatic compounds), has a lower melting and boiling points [155]. Furthermore, MA, an acrylic compound consisting of a carbon-carbon double bond (-C=C-) structure, possesses low-melting points at room temperature [71], which can be attributed to the relatively weak inter-molecular forces (van der Waals forces) between its small molecules. There is very little published literature on the WS of GMA, MA or 4VBC-functionalised collagen and gelatin, however of that currently published, all have shown to retain some monomer helix configuration [378][380], benefiting the overall mechanical strength of resulting WS fibres. Biocompatibility of functionalised polymers can also be improved through supplementary wash stages to remove surplus cytotoxic substances acquired during the functionalisation reaction [82]. All three bridging

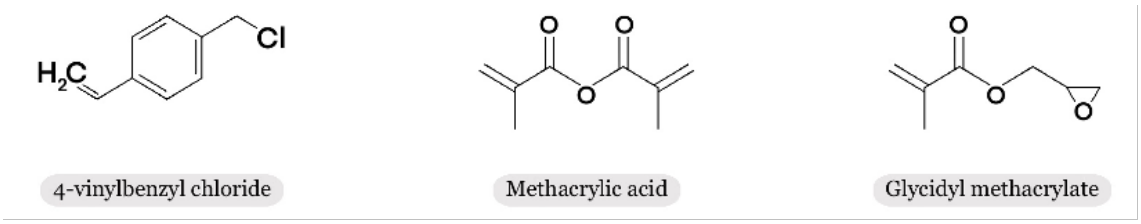

Figure 2.5: *Chemical structures for 4-Vinylbenzyl Chloride, methacrylic acid and glycidyl methacrylate bridging monomers.*

monomers possess good resistance to water and control over swelling in wet conditions, supporting their application in TE applications, through the formation of covalent bonds with prevent the ingress of water molecules into the polymer's structure. The process of chemical crosslinking gelatin with 4VBC is illustrated in **Figure 2.6a**.

2.3 Crosslinking

Crosslinking can also be achieved through the addition of supplementary photoactive monomers. Several papers have noted the functional groups in 4VBC, GMA and MA that enable the formation of molecular crosslinks upon exposure to UV light [377] [378] [380]; which initiates the formation of free radicals (wavelength dependent) from a photo-initiator. This instigates fracture of the carbon-carbon double bond (C=C) bonds from the vinyl group, enabling the formation of covalent bonds between bordering monomers (**Figure 2.6**). Photoactive crosslinkers permit polymer functionalisation prior to the manufacture of the material into gels or fibres, which enables the detoxification of any cytotoxic residues acquired during spinning.

2-Hydroxy-4-(2-hydroxyethoxy)-2-methylpropiophenone (herein referred to as "Irgacure 2959" or "I2959") is a photoinitiator which can be added to a polymer solution (e.g. WS dope) in order to enable a rapid curing/hardening reaction upon exposure to UV-light. This reaction is referred to as photopolymerisation and involves the generation of free radicals (at specific UV wavelengths), which facilitates the covalent bonding of adjacent polymer molecules. I2959 is generally used in Three-Dimensional Printing (3DP) [192], WS fibres [307], dental materials [251][401], resins [319], hydrogels [330][240], and other biomaterials [391][387][401].

2.3.1 4-Vinylbenzyl Chloride-Crosslinking

4VBC is a chemical compound with the molecular formula C8H7Cl, that contains a vinyl group and a chlorine atom attached to a benzene ring. This compound is often used as a monomer in the synthesis of various polymers through processes such as free radical polymerisation. Very little literature has been published on the crosslinking of collagen-based polypeptides with 4VBC for production of wet-spun filaments; however, the monomer has been shown to increase the overall toughness and swelling control of a material, through the obstruction of water binding sites. This inhibits excessive swelling of the material in wet conditions, and enables the control swelling and material properties [378][380]. Tronci et al. [378][380] also notes that the degree of chemical crosslinking can be modified based on the material application, which permits the tailoring of properties in gelatin-based materials for specific biomedical and biotechnological applications [378][380]. The high compressive strength of the 4VBC monomer (owed to its rigid benzene structure) make it well-suited for bone and tendon scaffolds.

2.4 *In Vivo* Applications and the Biological Response to Gel-4VBC Material

Numerous innovations within engineering and medicine have extended the applications of collagen and gelatin to the field of tissue engineering. Ramshaw et al. [299] discussed the applications of collagen-based materials within medical devices noting the successful implementation of the biological material in cardiology (e.g. heart valves, arterial/veinous replacements, etc.), surgery (e.g. sutures), and wound management [130][179][93][105][299][298]. Skin substitutes represent a middle ground between collagen-based wound dressings and scaffolds designed for tissue regeneration. As such, skin substitutes have been employed for treating diabetic ulcers, burns, and as protective barriers between the skin and the external environment [259][117]. The substitutes function similarly to wound dressings, gradually integrating into the epidermal tissue over time [16][65]. The IntegraTM bilayer wound matrix [141][291], which consists of bovine T1C, and shark chondroitin 6-sulfate Collagen–glycosaminoglycan matrix reinforced by an impermeable silicone membrane [213][277] has demonstrated the ability

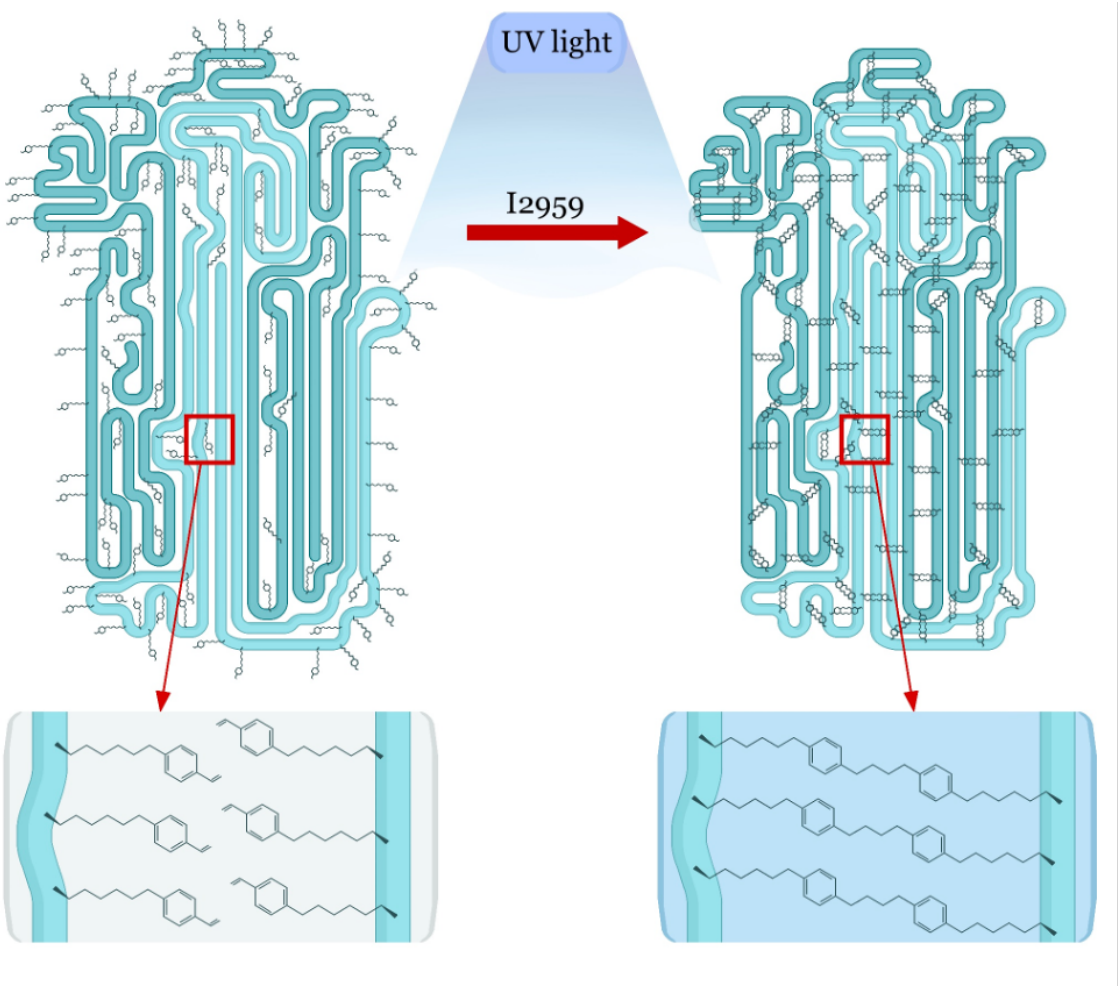

Figure 2.6: *Schematic illustration of the chemical crosslinking process of gelatin polypeptide chains with 4VBC, (a) before, and (b) after exposure to UV light.*

to facilitate tissue healing, through the forming of a complete seal over the wound. In turn this prevents biological fluid egressing through the dressing through the healing process [67]. TE and Tissue Regeneration (TR) are commonly utilised approaches for constructing collagen-based scaffolds and membranes. These methods aim to provide a biomimetic ECM that mechanically supports the tissue, encourages cell adhesion [7], tissue growth and eventual remodelling [7][218], and scaffold breakdown and reabsorption [405][404][199][425][396][301]. In TE, patient-specific stem cells are cultured onto the scaffold *in vitro*. In TR, the scaffold is directly implanted into the patient, relying on the recruitment of cells onto the scaffold *in vivo*. Both TE and TR need to support cell adhesion and viability of new tissue to ensure growth and survival. The scaffolds should be non-cytotoxic, degrade at the appropriate rate to provide mechanical stability during tissue remodelling, and possess the necessary mechanical properties in a wet

environment to mimic native tissue. The optimal dissolution rate would allow the implanted material to maintain its structural integrity for an adequate duration, facilitating the initial stages of tissue regeneration and wound healing. Subsequently, the gradual dissolution and clearance of the material would enable the progressive replacement by the regenerated native tissue, ultimately restoring the original tissue architecture and function without the persistent presence of a foreign body.

Biomimetic nonwoven gelatin meshes (normally electrospun) has been explored in some depththrough literature [223][43][311] due to their ability to structurally mimic components of biological tissue such as the fibrillar structure of the ECM [328], vascular grafts [405][404] and as biodegradable materials for *in vivo* drug delivery or cellular structural scaffolds [49][48][125][126][396]. Meshes such as these are three-dimensional in structure which aids in facilitating cellular attachment [222][352], proliferation [57][351], and differentiation during TR [131], making these materials useful for tissue engineering, where they can support the growth of specific tissues or organs. This category of biomaterial has also been proven beneficial in drug delivery systems, whereby drugs or bioactive molecules are embedded into the fibres [390][75] and (once *in vivo*) release slowly over time [390].

2.4.1 Chronic Wound and Burn Dressings

Chronic wounds, such as diabetic and pressure ulcers, and burns require specialised dressings to promote healing, control fluid discharge and reduce the risk of infection. Maintaining a moist environment is crucial for successful wound healing [106][340][174][390], as it aids in cell migration [144][266], TR [266], and aid in the removal of dead tissue from the site [174]. For these reasons, materials (such as gelatin) with good water absorption properties have been frequently investigated [260]. Collagen and gelatin fibres naturally have the capacity to swell and absorb substantial levels of exudate released by the wound site, making collagen an ideal material to form wound dressing [284].

During the process of wound healing, proteins, and amino acids such as fibroblast growth factors [348], glutamine and arginine [372][70] play a crucial role in attracting fibroblasts and keratinocytes to the site of the wound. This attraction facilitates essential stages

such as debridement, re-epithelialisation, and angiogenesis [441][33]. Collagen-based wound dressings can provide a conducive environment for cell migration, tissue repair, and the healing process; by assisting in stimulating the deposition of newly synthesised collagen and the promotion of wound granulation [324]. Matrix metalloproteases (MMPs) (collagen degrading enzymes), are released by the body during inflammation to aid in the remodelling of tissues, as such they are abundant within the wound healing environment [184][160]. In cases of chronic wounds, the abundance of MMPs can lead to the breakdown of healthy tissues, impeding the progress of tissue repair. As such, Bohn et al. [46] and Tronci et al. [379] developed collagen-based wound dressings that utilise the collagen as a sacrificial target for the MMPs, helping to preserve healthy tissue during the wound healing process.

Gelatin-based materials used in both wound and burn dressings can also promote the regrowth of fibroblasts, which are responsible for collagen production and wound contraction, further aiding in the healing process. Fibroblasts play a crucial role in wound healing by producing collagen, the main component of the extracellular matrix. Jang et al. [163] developed a dental gelatin paste to promote full thickness wound healing to enhance vascularisation in newly formed tissues around the healing site [163][259]. From this, researchers observed excellent native cell attachment to the gelatin matrix, facilitated by the fibroblast infiltration, encouraging neo-vascularisation, and encouraging native collagen production [196]. Alongside the biological/mechanical benefits discussed above, the use of wound dressings that incorporate gelatin to promote healing, have been shown to improve patient comfort [188][260]. Likely due to the fact that gelatin-based dressings are less adherent to the wound bed compared to traditional gauze dressings [188][260], minimising any risk of further tissue damage and pain during dressing changes.

2.4.2 Food Stuffs

Outside of the medical field, gelatin has been proven a valuable material in a range of other applications. Gelatin-based food packaging presents a promising solution in the pursuit of sustainable and eco-friendly packaging alternatives. Derived from animal collagen, gelatin offers a natural and biodegradable material source for creating packaging

materials that can effectively reduce the environmental impact of plastic waste [23]. As a meat-derivative, these packaging's are also often edible [23][153] and compostable [341][310]. Despite the environmental benefits, as an animal derivative, these materials are limited in their appropriateness in the food industry as they are not suitable for vegans and vegetarians, as well as some religions.

Despite these novel packaging materials exhibit versatility, with the ability to be formed into various shapes, films, and coatings tailored to different food products. Suderman et al. [354] discussed the extensive use of gelatin as a biomaterial within the food industry (films, packaging, etc.) proved successful in acting as a protective barrier to foods from the external environment (e.g. oxidisation, moisture, light, bacteria, etc.), and preserving the freshness and extending the food item's shelf life. Using bio-derived materials such as proteins (including casein, gelatin, and whey) [69] and polysaccharides (such as chitin, cellulose, starch, and chitosan) [63][17] can also contribute to lowering the environmental impact of non-biodegradable plastic waste. As with many gelatin-based materials, packaging films require significant treatment and crosslinking to limit their sensitivity to moisture [122]. Despite this, some gelatin-based films have been shown to offer good resistance to moisture [8][317]; an essential quality in preserving the freshness and quality of perishable food products.

Different food products require different types of packaging and environmental protection. Gelatin-based packaging have tuneable properties through modification of formulation and processing conditions [216], enabling the production of films with varying degrees of flexibility, strength, and external protection. These tuneable properties of gel-based films and packaging can be owed largely to the inclusion of polyol plasticisers into the material during production [354]. Polyols are organic compounds that contain several hydroxyl groups [344][156] and have been found to be efficient in plasticising hydrophilic polymers [371][119]. Benefits of the inclusion of polyols into gelatin-based materials includes improved mechanical properties, increased extensibility, flexibility and tensile resistance, plasticity, and rigidity [133][132]. Specifically, gelatin-compatible polyols that have been explored for use in biodegradable films include glycerol [256], mannitol [206][245], xylitol [375], and sorbitol [245][26]. Monosaccharide sugars in-

cluding glucose, mannose, fructose, and sucrose [294][289], as well as some fatty acids [207][169], have also been successfully used to improve gelatin film plasticity.

2.4.3 Wearable Textiles

The application of collagen-based materials outside of the medical and food industries may seem peculiar; however, the emergence of circular bio-economies (CBE) in recent years [361] has generated much interest in renewable biomaterials. Recent applications of gelatin in these fields include nonwoven mesh N95 respiratory filters [22], as a starch alternative to stiffening silk-based fabrics [189], and wearable conductive sensors [98]. Recent literature has presented collagen-based flexible electronic devices with applications in electrochemical energy storage, sensing, healthcare monitoring and thermal management [287][25][447]. Benefits of collagen-based textiles (aside from their biocompatibility) include good anti-static properties [346], ability to absorb UVA and UVB rays [346], flexibility and versatility [5][25][239].

2.5 Collagen and Gelatin Fibre Spinning Methods

WS fibres and fibrous scaffolds have been explored in a range of TE-related applications and have exhibited several advantageous properties such as possessing a substantial surface area; enabling enhanced cellular adhesion and re-growth; additionally good porosity of WS fibres permits effective migration of cells during proliferation [5]. The tunability of fibre qualities (to be discussed in detail in **Section 2.5**) through regulation of coagulation bath temperature, exterior surface quality [381][333], porosity [175][108], drawing conditions [426]. WS fibrous scaffolds offer unique advantages for tissue engineering, with their surface properties, porosity, and post-spinning treatments playing crucial roles in influencing cell behaviour and promoting tissue regeneration. Collagen is already widely utilised within textile manufacture to produce both single fibres (incl. filament, spun staple) and structured fabrics, through methods such as knitted, wovens and nonwovens.

Collagen-containing materials are attractive within the medical field due to their biocompatibility and biostability in physiological conditions. In addition, collagen deriva-

tive possesses certain characteristics that make the protein a highly attractive material; non-toxic, nonallergenic, and with suitable mechanical properties (strength, elasticity, durability). Within surgical applications, materials containing collagen are likely to be accepted *in vivo* as it is a non-immunogenic substance. This section discusses in brief detail alternate spinning methods. An overview of these have also been presented in in **Table 2.1**.

2.5.1 Wet Spinning

WS (**Figure 2.7**) is a fibre production technique that has been used to spin a wide variety of natural protein-based filament fibres including sodium alginate/soybean protein [80][81], casein [146][113][434], silk polymer [384], cellulose [428][271][183]; as well as collagen and gelatin [429][241][378][347][21].

WS has four key phases: dissolution, extrusion, coagulation, and fibre collection (**Figure 2.7**). The initial dissolution phase involves the state change of the polymer (gelatin) from a solid to a liquid by dissolving it in a compatible solvent to form a liquid dope. This dope is then loaded into a syringe and extruded at a continuous speed, through a blunt-tipped needle into a coagulation bath containing a solvent-non-solvent solution This initiates a solvent/non-solvent phase inversion of the dope stream from a liquid gel to a solid fibre. Finally, resulting fibres are treated (supplementary baths, drawing, curing, drying) and collected. During the coagulation stage, WS relies on diffusional exchange of solvents to generate the phase transition reaction; whereby the compatible solvent diffuses out, and the coagulation solvent diffuses into the polymer resulting in the formation of a solid fibre. The speed of this diffusional exchange reaction can significantly affect fibre morphology and properties.

WS is of particular interest as it can transform biopolymers (such as collagen) into solid fibres without denaturising the native protein structure (as there is no need to use excessively high temperatures, voltage, etc.). WS is advantageous compared to alternative fibre spinning methods, due to; good fibre permeability [175][334], and suitability for use with larger and thermally sensitive proteins as collagen and gelatin [334]. These properties make WS fibres suitable for *in vivo* applications, such as wound dressings

[151][376][385]. Alongside wound care, these fibres also have uses in other medical-related applications, such as: drug delivery [265], blood filtration/haemodialysis [389], tissue repair [422][5][58]. WS is particularly established as a practical fibre production method for naturally occurring plant and animal-based polymers [175]. Despite the advantages associated with WS, the method does have its drawbacks, Shirvan et al. [334] notes that a common limitation of WS fibre scaffolds is 'poor dimensional stability' [334], which can negatively affect a fibre's overall performance. Key factors that can negatively impact mechanical performance include disproportionate swelling and water uptake resulting in expansion and fibre buckling [334].

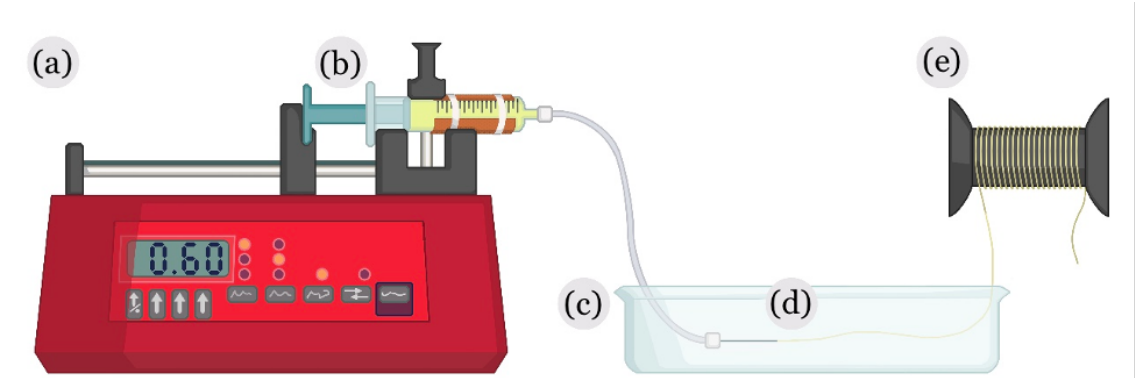

Figure 2.7: *Basic wet spinning set up. (a) Syringe pump; (b) syringe; (c) rubber tubing and blunt-tipped needle; (d) coagulation bath; (e) fibre collection method.*

2.5.2 Rotary Wet Spinning

Rotary wet spinning (RWS) (**Figure 2.8**) has shown good potential in the WS of polymeric fibres. The apparatus set up differs from conventional spinning, through the placement of the coagulation bath of a motorised rotary stage, which generates a circular flow to apply tension on the dope/fibre as is exits the needle. In high speed RWS, fibres are drawn, aligning polypeptide chains through the application of a light centrifugal force [54][307][334][64].

Shirvan et al. [334] notes that this set-up in principle can aid in overcoming Kelvin–Helmholtz instability (of the liquid dope in the coagulation solution), which describes the velocity difference across the interface between two fluids flowing in parallel [320][88], as ob-

served in WS. Kelvin– Helmholtz instability is driven by the faster moving fluid causing perturbations or ripples to develop on the interface between the two liquids [320]. These fibres can adopt a more uniform cross-section due to the rotation-induced shear force applied along the filament body. Through the application of a continuous draw in the early coagulation stages, resulting fibres possess enhanced overall mechanical performance [121][170]; addressing inconsistencies associated with conventional WS [247]. RWS fibres often exhibit smoother surface textures, with minimal crevices along the exterior [334].

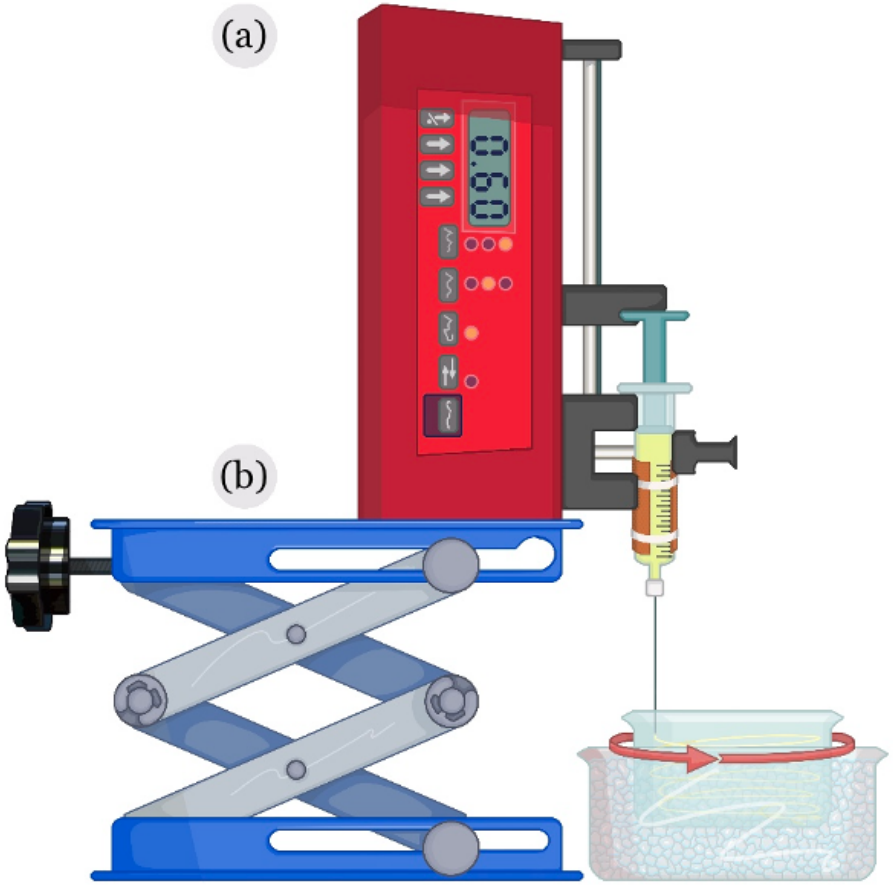

Figure 2.8: *Experimental rotary-assisted wet spinning set up. The (a) syringe pump has been turned 90° and raised on a (b) jack stand so that the needle can sit approximately 10 mm below the surface of the coagulation solution.*

2.5.3 Electrospinning

Electrospinning (**Figure 2.9**) employs an electric field to extrude the dope from a spinneret onto an oppositely charged collection plate [305]. The charge exerted upon the

polymer solution causes the formation of a Taylor cone from which the fibre is drawn, a volatile solvent is required to ensure this evaporates during this process such that the deposited mesh is dry. Fibre properties and morphology can be modified through the adjustment of variables such as dope flow speed, dope concentration, and holding temperature (in the syringe), molecular weight, spinning parameters (needle dimensions, flow speed, etc.), ambient conditions (temperature, humidity, etc.). Despite much research into collagen-based electrospun fibres and nonwovens, the high voltage required to facilitate fibre production [342] has been found to cause disruption of intramolecular H-bonds of the collagen polymer which results in an overall decrease in mechanical strength of polymeric material [444][143]. Collagen fibres can also possess low tensile strength, be sensitive to moisture, and possesses low thermal stability, limiting the use of these fibres in some physiological applications [45]. Despite these drawbacks, electrospun collagen has numerous advantages in the production of nonwoven biomimetic fibre meshes that replicate the structural and biological features of the physiological ECM tissues [152][339][165][55][328][195][104][83][182][14].

2.5.4 Dry Spinning and Gel Spinning

Dry spinning (DS) (**Figure 2.9**) follows the same four phases as WS, which are: dissolution, extrusion, solidification (coagulation), and fibre treatment/collection. The process involves dissolving a polymer in a volatile solvent to form a spinning dope. Polymer concentrations tend to be higher in dry spinning dopes (20-30%) as opposed to other spinning techniques; this will result in an increased liquid viscosity which can be reduced through heating prior to extrusion. The dope is filtered before extrusion from a nozzle into a heated air chamber, forming a continuous stream of liquid. The solvent within the polymer dope evaporates, leaving behind a polymer stream which becomes a solid fibre. Finally, fibres can be treated or processed (such as drawing or UV-curing [209][221] to alter properties. DS is best suited for polymers that have a melting temperature equivalent to the temperature at which the material will begin to thermally degrade [366].

Chaochai et al. [68] used DS to produce gelatin fibres with diameters ranging between 50-60 μm, that displayed good water resistance and maintained fibre morphology when

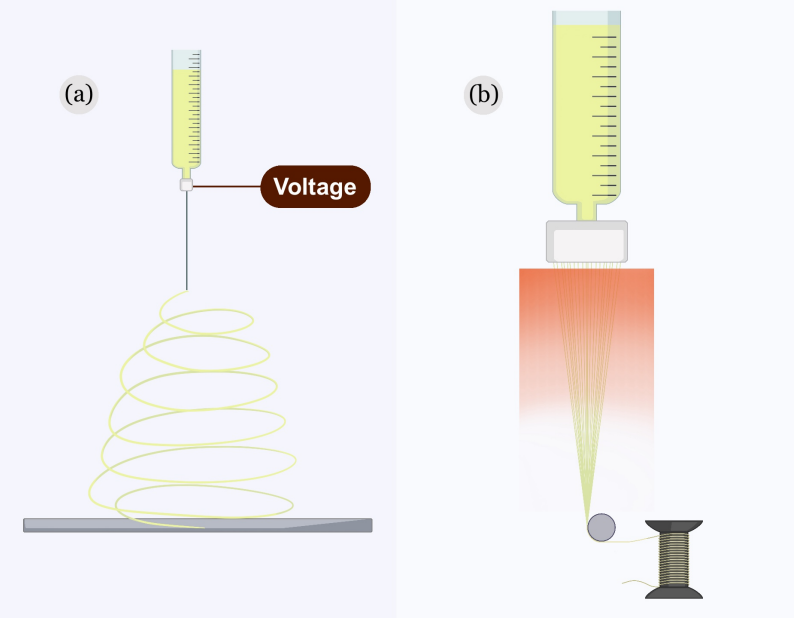

Figure 2.9: *Simplified illustrations of (a) an Electrospinning set-up, and (b) a Dry spinning set up.*

incubated for over 90 days, following extension and crosslinking with sugars [374][68], making these fibres suitable for biomaterials in applications such as gel-based drug delivery. Researchers noted that the fibres' internal structure were non-homogenous and porous, indicative of mechanical weakness, and that fibre morphology through the spinning process could not be fully regulated. Compared to gelatin there are few publications utilising DS to produce collagen-based fibres.

Gel-spinning (GS) (**Figure 2.10**)is a similar process to DS, with a secondary coagulation phase in the form of a coagulation bath, which strengthens the phase transition of the polymer from gel to solid fibre. Acting as an intermediate between wet and dry spinning, during extrusion, the dope stream will first pass through a heated air chamber (as utilised in DS) before further cooled, coagulated, and hardened in a coagulation bath (see WS). The dope will appear in a gel-like state (due to the ultra-high molecular-weight polymer) as it first travels through the heated chamber, which enables the dope stream to remain intact until it reaches the coagulation bath. At the molecular level, in its gel-state the polymer is held together by strong inter-chain bonds, aiding in an increased tensile strength. Fukae et al. [115] demonstrated this by producing GS-gelatin fibres with an average tensile strength of 146 MPa. These samples were tested to fail-

ure at a 1:16 rate of extension. Fibre diameter was not stated in this paper, however researchers noted that the WS needle used had an internal diameter of 0.3 mm [115]. Fukae and Midorikawa et al. [116] took this further by spinning gelatin dissolved in an ethylene glycol solution, resulting in fibres possessing an average tensile strength of 405 MPa; significantly higher than similar studies [115][116][242].

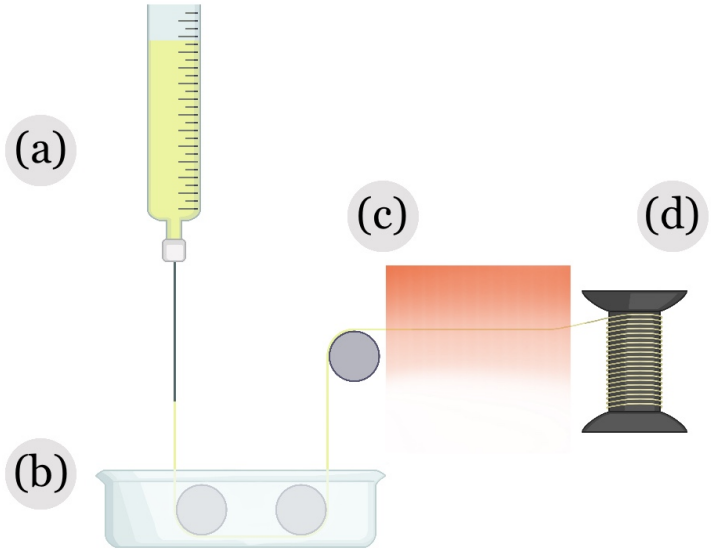

Figure 2.10: *Simplified illustrations of a Gel spinning set up. (a) dope extrusion; (b) coagulation bath, and (c) heating; (d) fibre collection.*

2.5.5 Centrifugal Spinning

Centrifugal spinning (CS)(**Figure 2.11**)is a fibre production method which employs force generated through centrifugal motion to produce fibres. In this method, a polymer or melt is introduced into a rapidly rotating spinneret or nozzle. As the spinneret revolves, centrifugal force forces the dope material through the tiny holes of the nozzle, forming fine fibres. The fibres created through centrifugal spinning can be manufactured in a range of diameters and lengths, depending on factors such as the polymer properties, spinneret design, rotational speed, and processing conditions. A recent paper by Arican et al. [22] employed CS to manufacture gelatin-based nanofibre meshes for use in N95 respiratory filters. CS gelatin fibres were sandwiched between two layers of nonwoven polypropylene material to produce the filter sheets which presented similar

breathability qualities to commercial benchmarks, indicating promising application of gelatin-based CS [22].

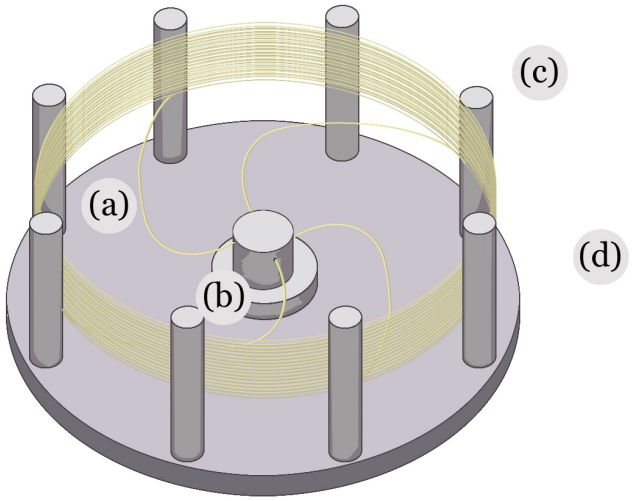

Figure 2.11: *Basic centrifugal spinning set up. (a) liquid polymer jet (b) spinneret (c) Fibre collectors (d) centrifuge.*

2.6 Fibre Manipulation and Optimisation of Wet Spun Fibres

Certain parameters during WS can have considerable influences on the thermodynamic attributes of the dope, as well as the resulting fibre morphology. This section will cover key parameters that should be considered throughout the WS process; including dope polymer concentration, dope and coagulation bath solvents, additional chemical additives, processing temperatures, extrusion and draw rates, and physical qualities of the nozzle and coagulation/supplementary baths [292]. The production of WS filaments relies on diffusional exchange of solvents between the coagulation bath and dope/fibre, in accordance with Fick's Law of counter diffusion, which describes the diffusion of particles, proportional to the concentration gradient [178][398], as well as post-spin treatments of the fibre, which will be discussed in the following sub-sections.

2.6.1 Dissolution: Dope Rheology and Solvent Polarity

Prior to the physical fibre production via WS, a spinning dope must be prepared whereby a polymer is dissolved into a compatible solvent. Factors that can affect dope consistency and end fibres include dope rheology, viscosity and solvent properties. Rheology of the spinning dope describes the flow behaviour of the polymeric solution) in the early stages of fibre production is a major contributing factor to the fibre's final structure and properties; and will determine both physical attributes, as well as solvent diffusion kinetics during later stages of WS.

Gelatin dopes exhibit viscoelastic behaviour, displaying properties of both viscous liquids and elastic solids when subjected to strain or stress [10]. Their rheological properties are influenced by factors like temperature, composition, concentration, and applied strain. The gel strength and viscosity are two important rheological properties of gelatin-based materials, as higher gelatin concentrations generally lead to higher gel strength and viscosity. Coordinated physical gelation (cooling below gelation temperature) and chemical crosslinking (e.g., photocuring) can be used to modulate and "lock in" the physical networks in f-gelatin hydrogels, influencing their rheological and swelling properties [439].

Viscosity is largely determined by the quantity of polymer wt.% dissolved into a solvent and plays an imperative role throughout the entire spinning process. As WS dopes tend to be higher in polymer concentration [384], solute/solvent solutions are often thick and viscous in consistency. With a higher polymer concentration, the rate of diffusional exchange will decrease during coagulation, which presents difficulties in producing a homogenous fibre [378]. Conversely, a disproportionately quick coagulation reaction may result in the fibre's exterior to solidify, preventing diffusional exchange at the fibre's centre; negatively impacting the overall homogeneity and crystallinity of the filament. Dope rheology (as it is extruded from the needle and into the coagulation bath) is essential to the resulting fibre's geometry [334]; as the flow behaviour will govern both fibre morphology and uniformity, as well as drawing tension throughout the coagulation reaction [394][334]. Dope viscosity can also impact the crystallinity of fibres [384]. Highly crystalline materials exhibit organised, repeating molecules, while amorphous materials will

display a far more random molecular structure, significantly influencing internal friction and resistance to deformation under axial stress [21]. The viscosity of a substance can be influenced by molecular weight as a result of heightened interlocking of polypeptide chains, leading to a decrease in chain mobility, due to an increased surface tension during coagulation.

The solvent must effectively dissolve the polymer to create a homogeneous dope. Non-uniform fibres caused by poor spinning or clogging of equipment can occur if the polymer is unable to fully dissolve into the solvent. This can also have an impact on the dope's rate of diffusional exchange, as different solvents will possess different rates of coagulation, which can impact the structure and properties of the resulting fibres. When using protein-based polymers, volatile solvents can induce polymer denaturisation, resulting in reduced stability and mechanical properties and tensile strength, irrespective of crosslinking treatments. Regarding this polymer denaturisation, it should be noted that in some cases a partial denaturation or "unfolding" of the protein is required for WS to facilitate alignment between protein molecules (globular proteins specifically need unfolding into a more linear state for spinning) [252].

Solubility of a polymer in a solvent is a significant factor in the production of dope. When there is a high solubility between polymer and solvent, intermolecular interactions are improved [334]. Regarding scaled-up WS, environmental and economic impacts of the solvent may have to be considered. Solvents that have high toxicity, and limited or complex disposal routes may limit large-scale production of the dope.

Solvent polarity plays a significant role in WS, as it impacts charge separation due to differences in electronegativity between the solvent and polymer [13][424]. In polar solvents, the negatively charged atoms induce charge separation within the polymer, which generates an electric field [238]. Polarity influences the alignment of polymer chains during WS and is a crucial factor in controlling fibre characteristics in WS applications. Polarity can also influence the WS process. During polymer dissolution, the degree of solvent-polymer interaction depends on the polarity of the solvent. More polar solvents will have a higher electronegativity difference, leading to stronger interactions with the

polymer. During charge separation, the more electronegative atoms in the solvent can pull electrons away from the polymer, leading to the creation of charged regions within the polymer. The charge separation within the polymer due to solvent polarity creates an electric field within the solution, which aids in the alignment of polymer chains during WS and can contribute to the formation of the desired fibre structure. As the polymer solution is extruded into a coagulation bath, the electric field generated by charge separation can influence the orientation and arrangement of polymer chains this affects the formation and properties of the resulting fibres.

2.6.2 Extrusion: Dope Temperature, Pumping Speed and Nozzle Features

Following dissolution of the polymer, the dope is pushed through a nozzle (needle or spinneret) into a coagulation bath. Factors that can affect resulting fibre morphology and characteristics include the temperature of the dope prior to extrusion, the rate at which the dope is pumped through the needle, and the physical features of the needle.

The high viscosity of WS dopes, which can often cause needle blockage or gelation at temperatures below taht of gelation [9][338]. By holding the gel at a temperature above that of gelation, the dope possesses an increased thermal kinetic energy potential [181][12], enhances mobility of the polypeptide chains within the solution and results in a decrease in viscosity immediately prior to extrusion [295].

The flow rate of dope through the nozzle should be compatible with the gel viscosity and should be high enough to enable the production of a continuous polymer stream as it is extruded into the coagulation bath. Within the case of lab-scale WS where this body of research situates itself, where syringes are more generally used (as opposed to industrial-scale machines) however, the pumping speed should not be so high to the point where it generates excessive back pressure on the syringe and needle, causing blockage, spillage, or breakage of the equipment. Matveev et al. [236] suggested that the rate of phase transition (during WS) increases if the pumping speed is increased; however, this finding was coupled with a finding of increased macrovoids within the fibre's internal structure [158][236]. The flow rate speeds of dope through the needle

will largely be dictated by the dope's rheology. Increased exterior roughness has been associated with employing an extrusion rate that is not best tailored to the rheological properties of the dope [334].

Dope parameters aside, the physical dimensions of the hole that the dope is extruded through can influence resulting fibre morphology. A smaller needle gauge (G) with a larger lumen diameter (<16 G) will produce thicker fibres which will require a longer period of incubation time in the coagulation bath to enable total solidification; as opposed to a higher gauge (>16 G), which will coagulate in a shorter duration, while also producing finer fibres. Different gauge sizes can also affect resultant fibre mechanical characteristics, such as tensile strength and drawing capacity, enabling fibre modification to specific performance requirements. The needle gauge will typically determine flow rates, as finer gauges will require a slower stream of dope through the channel [364][182]. H.C. Kim et al. [182]. also notes that both dope pumping speed and shear stress is largely determined by the needle's internal diameter. While this will not be explored within this body of research, spinnerets with non-circular cross-sections may also offer differing fibre properties.

2.6.3 Coagulation: Temperature and Solvent-Non-Solvent Compatibility

Like dope solvents, the choice of coagulant solvent/s play a central role in fibre formation. As the dope is extruded from the needle, the dope solvent diffuses out of the fibre, and is replaced by the anti-solvent in the coagulation bath. Factors that affect the rate of coagulation (other than those previously mentioned: dope characteristics, needle, and fibre diameter) include solution polarity, viscosity, volatility, and temperature [215].

Holding the coagulation solution at different temperatures will have an impact on resulting fibre properties. Several WS studies had noted holding the solvent-non-solvent solutions below zero (0°C) [116][333]. Oksuz and Erbil [269] observed that in reducing the temperature of the coagulation bath denser filaments with improved mechanical properties could be produced; while within the context of scaled-up production of fibres this paper hypothesises that decreasing the bath temperature to below zero could aid in dras-

tically reducing the rate of coagulation of the fibre from gel to solid (gel-sol reaction). One reason for this could be the significant change in temperature of dope/fibre (usually held at room temperature or heated) as it is extruded into the cold solvent-non-solvent, causes a reduction in thermal kinetic energy potential [230][39][181]. The decrease in kinetic energy reduces the mobility of polypeptide chains within the gel, increasing the viscosity of the dope, and initiating a slight phase change from liquid gel towards a more solid-like state [318][438], as molecules have limited mobility and maintain a fixed position. This temperature-induced phase change is temporary and can be reversed if total coagulation of fibre is not achieved; the extent of this phase change will depend largely on the specific composition of the gel and the temperature range involved.

Bath temperature will also have an impact on the exchange rate between the solvents. The rate of solidification is governed largely by the exchange behaviour of dope and coagulant solvent. In contrast to using a cold coagulation bath, Shirvan et al. [334] argue against dropping the solution temperature, stating that with this reduction in heat potential, mutual diffusion coefficient is decreased, which slows the rate of diffusion between the two solvents [345][437][449][334]. While excessively slow solidification speeds will limit both the consistent morphology and production of WS fibres, several studies have indicated that the slight deceleration in diffusional exchange caused by a temperature drop in the coagulation solution may decrease the porosity of the fibres internal structure [430][142][161]; which enables closer packing of polypeptide chains, and the production of a more uniform fibre [161].

The speed at which diffusional exchange takes place in a fibre will not only affect fibre morphology and properties, but also effect the rate at which fibres can be produced. Rickman et al. used a salt-based solution (Sodium chloride (NaCl) 20% (wt.%), Polyethylene Glycol (PEG) 20% Weight Value (w/v), dissolved into 0.1 M Phosphate buffered saline (PBS) solution, [307]) to spin Porcine skin gelatin (PSG)-crosslinked with 4VBC. Following extrusion, the fibre required a 60-minute incubation period in the salt-based coagulation bath (set to 5°C), followed a secondary 60-minute incubation phase in a wash bath containing distilled water to remove any sodium chloride from the fibre's surface. Very slow coagulation rates such as these may limit both the length of fibre that

can be spun at one time (as fibre length will be greatly determined by the size and dimensions of the physical bath), as well as feasibility of scaled-up production. Upon extrusion into the bath, the polymer within the dope begins to gel and coagulate because of solvent-non-solvent exchange phase inversion [334].

2.6.4 Post-Spin Treatments: Drawing and Curing

The fourth step in the WS process if fibre collection, which often involves some sort of drawing or post-spin treatment steps. Drawing is a critical step in the manufacture of WS fibres and involves stretching the newly formed fibre to improve mechanical stability [11]. Benefits of post-spin drawing include alignment of polymer chains/crystalline structure, which enhances the fibre's dimensional stability and tensile strength [288][334], making it more resistant to axial loading and breakage. An increased crystallinity has demonstrated improved resistance to higher temperatures, mechanical stresses, and enzymatic degradation [290]; as well as reducing susceptibility to moisture absorption through a reduction in porosity [334]. Drawing can also aid in attaining a more homogenous fibre diameter, which minimises any variations and non-uniformity in the final fibre [103], and enables control over fibre morphology, including its denier (linear density) and elongation. Drawing can be used to improve mechanical properties of a fibre. The draw-ratio describes the ratio between filament draw speed, and pumping speed [236]; it is controls polypeptide alignment at the molecular scale. Fahma et al. [103] indicated that an increase in draw ratio (> 1) would correlate with an increase in Young's modulus (YM) and tensile strength (TS) [426][103]. Yaari et al. [426] observed a significant different in surface quality between drawn and undrawn WS collagen fibres. In this study it was found that undrawn fibres exhibited a very non-homogenous cross-section along the length of the fibre, as well as displaying significant internal macrovoids and external crevices on the fibre's exterior; while drawn fibres displayed a far more homogenous and smooth surface quality [426]. The mechanical advantages of post-spin drawing have been demonstrated by Fukae et al. [115] who found a significant increase in both tensile strength and Young's modulus from 28 MPa and 0.7 GPa, respectively, to 180 MPa and 3.4 GPa following fibre drawing by 8x its original length.

Curing involves the chemical crosslinking of polymer chains using UV rays and a photo-

crosslinking agents dissolved either into the dope, or into the coagulation bath (which disperses into the polymer during diffusional exchange). Of particular interest to this project, the process of UV-curing involves the chemical crosslinking of polymer chains, which is achieved through the use of a photoinitiator, which a activates a network of covalent crosslinks upon exposure UV light. Upon exposure to this light, covalent bonds are formed between biomolecules in the dope, increasing stiffness and handleability of the fibres, as well as improving their resistance to higher temperatures (that may otherwise impact the uncured polymer) and water. Crosslinking of gelatin to stabilise the polypeptide chain structure under higher temperatures has been proven to reduce any potential immune reaction when used *in vivo* [124]. Gorgieva [124] suggested that these findings may be due to the removal of antigens which aids in material sterilisation.

The photo-crosslinking agents can be dissolved into the polymer dope solution prior to extrusion. Alternatively, they can be incorporated into the coagulation bath, where they diffuse into the polymer during the exchange of solvent and non-solvent. Upon exposure to UV light, the photo-crosslinking agents initiate the formation of covalent bonds between the polymer chains. This chemical crosslinking process results in the formation of a stable, three-dimensional network structure. The curing step is crucial for imparting desired mechanical properties, chemical resistance, and thermal stability to the final polymer product. It is commonly employed in various manufacturing processes, such as the production of coatings, adhesives, and composite materials.

2.7 Biomimetic Fibres for Artificial Tendon Reconstruction

This body of research sits within the context of biomaterials used within biomedical applications such as ATR. With the national life expectancy ever-increasing [2], and sport activity levels returning to pre-pandemic heights [4], tendon degeneration and rupture is of rising prevalence [138][397]. The Achilles tendon stands out due to its critical anatomical location and its prevalent susceptibility to injury and rupture. Presently, artificial tendon reconstruction methods primarily rely on synthetic polyester woven textiles, which lack adequate biomimetic properties and exhibit high rates of re-rupture.

This outcome is likely attributed to the challenge of effectively integrating biological tendon and muscle fibres with synthetic materials. In this context, the significance of collagen and gelatin as valuable biomaterials emerges, offering potential solutions to address the limitations of current reconstructive techniques and enhance overall treatment outcomes. The following sub-chapter will discuss the current state of artificial reconstruction, materials, and structures, as well as the impacts of these injuries on patients and the wider healthcare system.

2.7.1 The Achilles: Anatomy, Structure and Function

The AT (also referred to as the Calcaneal Tendon) is a thick, fibrous band of tissue that connects the gastrocnemius and soleus muscles of the calf to the heel bone (calcaneus) [226][96][200] (**Figure 2.12**). The AT is formed by the merging of the calf muscles' fibres (tendon-muscle interface) as they extend downward toward the heel bone, tapering into the calcaneal insertion site (tendon-bone interface). It is the strongest, largest, and thickest tendon in the human body; however, is also the most susceptible to injury due to (a) its location within the body and (b) the considerable forces it must withstand throughout day-to-day activities, such as weight bearing, walking, running, jumping [197][162][365]. The primary function of the AT is to facilitate plantarflexion; described as the transmission of force from the calf muscle through the ankle joint and on to the foot, through a movement is a downward pulling motion [96][200][1]. Additionally, the AT is central in the supination (outward rolling motion of the foot during the gait cycle) and pronation (inward rolling motion of the foot during the gait cycle) of the foot, enabling an individual to maintain a healthy gait. During plantarflexion, (push movements: running, jumping) the calf muscles will contract, producing tension that transmits through the AT to the calcaneus. This transmission of force propels the body forward and supports the body's weight during movements. A healthy tendon is therefore crucial in the withstanding shock forces and protecting the ankle joint and overall lower limb. With an average landing force of approximately 12.5-times the bodyweight of the runner [190][227][415] placed upon the AT during running, tendons act as natural shock absorbers, through their ability to stretch and store elastic energy during high-impact activities.

The Myotendinous Junction (MTJ) carries two main functions: to facilitate efficient

force distribution accross the span of the interface, and to mitigate focal stress concentrations during muscle contraction [274][35][403][388][359][427]. The interdigitated structure of the MTJ creates a larger interfacial region, allowing the contractile forces to be distributed over a broader area. This force dispersal mechanism helps to prevent the localisation of stress at specific points, which could otherwise lead to tissue damage or failure. Furthermore, the finger-like projections of the tendon fibres and myocytes provide a gradual transition between the dissimilar mechanical properties of the two tissue types, further reducing the risk of stress concentrations and potential failure at the interface [274] [35] [403] [388] [359] [427].

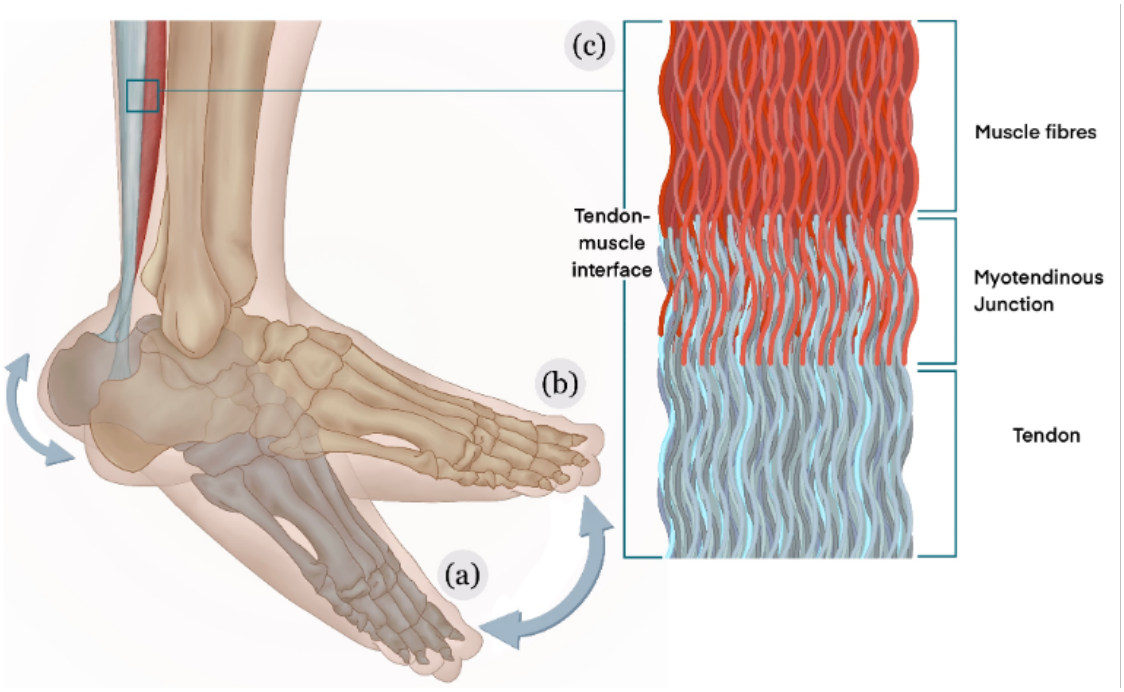

Figure 2.12: *The Achilles tendon (indicated with arrow) in its (a) plantarflexed and (b) dorsiflexed positions. A schematic illustration of the myotendinous junction (c) has been presented alongside.*

2.7.2 Tendon Injury, Rupture, and Degeneration

Tendon rupture refers to the complete or partial tearing or separation of a tendon from its attachment point to a bone [47][37]. Tendon ruptures can occur due to sudden trauma (sudden impact/injury), degenerative changes (long-term wear and tear/chronic tendinopathy), overuse, or a combination of these factors; often caused by exceeding the tendon's

capacity to withstand applied loads, resulting in material [tendon] failure [rupture]. AT rupture is a relatively common sporting injury; particularly in activities that involve explosive movements, quick changes in direction, and high-impact actions. AT ruptures often occur during dynamic movements that put excessive force on the tendon; and commonly occurs when the calf muscles contract forcefully while the foot is dorsiflexed (bent upward), causing an abrupt and powerful tension on the tendon body/interfaces [30][337][261]. These causes of injury/rupture are regarded as extrinsic factors; and within sport, have been largely attributed to excessive or repetitive mechanical stress on the tendon, poor training techniques, inadequate warm-up and stretching routines, and improper footwear. Several factors have been attributed to an increased risk in AT rupture. A correlation has been observed between natural aging, and risk of AT injury [138][358][393][185] (also observed in animal studies, [278], due to intrinsic physiological changes such as reduced blood flow to tendons [393], increased stiffness [138][212], decreased ability to withstand higher mechanical loads [138], mobility-induced atrophy [110], fibre disorganisation and the accumulation of non-functional tissue [402]. Genetic predisposition and underlying medical conditions can also contribute to injury risk. Many studies have noted adult men as the predominantly affected demographic [147][250][440][279][138][128][198][225][367]. Clayton and Court-Brown [73] found higher injury rates among male demographics; however the mean age of injury was higher in women, indicating that females may be more susceptible to age-induced tendon injury.

Similar findings were found in a Finnish study by Nyyssönen et al [267] who concluded the average of tendon injury from the Finnish National Hospital Discharge Register was 2-to-3 years older in women than their male counterparts, across a 12-year-span. Despite significant research supporting this, it may be important to note that much academic research on injuries (and sporting injuries) is carried out on this specific demographic, indicating a degree of gender bias. To counterbalance this, Chan et al. [66] observed higher operative rates in women's' sports as well as longer time lost from play, in comparison to male athletes; 77.8% vs 58.8%, and 96 vs 48 days respectively.

Degenerative changes over time can weaken tendons, making them more susceptible

to rupture even with less forceful actions. Chronic conditions such as tendinopathy [227][200] or chronic inflammation [85] can weaken the tendon structure and increase the risk of rupture [227][200][85][331], especially in individuals with repetitive movements [197] or those engaged in activities that put stress on specific tendons [217].

2.7.3 Treatment: Commercial Benchmarks for Artificial Tendon Reconstruction

The current approach to tendon reconstruction involves various surgical techniques, ranging from anti-inflammatory drugs for chronic injuries to surgical repair for acute cases [228]. While different suture techniques, such as four-strand cross-lock repair [321][32][31][19][94][79][139][285][414] and U-shaped repair [262][280][400], are employed in reconstruction surgery, complications and limited functionality can still occur post-surgery [101][302][410][202].

The specialisation of tendons to their specific role and anatomical location within the body, make them extremely difficult structures to repair/replace [193][210]. Current surgical treatments include suturing (ruptured ends are aligned and stitched together) and grafting, which involves the harvesting of a healthy tendon from one part of the body and transplanting it to the injury site [232][362]. Conventional techniques including autografts, allografts, and xenografts have proven successful in their ability to promote cell proliferation however, have also displayed several drawbacks such as high infection risks [370][168], inflammatory immune response, donor site morbidity [370][314], and high re-rupture incidences [281][331]. Post-operative re-rupture of tendons occurs most frequently during the critical healing period (less than 14 days) after surgery [51]. In cases of successful reconstruction, tendons rarely regain full mechanical strength [53][432][118], which can often result in chronic pain and a reduced quality of life [249][271][270][392]. These postoperative complications, therefore, prevent traditional methods such as these, from offering suitable long-term treatment [51].

In recent years, researchers have looked toward novel artificial methods of reconstructing tendons [6]. Artificial neo-tendons, (made from man-made materials such as polyester), have been recommended as an alternative to surgical tendon autografts in the case of

significant tendon damage and tendon loss [6], and have delivered promising results in recent years [51].

Leeds-Keio (LK) polyester (**Figure 2.13**)[325] was developed as a synthetic alternative to conventional knee ligament suturing by Xeros/Neoligaments [114][235]. LK polyester fibres (22 μm diameter) are manufactured into a rigid open-weave mesh structure [114][264]. Since the material's launch, LK polyester has been manufactured into a range of tendon/ligament reconstructive products, such as the AchilloCordPLUS™ System (AT reconstruction) [417]), JewelACL™ (anterior cruciate ligament (ACL) reconstruction) [418]), the PatellarTape System™, Infinity-Lock, and Poly-Tapes (Patellar tendon reconstruction) [419][420][421]). The polyester material has displayed tensile properties equivalent to those of a human ACL, with an ultimate load strength of 2200 N [114]. Regarding long term performance and durability of the material, Nomura et al. [264] investigated neo-cellular attachment to the woven mesh using ultrasound imaging; observing good collagen and surrounding ECM integration.

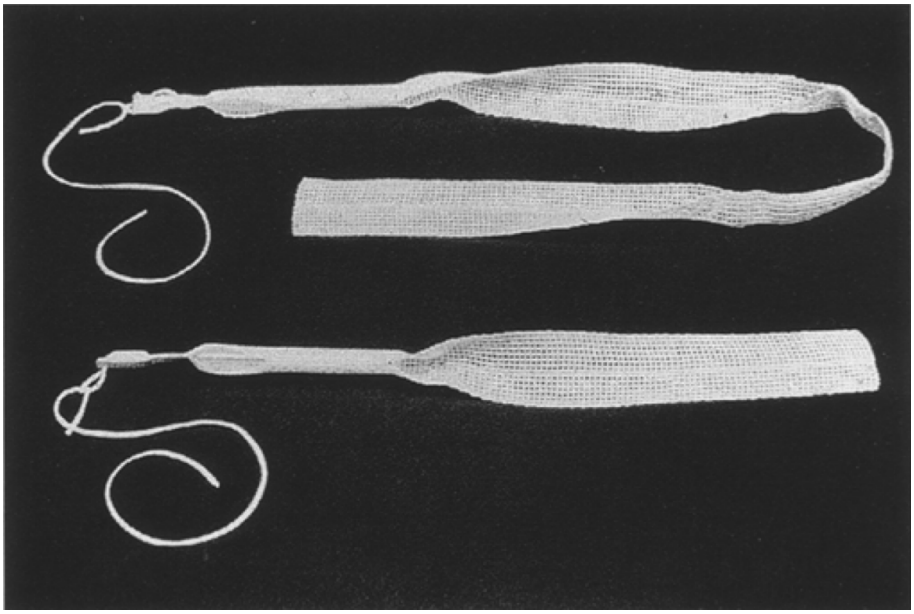

Figure 2.13: *'The Leeds-Keio artificial ligament with typical woven polyester structure'; adapted from Schroven et al. [325].*

Carbon fibre-based synthetic tendons were developed by Johnson and Johnson for use in AT reconstruction [6] to act as surrogate native carbon fibres following rupture [172].

These have exhibited similar mechanical dimensions and properties to other graft transplantation techniques [166][172]. Surgicraft developed a composite carbon-polyester synthetic tendon [166][6][51], which utilised the respective benefits of strength and rigidity of carbon, and the flexibility and elasticity of polyester [51], combined to form the Surgicraft Surgical Mesh System and Surgicraft ABC prosthetic [248].

2.7.4 Impacts of Tendon Injury on Healthcare

Many sources recommend reconstructive surgery in younger demographics and in physically active/sudden rupture cases [164]. The impact of Achilles tendon rupture on the NHS is significant, with over 11,000 cases per year [77][145].

Tendon injuries place a significant burden on healthcare providers [406][183][72]. The financial strain, largely a product of extensive (often long-term) medical treatments, including consultations, imaging, surgeries, and rehabilitation, imposing burdens on healthcare systems and individuals alike [406]. Ruptured tendons sometimes require a period of immobilisation to heal [84][226], and even after this, rarely regain full mechanical function [432] and so rehabilitation of the tendon and surrounding joint is imperative to increasing the outcomes of recovery and functional restoration. The repercussions of tendon rupture extend to workforce productivity, with injuries causing temporary or permanent disability, sometimes leading to a decrease in productivity.

2.8 Chapter Conclusion

This project looks to build upon knowledge in two distinct areas. The first being to examine the current state of tendon reconstructive methods. As previously mentioned, repair of ruptured tendons at the MTJ presents significant surgical challenges due to the intermeshing of native tendon and muscle tissues (**Figure 2.12c**). Additionally, it is the gradient transition of the MTJ region from dissimilar tendon-to-muscle fibre exhibits further complicates the application of synthetic woven tendon implants through the introduction of a third dissimilar material (this time synthetic) into the tendon-system. This complex interface, exhibits a low healing process attributed to their hypo-cellular and hypo-vascular nature, resulting in limited cell presence and blood supply, reducing

both the rate of healing, and also the healing quality. Moreover, the absence of a universally accepted standard for suture materials, techniques, and rehabilitation protocols adds complexity to tendon repair procedures.

To build upon the issues mentioned above, the author looked to fill this gap in knowledge through building upon a second area of research; that is the manufacture biocompatible filament fibres through fibre spinning methodologies, with material properties optimised from earlier initial fibres reported in Rickman et al. [307]. As discussed throughout this chapter, WS-fibre-based scaffolds have been shown to offer considerable potential for tendon tissue engineering applications through the biomimicry of microenvironment that supports cell attachment, orientation, migration, and proliferation [414] [309] [149] [102]. Recent developments by Rinoldi et al. [308] employed a three-dimensional microfluidic WS system in the manufacture of highly-aligned cell-laden hydrogel yarns made from human-bone-marrow-mesenchymal stem cells dissolved in a Gel-MA bio-ink [308]. Findings of T1C and T3C cellular expression, indicate hope for total regrowth of tendon-forming cells and TR, showing great promise for the future of biocompatible WS fibres for *in vivo* applications.

Similarly, recent advancements by Wu et al. [411], Rinoldi er al., [308], Dong et al. [95], and Deng et al. [89] have shown promising application of WS in the production of biomimetic ligament scaffolds. In addressing ACL reconstruction, re- searchers concluded that resultant fibres exhibited cytocompatibility and osteogenic differentiation qualities, superior to natural degummed natural silkworm silks.

Gelatin is a valuable biomaterial, with many current applications in the medical, pharmaceutical and food industries. Processing gelatin, however, presents challenges for extended application in the field of biomaterials for *in vivo* application. The production of high-quality, uncontaminated collagen-based fibres is essential for advanced wound care and tissue regeneration devices. WS is capable of producing such fibres, but enhancing the wet stability and mechanical properties without resorting to chemical crosslinking remains a challenge across current literature.

The subsequent experimental work concentrates on exploring an alternative method for

preparing F-gelatin-based fibres. The subsequent research assesses the feasibility of WS and supplementary UV-crosslinking of photoactive gelatin-based fibres. Following this further optimisation of fibres through drawing and curing investigation is conducted to thoroughly evaluate the fibre properties.

Chapter 3

Experimental: Materials and Methods

3.1 Chapter Introduction

The literature reviewed, has evaluated the current approaches to gelatin-based wet-spun biomaterials and highlights a gap in current literature and practice, regarding the ability to successfully treat and heal tendon tiussue to prior mechanical strength and function **(Objective 1)**.

This chapter outlines all experiments and optimisation processes carried out throughout this research project in order to manufacture UV-cured Gel-4VBC filament fibres through WS methodologies at a laboratory-scale. The research process involves several key steps, catagorised by their stage in the WS process (as discussed in **Section 2.5.1**). Each experiment was designed to optimise the properties and performance of the resulting f-gelatin fibres.

3.2 Materials

High bloom strength gelatin from porcine skin (PSG) (Sigma-aldrich, Gillingham); Phosphate buffered saline (PBS) tablets (Sigma-aldrich, Gillingham); Polysorbate 20 (EMD Millipore, Massachusetts, United States); 4-vinylbenzyl chloride (4VBC) (Fisher Scientific, Massachusetts, United States); Triethylamine (TEA) (Sigma-aldrich, Gillingham); Absolute Ethanol (EtOH) (Sigma-aldrich, Gillingham); 2-Propanol (IPA) (Sigma-

aldrich, Gillingham); Acetic acid (AcOH) (Merck millipore, Gillingham); Hydrochloric acid (HCl) (Sigma-aldrich, Gillingham); 2-Hydroxy-4- (2-hydroxyethoxy)-2- methyl-propiophenone (I2959) (Sigma-aldrich, Gillingham); Sodium bicarbonate (NaHCO_3); 2,4,6-Trinitrobenzene sulfonic acid (TNBS) (Fisher Scientific, Massachusetts, United States); Diethyl Ether (Sigma-aldrich, Gillingham); Polyethylene Glycol 8000 (PEG 8000) (Sigma-aldrich, Gillingham); Polyethylene Glycol 400 (PEG 400) (Sigma-aldrich, Gillingham); Sodium chloride (NaCl) (Tesco PLC, Hertfordshire).

3.3 Synthesis of Collagen-Based Polymers

The following experiments describes optimisation of methodologies within the dissolution stage of the WS process. The synthesis of collagen-based polymers is a crucial aspect of the methodology, and included the crosslinking of gelatin with 4VBC and subsequent quantification of functionalisation degree through the use of colourimetric assays. The dissolution of the functionalised polymer (at different wt.%) in various acids is also explored to determine the optimal conditions for the polymer dope. Stability and compatibility of the polymer dope are extensively investigated, with a focus on thermal and wet stability, as well as the interaction between the dope and different coagulation solutions; including the salt-based bath as described in Rickman et al. [307].

3.3.1 Gel-4VBC Functionalisation

High bloom strength PSG, was dissolved in distilled water at 10 wt% and heated to 50°C. The following materials were then added in sequential order; 1% w/v Polyoxyethylene sorbitol ester, 4VBC 14.8% w/v, and TEA a14.6% w/v. These measurements were followed in accordance with the methodology states in Rickman et al. [307]. The solution was mixed vigorously at 600 rpm for five hours at 50°C. Subsequently, the reaction mixture was added to absolute ethanol at a 1:10 volumetric ratio and left overnight to terminate further reactions and allow for precipitation of the functionalised gelatin. Following this, the gel-4VBC was removed from the solvent, and placed into a fume cupboard to allow any residual IPA to evaporate off, before drying at 60°C for 48 hours. This procedure is illustrated in **Figure 3.1**.

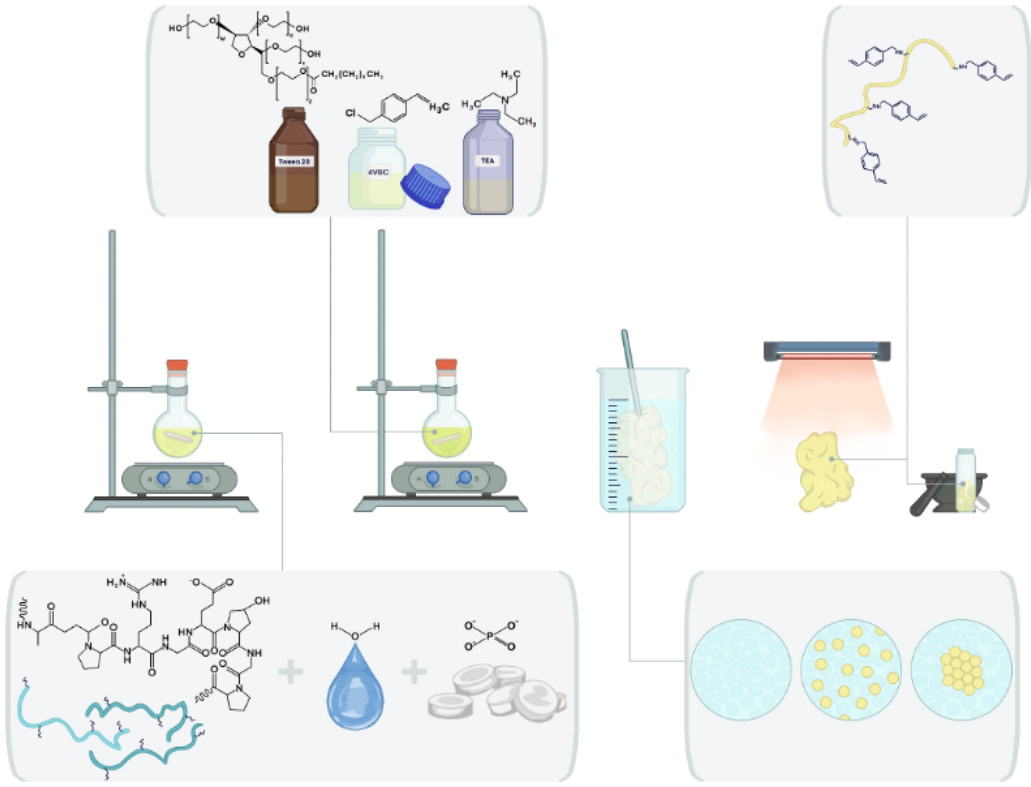

Figure 3.1: *Chemical crosslinking functionalisation of PSG with 4VBC. The key steps within this reaction are outlined as: (a) dissolution of native PSG in PBS solution, (b) combination of the PSG/PBS solution with Polyoxyethylene sorbitol ester, 4VBC and TEA in the quantities listed in section 3.2.1.; (c) precipitation of the gelatin solution in IPA; (d) removal of remaining IPA and drying of the crosslinked gelatin in an oven; (e) crushing down large pieces of polymer (pestle and mortar) into a powder and storing in a glass jar.*

3.3.2 2,4,6-Trinitrobenzene Sulfonic Acid Colourimetric Assay

The extent of 4VBC-functionalisation of gelatin was measured through the 2,4,6-Trinitrobenzene Sulfonic Acid (TNBS) colourimetric assay, following the procedure outlined by Bubnis and Ofner (1992). Gel-4VBC (11 mg) was placed in a falcon tube, to which 1 ml of a 4 vol.% NaHCO3 solution was added followed by. 1mL 0.5 vol.% TNBS solution. Simultaneously, native gelatin blank samples (11 mg) with 3mL of 6N HCl were prepared. All samples were agitated at 200 revolutions per minute (r·min-1) and maintained at a temperature of 40°C for 4 hours. Following this, 3mL of 6M HCl is added to the gel-4VBC samples and 1mL 0.5 vol.% TNBS solution is added to the blanks. All samples were incubated again for 1 hour at 60°C. Once cooled to room temperature, all samples were diluted with 5 ml de-ionised (DI) water. Unreacted TNBS was extracted through mixing

with diethyl ether in a separation funnel, the aqueous component was kept, and the solvent discarded. From the remaining solution, 5 ml was collected and then diluted with 15 ml of DI water. This resulting solution was heated in a water bath at 50°C to allow any remaining diethyl ether to evaporate off.

Each gel-4VBC solution was analysed using UV-Vis spectrophotometry (6315 UV/Visible Spectrophotometer by Jenway, UK; St James' Hospital, Leeds), and the recorded absorbance value at 346 nm was compared against the blank sample. **Equations 3.1** and **3.2**, were used to calculate both the molar content of remaining lysines (per gram of gelatin) and the degree of gelatin functionalisation, respectively.

$$\frac{Moles(lys)}{Gelatin} = \frac{2 * Abs * 0.02}{1.46 * 10^4 * p * m} \tag{3.1}$$

Where *Abs* is the absorbance at 346 nm, *1.46 x 104* is the molar absorption (M-1cm-1), *p* is the spectrophotometer cell path length (1 cm), *m* refers to the weight of gel-4VBC (0.011 g), and *0.02* is the total volume of diluted (diethyl ether-) extracted solution (litres).

$$F = (1 - \frac{Gel_F}{Gel_N}) * 10 \tag{3.2}$$

Where Gel_F is the molar lysine content of functionalised gelatin,Gel_N" is the molar lysine content of native gelatin, and *F* is the degree of functionalisation of 4VBC onto the gelatin.

The TNBS assay relies on the reaction between TNBS and the primary amino groups (lysines) on gelatin [377][203]. By quantifying the decrease in free amino groups after 4VBC functionalisation, the degree of substitution can be indirectly determined [377][203]. This colourimetric method has been widely used to characterise the functionalisation of collagen and gelatin with various monomers like 4VBC and MA [377][203][307].

3.3.3 Polymer Dissolution in Acetic and Hydrochloric Acids

Gel-4VBC polymer was dissolved in AcOH and HCl acids using the conditions defined in **Table 3.1**. 5ml of each solution were prepared in glass vials, placed into a large water

bath, and held at 55°C for 60 minutes. Stirring was set to 6500 rpm. The chosen stirring speed was carefully determined to strike a balance between two key factors. On one hand, it needed to be sufficiently high to ensure thorough mixing of the highly viscous dope solution, ensuring complete dissolution of the gel-4vbc solute into the solvent. However, on the other hand, the stirring speed had to be slow enough to prevent a ”whipping” effect, which could introduce a significant amount of unwanted air bubbles into the solution. After this, stirring was turned off and solutions were heated for a further 10 minutes to allow any air bubbles to accumulate at the top surface of the liquid, and burst. This is illustrated in **Figure 3.2**.

Table 3.1: *Experimental conditions investigated to determine polymer dissolution.*

Sample	**Gel-4VBC w/v (%)**	**Polymer quantity (g)**	**Solvent**	**Solvent quantity (ml)**
1	5	0.25	50 mM HCl	4.75
2	10	0.5	50 mM HCl	4.5
3	5	0.25	100 mM HCl	4.75
4	10	0.5	100 mM HCl	4.5
5	5	0.25	50 mM HCl	4.75
6	10	0.5	50 mM HCl	4.5
7	5	0.25	100 mM HCl	4.75
8	10	0.5	100 mM HCl	4.5
9	5	0.25	DI water	4.75
10	10	0.5	DI water	4.5

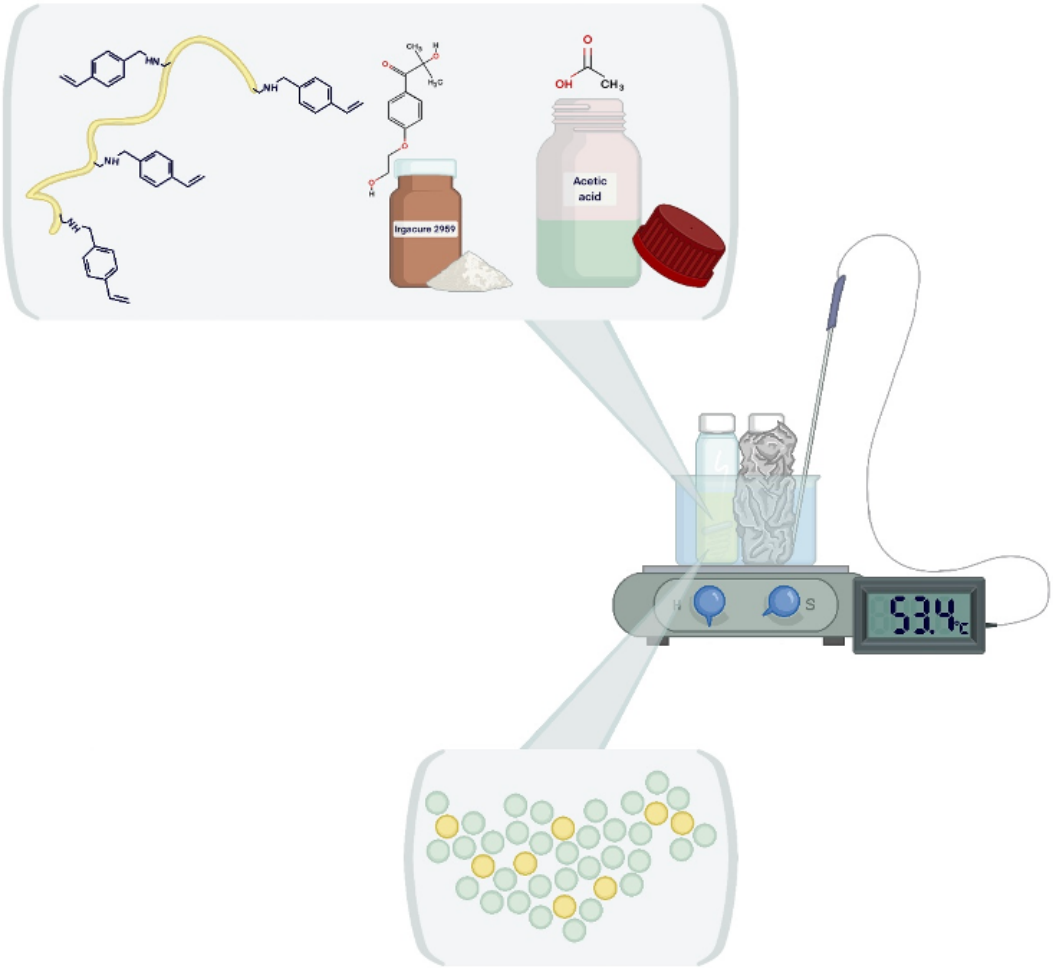

Figure 3.2: *Dissolution of Gel-4VBC and I2959 into 50mM AcOH.*

3.4 Dope Thermal and Wet Stability

This experiment series addresses the benefits of both chemical and UV crosslinking of gelatin. The gelation of Gel-4VBC was investigated in order to ascertain feasibility that the polymer would be able to undergo the gel-sol reaction and eventually spin into fibres. Here, the properties of native PSG and gel-4VBC were compared with respect to gelation and temperature stability. Four dope samples were prepared (**Figure 3.3**) for this experiment; as set out in **Table 3.2**. All solutions were dissolved at 55°C for 2 hours and decanted onto a sheet of parafilm to solidify. Dopes 2 and 4 (containing I2959) were cured for 40 minutes to generate UV-crosslinks. Three $20mm_2$ samples were taken from each dope and labelled as (a), (b), or (c) (**Table 3.2**). One dry sample from each dope condition was placed into incubator set to 37°C and 60°C respectively, while the remaining samples were left at room temperature (RT). All samples were inspected every 15

minutes for the first hour of incubation, hourly for three hours and then left under heat for a further 24 hours, to determine gel stability at physiological temperatures. Following this, samples were fully saturated in DI water and re-incubated in the 37°C and 60°C ovens. These gels were examined every 15 minutes for the first hour and again after a second hour to assess their properties (**Table 3.3**). The time steps for these have been noted in hours and minutes (hh:mm).

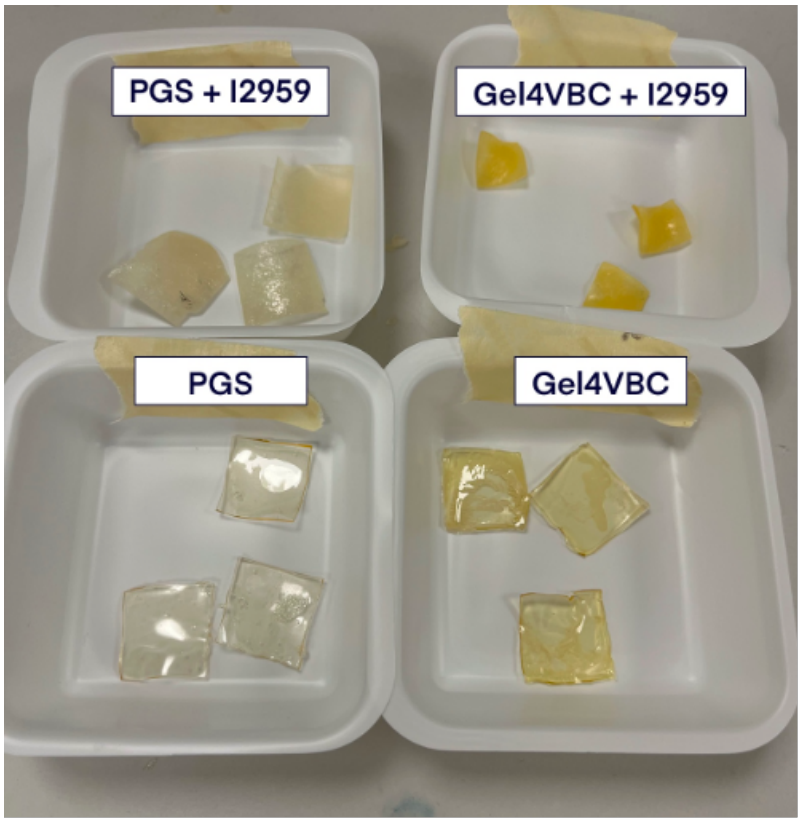

Figure 3.3: *Dope samples prior to heating experiment.*

Table 3.2: *Experimental conditions to investigate the effect of increased temperature on dry dope samples.*

Sample	Polymer	Incubation temperature (°C)	Time steps (hh:mm)
1a	Gel-4VBC	RT	00:15; 00:30; 00:45; 01:00; 02:00; 03:00; 24:00
1b		37	
1c		60	
2a	Gel-4VBC, 2% I2959	RT	
2b		37	
2c		60	
3a	Native PSG	RT	
3b		37	
3c		60	
4a	Native PSG, 2% I2959	RT	
4b		37	
4d		60	

Table 3.3: *Experimental conditions to investigate the effect of increased temperature on wet dope samples.*

Sample	Polymer	Incubation temperature (°C)	Time steps (hh:mm)
1b	Gel-4VBC	37	00:15; 00:30; 00:45; 01:00; 02:00; 03:00; 24:00
1c		60	
2b	**Gel-4VBC, 2% I2959**	37	
2c		60	
3b	Native PSG	37	
3c		60	
4b	Native PSG, 2% I2959	37	
4c		60	

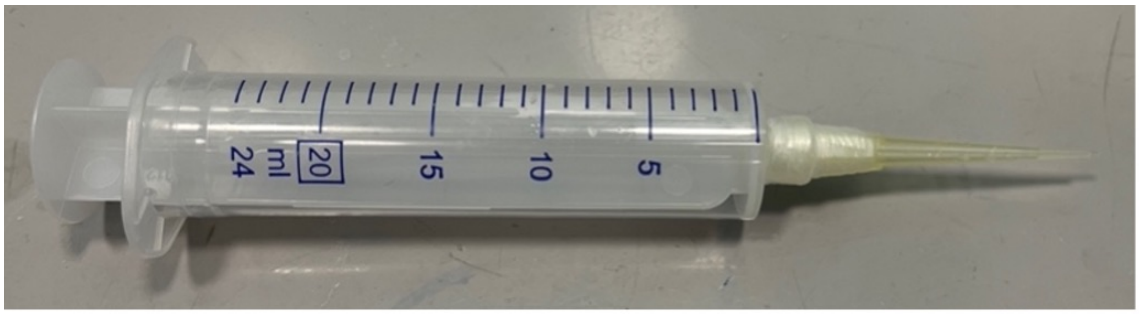

Figure 3.4: *Manual needle constructed from a 0.2 ml pipette-tip and 24 ml luer-lock syringe.*

3.5 Compatibility of Dope with Coagulation Solutions

The following experiments describes optimisation of methodologies within the coagulation stage of the WS process. Drop tests and phase transition studies are conducted to identify the most suitable coagulation bath composition and temperature. The WS process itself is optimised using a both a conventional (**Section 2.5.1**) and rotating (**Section 2.5.2**) lab-scale rig, with parameters such as needle gauge, pumping speed, rotational drawing, temperature, and spinning duration systematically varied to achieve the optimised fibre properties.

3.5.1 Drop Tests into Different Coagulation Baths

Following optimisation of the dope solution, drop tests were carried out to determine the best solvent for the coagulation bath. The different coagulation conditions have been set out in **Table 3.4**. 5 ml dope was prepared at 10% and 20% polymer w/v in 50 mM AcOH. Both dopes were pre-heated to 55°C. Six coagulation baths were prepared; bath 1 contained follows the salt-based bath as described in Rickman et al. [307] 20% w/v PEG 8000, 80% w/v 0.1M PBS solution, and 20wt.% NaCl in a total ratio of 1:1:4 [61][444][443][307]. Baths 2 contained 100% IPA, and bath 3 contained 100% EtOH. Herein referred to by its source as ”Rickman et al., 2019”. All six baths each contained 20 ml of liquid and were all held at room temperature. A single droplet of each dope was pipetted into each bath and left to coagulate. This gel-sol reaction was timed (seconds, s). Following coagulation, each bath was visually assessed to determine whether droplet coagulation had been achieved. The droplet would then be removed from the bath using a pair of stainless-steel tweezers, and the process was repeated to ascertain an

Table 3.4: *Experimental conditions considered to determine the compatibility of different coagulation solutions with Gel-4VBC dope.*

Dope	Coagulation bath	
10% Gel-4VBC*50mMAcOH	Bath 1a	*Rickman et al., 2019*
	Bath 2a	IPA
	Bath 3a	EtOH
20% Gel-4VBC*50mMAcOH	Bath 1a	*Rickman et al., 2019*
	Bath 2a	IPA
	Bath 3a	EtOH

average coagulation time (**Table 3.4**). IPA and EtOH were investigated as potential coagulation baths as they are both organic solvents that are unable to form hydrogen bonds with the charged groups in the gel-4VBC. Because of this, the polymer will remain unstable and clump together, enabling the phase transition from gel to solid fibre.

3.5.2 Effect of Coagulation Bath Temperature on Rate of Phase Transition

The effect of coagulation bath temperature was investigated. Several WS studies had noted holding the solvent-non-solvent solutions below freezing [116][333][269][307]. The purpose of cooling the coagulation baths was to examine how lower temperatures might impact the phase transition and fibre formation during the WS process; a decrease in coagulation bath temperature has been shown in previous studies to influence the morphology and properties of the resulting fibres, such as by promoting the formation of macrovoids and altering the porosity [18][204][307][445]. Each 15 ml coagulation bath (as previously described in **Table 3.4**) was set in an ice bath for 10 minutes prior to the drop tests being carried out, to allow the solution temperature to cool. Coagulation baths would remain in the ice bath throughout the experiment. Using a 20% gel-4VBC w/v dope, the drop tests were repeated (**Table 3.5**).

Table 3.5: *Experimental conditions to test the effect of decreased solvent temperature on rate of coagulation.*

Dope	Coagulation bath	
20% Gel-4VBC*50mMAcOH	Bath 1	*Rickman et al., 2019*
	Bath 2	IPA
	Bath 3	EtOH

3.6 Optimisation of Gel-4VBC Fibres and Lab-Scale Wet Spinning Rig

The following experiments describes optimisation of methodologies within the extrusion and coagulation [of fibres] stages of the WS process. The feasibility of fibre spinning, and the recycling of coagulation solvent are also considered. The drawn fibres are then subjected to UV-crosslinking to enhance their mechanical and chemical stability. Optical microscopy, mechanical testing, and SEM are employed to characterise the fibres' water uptake, stress-strain behaviour, and morphology, respectively. The wetting and heating of the fibres are finally investigated to assess their performance under physiologically-similar conditions. By following this comprehensive methodology, the research aims to develop UV-cured gelatin-4VBC fibres with optimised properties for use in various biomedical applications, such as tissue engineering scaffolds, wound dressings, and drug delivery systems.

3.6.1 Feasibility of Fibre Spinning

Initial WS experiments were first carried out using a 0.2 ml pipette tip with an internal needle diameter of 1 mm, attached onto a 24 ml syringe (**Figure 3.4**). The dope was prepared with a polymer concentration of 20% in 50 mM concentration AcOH. The dope was held at 55°C until the polymer was fully dissolved, where it was transferred to the 24 ml syringe. To minimise the risk of needle blockage during spinning, the pipette-tip needle was inserted into the coagulation bath (maintained at 1°C in an ice bath) at a 45° angle, and dope was manually extruded into the solution. Resultant short fibres were incubated in the coagulant for two minutes before being removed from the solution. Fibres

were then wound around a glass rod covered in parafilm and left to air dry.

3.6.2 Needle Gauge

Various needle gauges (G) were explored to determine the most successful fibre size. Blunt-tipped luer lock needles with a length of 50 mm were investigated in a range of lumen sizes; 16G, 18G, 20G, and 21G (purchased from Science Warehouse) Fibre bundles were spun using a RWS set-up and incubated in the coagulation bath for 30 seconds, before they were removed from the bath and air-dried. The dope used contained 20 wt.% gel-4VBC dissolved into 50 mM AcOH. The dope did not include I2959 to evaluate the properties of the fibres before curing. This omission allowed for an assessment of the fibre properties in their uncured state, as the crosslinking network formed during the curing process tends to make the fibres more brittle. These mechanical properties were assessed visually and in terms of fibre handleability.

3.6.3 Pumping Speed

Pumping speed was assessed to determine flow rate of the dope through the needle and into the coagulation solution. The successful pumping speed for the WS process will be defined as a flow rate that is simultaneously fast enough to maintain a continuous, uninterrupted flow of the polymer dope through the spinneret, but slow enough to avoid producing excessive back pressure within the system. Dope was extruded using an automated syringe driver (purchased from Science Warehouse) for 3 minutes and the rate was decreased from 3.00 ml/min down to 1.2 ml/min. Dope flow behaviour and back pressure was noted before the experiment was repeated at a speed 0.2 ml/min slower. The speed increments have been specified in **Table 3.6**. Pumping speed was assessed to determine flow rate of the dope through the needle and into the coagulation solution during the WS process. These parameters are crucial for maintaining a continuous, uninterrupted flow of the dope through the spinneret while avoiding excessive back pressure within the system. To achieve this, they extruded the dope using an automated syringe driver for 3 minutes, gradually decreasing the flow rate from 3.00 ml/min to 1.2 ml/min and observing the dope flow behaviour and back pressure at each step; in order to identify the optimal pumping speed that meets the desired criteria for the WS process. Preliminary WS studies were carried out prior to this experiment, with a pumping speed of

Table 3.6: *Experimental pumping speeds to determine most compatible flow rate using a 21G needle.*

Dope pumping speed steps (ml/min)
3.00; 2.80; 2.60; 2.40; 2.20; 2.00; 1.80; 1.60; 1.40; 1.20

0.5 ml/min as informed by Rickman et al. [307], (stating a pumping speed of 30 ml/h), however a continuous and unbroken dope stream could not be achieved; hence, exploring faster flow rates into the coagulation bath. Rationale for this are discussed in greater detail in **Chapter 4**.

3.6.4 Rotational Drawing

A rotating coagulation bath (previously illustrated **Figure 2.8**) was explored to overcome limitations related to using a stationary bath with the needle inserted at a 45°. The dope was prepared with a polymer concentration of 20% in 50 mM concentration AcOH. The dope was held at 55°C until the polymer was fully dissolved, where it was transferred to the 24 ml syringe. During WS, the syringe driver was rotated 90° and raised on a jack stand. The needle was inserted vertically into the bath, 10 mm from the bath's edge. The tip held 10 mm below surface of the solution. During extrusion of the fibre, the bath was rotated within the ice bath, applying a slight tension to the fibre as it was drawn from the needle. A 50 ml cylindrical glass bath (sitting within a 250 ml ice bath) was used to hold the coagulation solvent . The cylindrical shape of the dish permitted rotation of the coagulation bath during spinning. Fibre bundles were gathered at the bottom of the bath before they were removed, unravelled, and cured.

3.6.5 Temperature

A decreased coagulation bath temperature was previously investigated in **Section 3.5.2** to investigate the effect of decreasing temperature on the rate of phase transition. Now, as part of s WS set-up, this decreased temperature of the coagulant was explored in combination with an increased temperature of dope. A syringe heating sleeve (purchased from Science Warehouse) was used to hold the syringe containing the polymer dope at a constant temperature of 65°C throughout the spinning process. Heated dope was

extruded into the coagulation bath held over ice. This was repeated with a dope held at room temperature (no heating sleeve), and spinnability was compared between the two dope temperatures. It was noted that in Rickman et al. [307], the polymer dope was maintained at 50°C prior to extrusion. A higher holding temperature of 65°C was selected in order to mitigate any potential adverse effects from additional factors such as the coagulation ice bath, and the increased polymer wt.% in the dope; from 15 wt.% in Rickman et al., 2019, to 20 wt.% in this experiment.

3.6.6 Recycling Coagulation Solvent

During coagulation diffusional exchange of solvents takes place, whereby the dope solvent diffuses out of the fibre, and is replaced by the coagulant solvent, initiating the phase transition from gel to solid. To maintain fibre quality, the total amount of dope that could be coagulated by a known quantity of coagulant solution was qualitatively assessed. A syringe containing gel dope was held at 55°C. Fibres were spun at a pump speed of 0.6 ml/min, using the rotation-assisted method (as described in **Figure 2.8**) into a 100 ml coagulation bath containing IPA on ice. The WS was paused every 60s and the fibre was visually examined, following incubation in the coagulation bath for 20 s. This process was repeated until the quality of fibre and rate of coagulation (solvent diffusional exchange) decreased. Once it was determined that fibre quality had decreased, all dope remaining in the syringes was decanted into a measuring cylinder. The quantity of remaining dope (in ml) was subtracted from the original amount of dope to calculate how much dope could be spun in 100ml of IPA.

3.7 Fibre Drawing and UV-Crosslinking

The following experiments describes optimisation of methodologies within the post-spinning-treatment stage of the WS process. The impacts of both extension (drawing) and UV-crosslinking were investigated simultaneously (**Table 3.7**). Fibres were spun using a 21 G needle, with a 0.3 ml/min pumping speed, into a rotating coagulation bath containing EtOH. Fibres were incubated for 10 seconds before they were loaded into an Instron 3365 (Oral Biology, St James' Hospital, Leeds). The internal boundaries of the fibre clamps were set 50 mm apart so that a 5 cm length of fibre could be drawn. Using

Table 3.7: *Experimental conditions investigating the simultaneous effects of fibre drawing and UV-curing on fibre properties.*

Percentage increase in length during fibre drawing	Curing duration (hh:mm)
25 %	00:01; 00:15; 00:30; 00:45
50 %	
75 %	
100 %	

Bluehill Universal Software, the draw speed was set to 25 mm/min and extension was set to 12.5 mm to allow for a 25% extension from the fibre's original length. Following this, fibres were spun under the same conditions as above, and extended by 25mm (a 50% length increase), 37.5 mm (75%) and 50mm (100%) (40 fibres total) (**Table 3.7**). 10 replicate fibres were produced for each condition. Dry fibres were placed on a dry glass petri dish and exposed to UV light with a wavelength of 365 nm and an intensity of 8 mW·cm-2. All fibres were cured for 1 minute. Mechanical testing (**Section 3.9**) was carried out on all fibres. This process was repeated four times with the curing duration increased up to 45 minutes (**Table 3.7**). The purpose of these experiments was to determine the optimal drawing and curing conditions, and to compare the uniformity of fibre repetitions within each condition. In simultaneously investigating the effects of both extension (drawing) and UV-crosslinking, the author aimed to understand how these two key processing steps interact to influence the final properties of the Gel-4VBC fibres.

3.8 Optical Microscopy

Craft card (purchased from the University of Leeds Student Union) was cut into 3-6 cm rectangles, with a 20mm diameter circle cut in the centre of each piece. These rectangle cards acted as a mounting frame for spun fibres (**Figure 3.5**). Individual dry fibres were attached to each rectangle, first with double-sided-tape and reinforced with Sellotape. Each frame was placed onto the specimen stage of a Leica M205C Light Microscope (Nonwovens Laboratory, School of Design) and magnified to x50. Digital microscope images were taken of each fibre. Following this, each mounted fibre incubated in DI water at 40°C for 5 minutes immediately before reloading them onto the specimen stage

and reimaging. The fibre diameters (and subsequently, the cross-sectional area) were obtained using ”ImageJ” software. This was done by using the features ”Analyse $>$ Set Scale” to calibrate the pixel dimensions to real-world units; followed by ”Analyse $>$ Measure” to obtain the area and other measurements of the selected fibre diameter. The water was held at that slightly higher than the human body's internal temperature, so to mimic physiological conditions.

3.8.1 Calculating Water Uptake

The swelling index (SI) of the fibres was determined as the percentage increase in cross-sectional area following to the incubation of the samples with water. The following equation was used:

$$SI = 100 * \frac{x_s - x_d}{x_d} \tag{3.3}$$

Where *SI* is the swelling index, x_s is the wet diameter, and x_d is the dry (original) diameter.

3.9 Mechanical Testing

Following microscopy of wet samples, mounted fibres were re-incubated in DI water for a further 2 minutes and loaded onto the Instron 5544 (Universal Strength Tester, School of Design, University of Leeds); using a $< 5N$ load cell. Mechanical testing was carried out in accordance with section 7 of the ISO 5079:2020 [368]; which dictates for filament fibres, the distance between the two clamping points (gauge length) should be 20 mm. This was measured using a caliper. The internal boundaries of the jaws would align with the circle boundary of the card fibre mounts, which also acted as a protective barrier to minimise fibre breakage at the clamps. Fibres that broke during clamping were excluded from results. Once loaded, the gauge length was set to zero on the Bluehill Universal software. The rate of extension was set to 25 mm/min and would continue to apply tensile load until mechanical failure of the fibre. The rate of extension between the Instron clamps for both the aforementioned drawing of wet fibres (**Section 3.7**), and during mechanical testing were set to the same speed. In maintaining the same rate of exten-

sion/strain rate during both the wet fibre drawing and mechanical testing stages ensures consistency in fibre microstructure, deformation behavior, and avoids potential structural changes, ultimately enabling accurate and reproducible measurement of the mechanical properties resulting from the specific drawing conditions [182]. The yield point is the stress value at which a material transitions from elastic deformation to plastic deformation. It marks the onset of permanent deformation of the fibre. On a stress-strain curve, this is identified as the region where the curve starts to deviate from its linear progression. The ultimate tensile strength (UTS) is the highest point on the stress-strain curve indicating the maximum stress a material can withstand before it deforms/ruptures. Beyond this point, the material experiences mechanical deformation and failure.

3.9.1 Stress and Strain

The stress value for each fibre was calculated using **Equation 3.4**.

$$\sigma = \frac{F}{A} \tag{3.4}$$

Where σ is the Stress value (Nm-2 or Pa), *F* is the applied force (mN) at mechanical failure, and *A* is the cross-sectional area (μm_2).

The strain value for each fibre was calculated using **Equation 3.5**.

$$\epsilon = \frac{\Delta l}{l_0} \tag{3.5}$$

Where: ϵ is the Strain value, Δl is the change in length (mm), recorded as the fibre length at mechanical failure, and l_0 is the original fibre length (mm). Using MATLAB, the mean stress value for each condition was plotted along the y-axis, and mean strain along the x-axis. From here the yield point (plastic deformation) and UTS could be ascertained.

The relationship between stress and strain was calculated using the following equation,

$$E = \frac{\sigma}{\epsilon} \tag{3.6}$$

Where E is the relationship between stress and strain, σ is the strain value, and ϵ is the Stress value.

3.10 Wetting and Heating Drawn and Cured Fibres

RWS fibre bundles were investigated using the same methodology set out previously in **Section 3.4**. In this experiment, two RWS fibre bundles were spun, dried and cured for 30 minutes in a cure box (Chromato-Vue C-71). Both fibre bundles were weighed as dry samples, before being incubated in separate water baths containing 200 ml DI water and placed into a 37°C oven. One bundle was incubated under these conditions for a 24-hour period, while the second was left to incubate for a 30-day period (one month). Once the incubation period was up, each bundle was removed from its water bath, excess water was removed, and the sample was re-weighed in its semi-dry state. A percentage increase in weight was calculated using **Equation 3.3**.

3.11 Scanning Electron Microscopy

Fibre surface texture was examined using SEM (School of Chemistry, University of Leeds). Imaging was conducted at a magnification of x40, and image analysis and quantification of fibre diameter distribution were performed using ImageJ software.

3.12 Chapter Conclusions

The WS process has been broken down into four key stages; dissolution, extrusion, coagulation, and post-spin treatments; with the view to systematically investigate and optimise each of these key stages. The aforementioned experimental methods described within this chapter were designed in order to answer **Objective 3** (**Section 1.3**) of this research project, which was to carry out fibre optimisation processes with a view to improve fibre properties and morphology.

Chapter 4

Results and Discussion

4.1 Chapter Introduction

This chapter presents the results of experimental conditions set out in Chapter 3. As previously discussed, this body of research looks to present the development of wet spun, UV-cured, functionalised gelatin fibres; building on previous research by Rickman et al. [307]. The following results are presented in the following order: optimisation of polymer dope (**Sections 4.2** to **4.4**), coagulation (**Section 4.5**), optimisation of WS rig, (**Section 4.6**), and post-spin optimisation and analysis (**Sections 4.7** to **4.8**).

The key objectives investigated in this chapter are to determine the feasibility of (a) f-gelatin as a bioresceptive material (**Objective 2**), (b) manufacturing UV-cured Gel-4VBC filament fibres through WS methodologies at a laboratory-scale (**Objective 3**), and (c) conduct a systematic optimisation of the fibre production processes, aimed at enhancing the structural and functional characteristics of the resulting fibers (**Objective 4**).

4.2 2,4,6-Trinitrobenzene Sulfonic Acid Colourimetric Assay

The TNBS colourimetric assay was used to indirectly evaluate the modification of lysine amino groups in gelatin through the addition of 4VBC. The results of the reaction

(as specified in **Section 3.3.2**) indicated successful functionalisation of the PSG to form gel-4VBC, with functionalisation degrees of 86.74%. TNBS assays were conducted on different batches of gel-4VBC throughout this project's duration (results in **Table 4.1**, and a mean standard deviation of ±2.59. These results align with research presented in Hoch et al. [140], Rickman et al. [307] and Tronci et al. [378]. Degree of functionalisation was higher in the gel-4VBC presented in this research, in comparison to rat's tail T1C-functionalised-4VBC as previously reported in Tronci et al. [377] and Rickman et al., [307]; and this has been attributed to the thermal denaturisation of the triple helix, enhancing the polymer's chemical accessibility [268].

Table 4.1: *TNBS colourimetric assay absorbance peaks, where 'L' is the Free lysine content and 'Y' is the yield of functionalisation. Results shown to three decimal places*

Batch	Mean F	SD (±)
Native PSG	0	2.3.44
Gel-4VBC Batch 1	83.420	2.74
Gel-4VBC Batch 2	89.729	1.83
Gel-4VBC Batch 3	87.06	3.89

4.3 Dope Optimisation

4.3.1 Polymer Dissolution in Acetic and Hydrochloric Acids

Both AcOH and HCl was investigated as potential dope solvents. Rickman et al. [307] has previously shown the compatibility of AcOH with gel-4VBC when the polymer was dissolved into a concentration of 17.4mM [307]. Employing a slightly higher molar concentration, 20 wt.% gel-4VBC was dissolved into 50 mM AcOH. Molar concentration was increased from the methodology proposed in Rickman et al. [307] to control and prevent the gel dope from congealing and clotting at room temperature. This dope was compared to a 20 wt.% gel-4VBC dissolved into 50 mM HCl. While HCl has not been explicitly used as a dope solvent for gel-4VBC, many researchers have used very low concentrations of HCl to dissolve collagen-based materials in other biomedical applications [187]. No significant difference in dope consistency or later compatibility with coagulation solvents (during drop tests or spinning) was detected from a vi-

sual/handleability perspective. AcOH was ultimately selected for continued use during this project.

Within the context of producing fibres that would be theoretically safe for use *in vivo*, AcOH is relatively biocompatible and can be cleared from the body through normal metabolic pathways. In contrast, HCl is a strong inorganic acid that would be highly cytotoxic, corrosive, and incompatible with biological systems. Regarding the manufacture of biomaterials for healthcare applications, AcOH is also relatively stable and can be lyophilized/freeze-dried for long-term storage, making it suitable for commercial manufacturing and regulatory approval for biomaterials and pharmaceuticals [191].

4.3.2 Photoinitiator: I2959 in Dope vs Coagulation Bath

I2959 was investigated as both a dope component and coagulation solution component. In Rickman et al., [307] researchers dissolved the curing agent into the coagulation bath, which held the fibres for an hour during the incubation period. It was found that I2959 could dissolve into both the dope and EtOH. This finding raised questions followup questions as to whether it might be more beneficial to dissolve I2959 in the dope OR in the coagulation solvent.

I2959 photoinitiator is a compound that is sensitive to UV light and when activated, initiates the formation of a chemical crosslink network within the material, in a process is called polymerisation [373]. As the polymerisation reaction progresses, the material changes from a liquid or gel-like state to a solid, hardened state. When activated by UV light, typically at a wavelength of 365 nm, I2959 breaks down into two free radicals: a benzoyl radical and an alkyl radical [373]. These free radicals react with, and crosslink monomers or polymers that contain reactive groups, such as methacrylate groups [373], to form a stable network of crosslinks. I2959 is preferred for biomedical applications due to its moderate water solubility, low cytotoxicity, and minimal immunogenicity compared to other photoinitiators [100].

Three methods of integrating I2959 into fibres was investigated. Initially, dissolvability of 2 w/v.% I2959 in 10 ml DI water, EtOH and AcOH was established. Following confirmation of solubility, a water-based curing bath containing 2 wt.% I2959 was ex-

plored. Gel-4VBC fibres were spun from a gel-4VBC/50 mM AcOH dope into a EtOH coagulation bath. Following a successful phase transition, fibres were transferred to a supplementary curing bath containing DI water containing 2 w/v.% I2959. **Figure 4.1** shows the quick dissolution of fibres during the curing process when placed in this water-based curing bath. Following this, 2 w/v.% I2959 was dissolved in EtOH to act as a single coagulation-curing bath. While this seemed to work, the fast rate of coagulation (in comparison to findings in Rickman et al. [307]) made it that WS fibres would have to remain in the coagulation bath for a prolonged duration of time (up to 30 minutes) during the curing process, causing fibres to over-coagulate and become extremely brittle once removed from the bath. While this process of introducing a PI into the f-gelatin fibres, was not successful in producing fibres with good handleability, cured fibres displayed good wet stability when placed in a water bath for 20 minutes.

Finally, 2 w/v.% I2959 was dissolved into the dope, spun, dried, and cured. This method enabled the fibre formation and quick removal from the coagulation solvent (preventing extreme brittleness). This process involved dissolving 2 wt.% I2959 into the dope (in glassware covered in tin foil so to prevent natural/UV light from prematurely activating the UV-curing process). Light was further prevented from initiating crosslinks in the

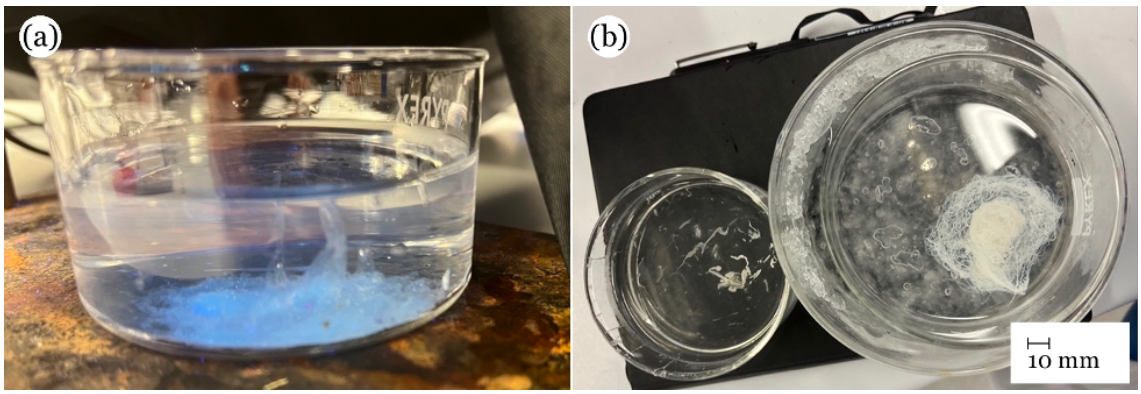

Figure 4.1: *(a) Dissolution of gel-4VBC fibres in a water-based curing bath containing 2% wt.% I2959. Photo taken inside the curing box following 60 seconds of incubation in the curing bath; and (b) behaviour of fibre bundles spun from a dope containing 20% gel-4VBC in DI water with no curing (left bath), and 30 minutes in a cure box (right bath). A curing bath of 2% I2959 dissolved into IPA was used to integrate the photoinitiator into the fibres. Scale bar is applicable for both images.*

gel dope in the syringe as it was covered in the heating sleeve. Following extrusion and phase transition, fibres would be left to air dry for 5 minutes before being transferred to a UV-cure box (chromate-Vue C-71, Oral Biology, St James' Hospital, Leeds), and irradiated at 365 nm for 30 minutes. It was concluded that by integrating I2959 into the dope (as opposed to the coagulation solution or as a supplementary bath) produced the highest quality fibres with regards to flexibility and handleability. This is likely due to the in-situ crosslinking of the fibres during the WS process, which can help stabilise the fibre structure and improve the mechanical properties, such as flexibility and handleability, compared to post-treatment approaches [307]. Integrating I2959 into the dope also ensures a more homogeneous distribution of the photoinitiator throughout the fibres, leading to more uniform crosslinking and enhanced mechanical performance [307]. In contrast, adding I2959 to the coagulation solution or as a supplementary bath after spinning may result in less efficient crosslinking and potentially uneven distribution of the photoinitiator within the fibres [307].

4.4 Determining Dope thermal and Wet Stability

Photoactive covalent bonding was investigated so to assess the benefits of chemical and UV crosslinking, both separately, and in combination. As defined in **Section 3.4**, four dopes were prepared; the first dope, containing only Native PSG dissolved into 50 mM AcOH, acted as the control sample. The remaining dopes, Native PSG with 2 wt.% I2959, gel-4VBC, and gel-4VBC with 2 wt.% I2959 were all dissolved in the same 50 mM AcOH as the control. The two separate samples containing Native PSG with 2 wt.% I2959 and gel-4VBC sought to assess the stand-alone effects of chemical crosslinking in comparison to UV-crosslinking. Furthermore, these were used in conjunction for the final (gel-4VBC with 2 wt.% I2959) sample to evaluate these properties in tandem. Initially, dry samples (20 mm2 squares, 3 mm thickness) of each dope were placed into an oven set to 37°C and 60°C ovens and visually assessed every 15 minutes for the first hour (**Figure 4.2**). Samples were then incubated for a further 24h and visually assessed. The 37°C oven was selected as this project focuses on the production of gelatin-based fibres that can survive within the human body. The 60°C oven was selected to ensure that the fibres would be able to withstand significantly higher temperatures- proving the

dope's feasibility of survival (on a purely chemical level) within the body.

Other than the Native PSG sample (**Figure 4.2i**) in the 60°C (where a slight softening of the sample was observed), there was no change between the control dry samples and the samples incubated at high temperatures for 24h in both ovens. Photographs of all samples, prior to, and after heating for 24 hours, have been presented in **Figure 4.2**. It may be worth noting the differences in surface texture between the samples containing I2959 (**Figures 4.2c, d, g, h**), and the samples that did not contain the curing agent (**Figures 4.2a, b, e, f**). Samples containing I2959 exhibited a rougher, matte surface quality and appeared to be opaquer in appearance. As the samples containing no I2959 were translucent in appearance, this opacity may indicate the formation of crosslinks, as these samples had already gone through the UV-crosslinking process. As could be expected, both samples containing gel-4VBC (**Figures 4.2a, b, c, d**) were more saturated in colour when compared to the native PSG. This is due to the yellow colour of chemical 4VBC, which binds to the gelatin molecule during the functionalisation process. As shown in **Figure 4.2**, no colour change was observed in any sample following heating, regardless of duration or oven temperature, indicating dry stability across all four samples.

This body of research, however, looks to produce gelatin fibres that would be stable within the human body. To mimic this *in vitro*, all samples were incubated in 10ml DI water and returned to their respective ovens. Findings of this experiment have been presented in **Figure 4.3**. After 15 minutes, no real changes were observed in the 37°C oven in any sample; however, significant dissolution of the gel-4VBC (**Figure 4.3c**) and Native PSG (**Figure 4.3k**) samples were observed in the 60°C oven after only 15 minutes. During this initial 15 minutes, sample thickness had decreased the most in the native PSG (**Figure 4.3k**, 60°C), followed by the gel-4VBC (**Figure 4.3c**). Similar findings were found in the dopes containing no I2959 in the 60°C oven. For each sample, 5 thickness measurements were taken in mm with digital calipers, and the mean was calculated. These mean thicknesses have been presented in **Table 4.2**. Due to the dissolution of I2959 into the dopes, the gel-4VBC + 2% I2959 and the native PSG + 2% wt.% I2959, were the least affected by heating in both the 37°C and 60°C ovens.

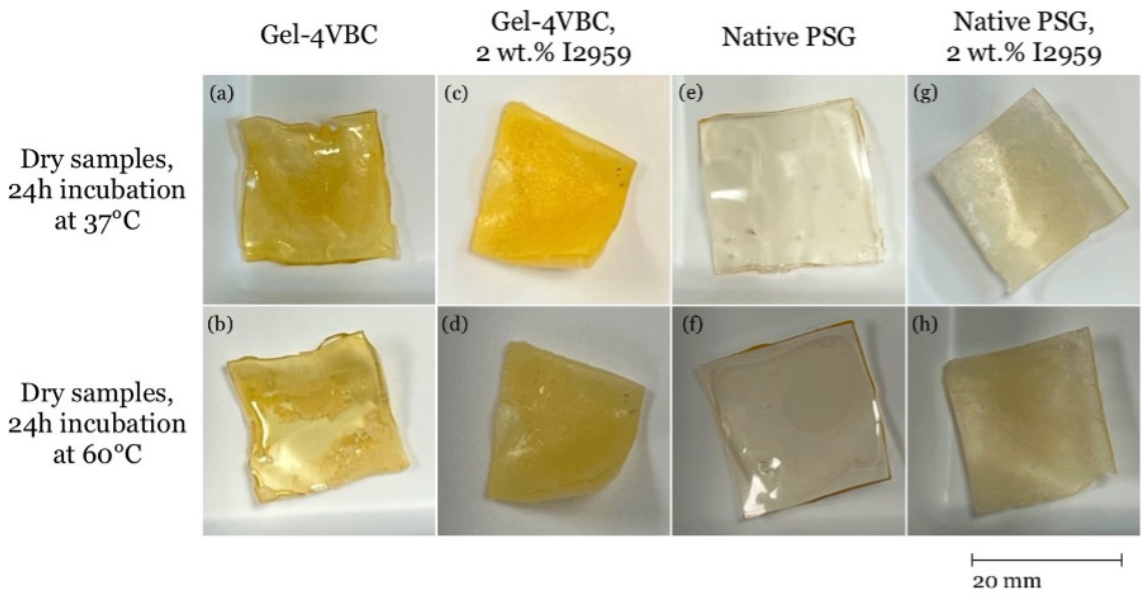

Figure 4.2: *Images showing change in surface texture of dry gelatin samples after incubation.*

4.4.1 Native PSG Control Sample

As the control dope, the native PSG polymer reacted poorly to wet heating in both oven temperatures. Of all samples heated to 37°C, the native PSG sample has the most significant decrease in thickness after 15 minutes (-0.249 mm from original thickness) and greater still after 60 minutes (-0.681 mm from original thickness). At 37°C, general structural integrity was maintained after 60 minutes, however the reduction in thickness indicated significant dissolution of the gel into the surrounding water. Similarly, to the sample heated to 37°C, the sample heated to 60°C experienced the most considerable decrease in thickness after 15 minutes (-0.9 mm from original thickness) and 60 minutes (-2.54 mm from original thickness). The sample had also completely stuck to the plastic sheet after 60 minutes and had returned to its liquid gel-state (in comparison to samples containing a UV-crosslinking agent, which were able to maintain their solid state). The high susceptibility of native PSG to water and thermal degradation is likely due to the lack of free radicals (that can form covalent bonds between gelatin chains) or aromatic rings, present in further enhancing the thermal and water stability of the material.

4.4.2 Effect of 4VBC Crosslinking Only

In the gel-4VBC heated to 37°C (**Figure 4.3a**), some slight puckering was observed around the edges of the sample and some dissolution (indicated by a slight-yellowing

Table 4.2: *Wet sample thickness measurements in mm to 3 decimal points.*

Sample	Starting thickness	00:15 incubation at 37°C	01:00 incubation at 37°C	00:15 incubation at 60°C	01:00 incubation at 60°C
Gel-4VBC	3.003	3.001	2.871	2.498	1.674
Gel-4VBC, 2 wt.% I2959	3.004	3.004	3.003	3.004	3.002
Native gelatin	3.005	2.756	2.324	2.105	0.465
Native gelatin, 2 wt.% I2959	3.004	3.002	2.997	2.994	2.898

of the surrounding water) was evident; however, there was no real change in overall thickness (-0.002 mm). The sample developed a tacky surface following 60 minutes incubation at 37°C, however the sample still maintained overall form. When heated to 60°C (**Figure 4.3c**), a reduction in thickness of 0.505 mm was observed (when compared to the original thickness taken at room temperature) in the first 15 minutes. After 15 minutes of incubation at 60°C (**Figure 4.3c**), a reduction of 0.505 mm thickness was observed (when compared to the original thickness taken at room temperature). As could be expected, after 15 minutes, the sample in the 60°C was evidently dissolving at a faster rate than the sample incubated at 37°C (**Figure 4.3a**).

The sample dissolved at a faster rate when compared to the sample at the same time step in the 37°C oven, had become fixed to the plastic sheet it was placed on, and an air bubble had started to form. Following 60 minutes incubation, significant bubbling of the surface was evident, and a considerable amount of the sample had dissolved into the surrounding water. The sample's thickness had reduced by a further 0.824 mm (-1.329 mm total reduction) and could not be removed from the sheet without damaging the sample further. Overall findings of the gel-4VBC sample indicates that chemical crosslinking (4VBC onto the gelatin) alone is not sufficient for a dope/gel to withstand the physiological conditions present within the human body. For each sample, 5 thickness measurements were taken in mm with digital calipers, and the mean was calculated.

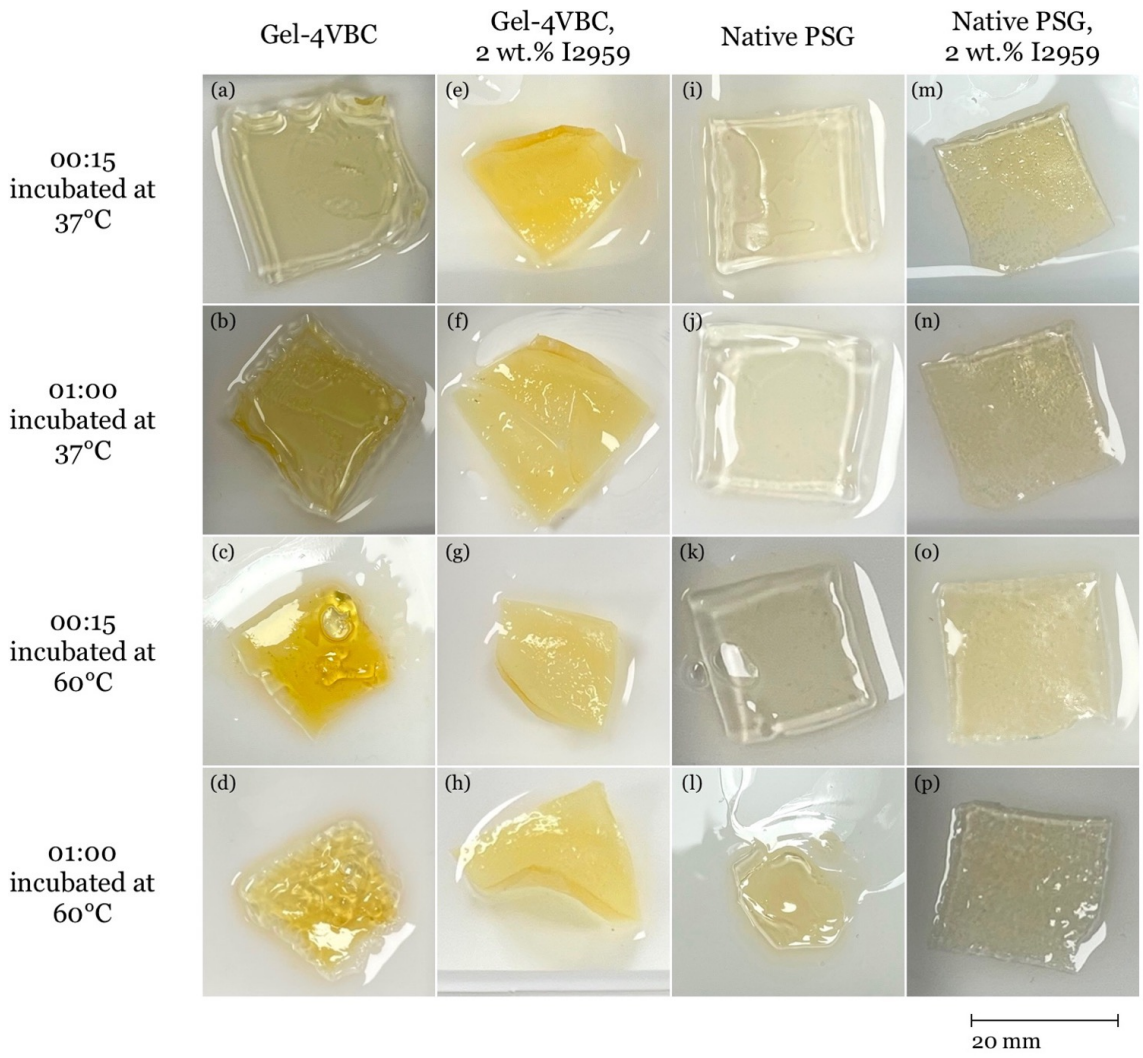

Figure 4.3: *Wet gelatin samples after 15 and 60 minutes.*

4.4.3 Effect of UV-Crosslinking Only

To investigate the sole effects of UV-curing, 2 wt.% I2959 was dissolved into a dope containing native PSG and 50 mM AcOH. As no chemical crosslinking of the gelatin polymer had been carried out, this sample was not expected to be wet stable at increased temperatures; however, proved to be the second-most successful sample after gel-4VBC + 2 wt.% I2959. In the 37°C oven, no significant differences in thickness were observed after 15 minutes (-0.002 mm), and only a reduction of -0.007 mm after 60 minutes. Structurally, the sample remained intact throughout the experiment and did not stick to the plastic surface as opposed to the gel-4VBC and Native PSG samples.

In the 60°C oven, a reduction of -0.01 mm was observed after 15 minutes at 60°C and

a further -0.096 mm after 60 minutes (totalling -0.106 mm). After the 60 mins heating, however, the sample was significantly tackier in comparison to the gel-4VBC + 2 wt.% I2959 sample; and while the sample had not become fixed to the plastic sheet (as with the case of the two dopes not containing I2959), it was slightly sticker than the gel-4VBC + 2 wt.% I2959 sample.

4.4.4 4VBC/UV Combination Crosslinking

Both forms of polymer crosslinking were investigated in tandem in the final dope sample. Here, 2 wt.% I2959 was dissolved into a dope containing 20 w/v gel-4VBC in 50 mM AcOH and cured for 30 minutes. After 60 minutes in the 37°C oven, A reduction in thickness of only -0.001 mm was observed. This change in thickness was not deemed to be a significant, indicating good wet and thermal stability. No dissolution of the gel into the surrounding water was observed at any point.

No significant changes were observed between the sample heated to 60°C and the sample heated to 37°C. Even after 60 minutes at the higher temperature, no dissolution or reduction in structural integrity was observed. In both ovens, the sharp edge (produced from slicing the samples with a medical-grade scalpel, St James' Hospital, Leeds) was maintained, proving the preservation of shape. A reduction in thickness of -0.002 mm was observed in the sample heated at 60°C for 60 minutes. This was not deemed a significant reduction. Unlike the sample containing native PSG and I2959, the combination sample (gel-4VBC + 2 wt.% I2959) did not present any change in surface texture as a result of thermal degradation. This stability under the applied conditions was exemplified by the gel-4VBC + 2 wt.% I2959 sample's ability to maintain a distinctive boundary edge (**Figure 4.3e, f, g, h**), whereas the samples that had only undergone chemical crosslinking (**Figure 4.3a, b, c, d**) and the control samples (**Figure 4.3i, j, k, l**) presented significant dissolution around the sample boundaries. This shape integrity was also observed in the native PSG + 2 wt.% I2959 sample to an extent.

4.4.5 Discussion on Dope Characterisation

Findings indicate that chemical functionalisation of gelatin is not enough to enable both wet and thermal stability. Within the context of this research, these are imperative qual-

ities in ensuring the survival and longevity of WS gelatin fibres within homeostatic conditions. The wet/thermal stability of the native PSG + 2 wt.% I2959 was a surprising result as it was previously hypothesised that the polymer would be somewhat unstable due to the hydrophilic nature of the material. As previously mentioned, when exposed to UV light, I2959 binds the polypeptides via photo-crosslinks which create a network that traps and immobilises water molecules, rendering the gelatin water-insoluble. Overall, both dopes containing I2959 were the least affected by wetting and heating (in terms of overall resulting thickness), with the gel-4VBC polymer generally performing the best under the set conditions.

4.5 Dope Compatibility with Coagulation Solutions

This section of results specifically focuses on optimisation of the chemical solutions used in the dope and coagulation bath. Chemical compatibility plays a critical role in WS for several reasons. Firstly, compatibility between the dope solvent and the solvent-non-solvent (coagulant) influences the coagulation process, ensuring that the transition from a liquid solution to solid fibres occurs efficiently and produces the desired properties. Secondly, it enables control over the phase transition that occurs during coagulation, preventing any undesirable chemical reactions or by-product formation as the solvent in the polymer solution rapidly exchanges with the non-solvent in the coagulation bath. These factors collectively contribute to the production of biopolymer fibres, the efficient use of materials, and the safety of the manufacturing environment in WS.

4.5.1 Drop Tests: Varying Polymer Concentrations in Coagulation baths

Drop tests carried out using both 10% and 20% w/v Gel-4VBC in AcOH in three coagulation bath solutions. These have been specified in **Table 3.4**, following the methodology set out in **Section 3.5.1**, and results have been presented in **Table 4.3**. A 0.2 ml pipette tip was fixed to a 15 ml syringe containing the dope; and single droplets were allowed to form and fall into each coagulation bath (room temperature). Coagulation was timed from the point of the drop hitting the bath and was judged visually and physically (using point-tipped tweezers). The initial formation of gel droplets is characterised

by the formation of a dope droplet in a semi-gelled, but reversible state. These semi-coagulated droplets, once removed from the coagulation bath, revert to a fully gelled state because their structural integrity relies on the presence of the non-solvent bath. Under room temperature conditions, it was difficult to form a solid dope droplet in the salt-based bath as described by Rickman et al. [307]. The results from this experiment show that while the polymer did not disperse out into the bath (remaining somewhat intact), no successful phase transition (gel-sol) was achieved, indicating a reversible-gelation state. The results of these drop tests are depicted in **Figures 4.4a** and **4.4d**. Both EtOH and IPA produced quick gel-sol reactions in droplets for both polymer w/v conditions.

Droplets appeared to shrink more when 10 wt.% gel-4VBC was used as opposed to the higher polymer wt. dope in both the IPA and EtOH coagulation baths. This is likely due to a larger quantity of solvent (50 mMAcOH) undergoing diffusional exchange. No difference was observed when the same wt.% dope was used in IPA or EtOH. The author theorised this similarity in drop test results to be likely due to the chemical similarities in between the two solvents. EtOH and IPA are both alcohol compounds that share similar commercial uses, including being solvents, disinfectants, and having antiseptic properties [24][134]. They both evaporate quickly, are flammable, used in pharmaceuticals, and possess polar properties (allowing them to function as dehydrating agents) [253]. In addition, both substances are similar in chemical structure: C2H5OH (EtOH) and C3H7OH (IPA).

Overall, the results of the drop tests indicate that both IPA and EtOH are very effective as coagulant solvents. Upon visual and physical examination of dope droplets, no differences in characteristics, size, shrinkage, hardness, etc. could be detected. In contrast to findings by Rickman et al. [307], the salt-based coagulation bath (**Figure 4.4a** and **4.4d**) did not produce successful droplets, indicating that a gel-sol phase transition could not be achieved within a 5-minute incubation period. Coagulation times have been presented in **Table 4.3**, showing the differences in droplet formation and coagulation time at RT and on ice. In the salt bath (20% PEG 8000, 80% 0.1M PBS solution 20 wt.% NaCl) a solid 10% Gel-4VBC did not form, even after being left to coagulate for longer than 5 minutes (300s) (**Figure 4.4a**); while it took the 20% Gel-4VBC sample 08.98s for a gel

droplet to form, however, was not fully coagulated following 300s incubation (**Figure 4.4d**).

Table 4.3: *Mean time taken (seconds, s) for a gel droplet (20% w/v Gel-4VBC) to form in each coagulation bath held on ice.*

Sample	Rickman et al., 2019	EtOH	IPA
10% Gel-4VBC	n/a.	11.18s (±1.89) for a gel droplet to form; 25.24s (±2.72) to fully undergo gel-sol	10.34s (±2.35) for a gel droplet to form; 27.51s (±3.52) to fully undergo gel-sol
20% Gel-4VBC	208.98s for a gel droplet to form. No full gel-sol	6.42s (±0.29) for a gel droplet to form; 16.17s (±2.03) to fully undergo gel-sol	5.96s (±0.74) for a gel droplet to form; 18.47s (±1.59) to fully undergo gel-sol

It should be noted the time taken to form a droplet in the salt-bath was halved when the bath was cooled over ice (208.98 s to 104.23 s), however in both instances, no full coagulation reaction was achieved when the droplet was removed from the coagulation bath. These times are significantly longer than those recorded using an EtOH bath. As can be extracted from **Table 4.3**, a full gel-sol coagulation reaction could be achieved in less than 20 seconds using an EtOH bath at RT, and less than 10 seconds when the temperature was further reduced.

4.5.2 Effect of Coagulation Bath Temperature on Rate of Phase Transition

In a second experiment, the effect of decreasing the ambient temperature of the coagulation bath was considered to investigate the impact on coagulation speed. For this experiment a 20 wt.% gel-4VBC dope was prepared in following with the procedure set out in **Section 3.5.2**. Two coagulation baths were prepared; the salt-based bath as described in **Table 4.4** and EtOH and placed in an ice bath 20 minutes prior to the experiment. The ice bath was replenished, when necessary, throughout this process. The mean coagula-

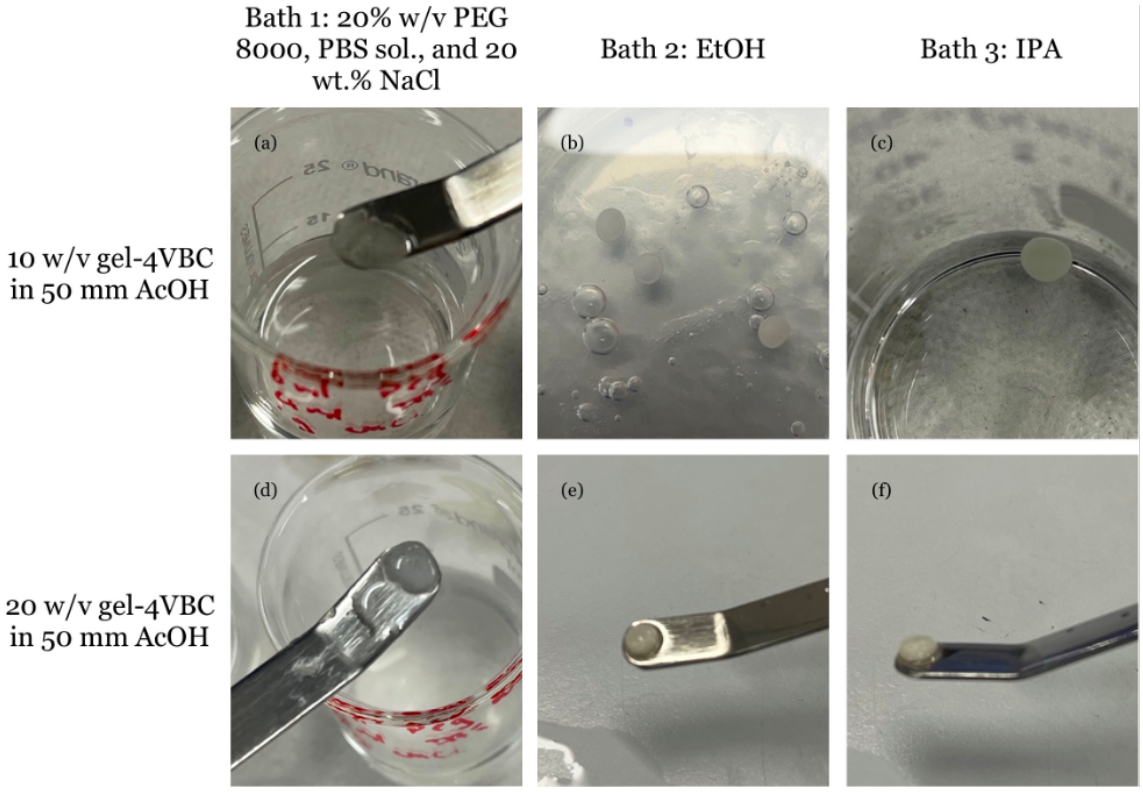

Figure 4.4: *Wet gelatin samples after 15 and 60 minutes.*

tion times have been set out in **Table 4.4**. These findings show a significant reduction in mean coagulation time of gel droplets because of the decreased bath temperature.

Table 4.4: *Mean time taken (seconds, s) for a gel droplet (20% w/v Gel-4VBC) to form in each coagulation bath held on ice.*

Bath	**Room temperature (18°C)**		**On ice (2°C)**	
	Gel-droplet formation	**Full gel-sol transition**	**Gel-droplet formation**	**Full gel-sol transition**
Rickman et al., 2019	208.98s	n/a	104.23	n/a
EtOH	6.42s (±0.29)	16.17s (±2.03)	3.98 (±1.64)	9.81 (±1.51)

4.5.3 Feasibility of Fibre Spinning (Manual Pipetting)

Drop tests indicated that EtOH (on ice) was the most successful coagulation bath solution, however as there is minimal literature on WS gel-4VBC fibres, the author felt it important to continue using the salt-based coagulation solution (as presented in Rickman et al.[307]) to act as a direct comparison. To prove the feasibility of WS of gel-4VBC,

dope (20 wt.% gel-4VBC polymer, 2% w/v. I2959) was pipetted into the two coagulation solutions (held in an ice bath) using the manual pipette (**Figure 3.4**) and left to coagulate. The maximum time each fibre spent in the coagulation was up to 5 minutes.

Findings echoed results presented in **Section 4.5.1**; fibres pipetted into the salt-based bath (**Figure 4.5**) did not fully coagulate, and after 5 minutes, could not be removed from the bath without reverting to a liquid state. Interestingly, the fibres spun into the salt bath displayed an affinity to the glassware that contained the coagulation solution. Fibres spun would migrate towards the edges of the glassware, making it difficult to remove any polymer without damaging the semi-coagulated fibre. While a fibre shape was formed in the salt-based bath, it quickly returned to its liquid state if removed from the non-solvent. As expected, fibres pipetted into the EtOH bath coagulated quickly and could be removed from the bath after 60 seconds while maintaining form; indicating successful gel-sol transition within a quick time frame. These findings are positive in terms of scaling-up fibre production as coagulation speed had been reduced from a 60-minute incubation period [307] to roughly 30 seconds.

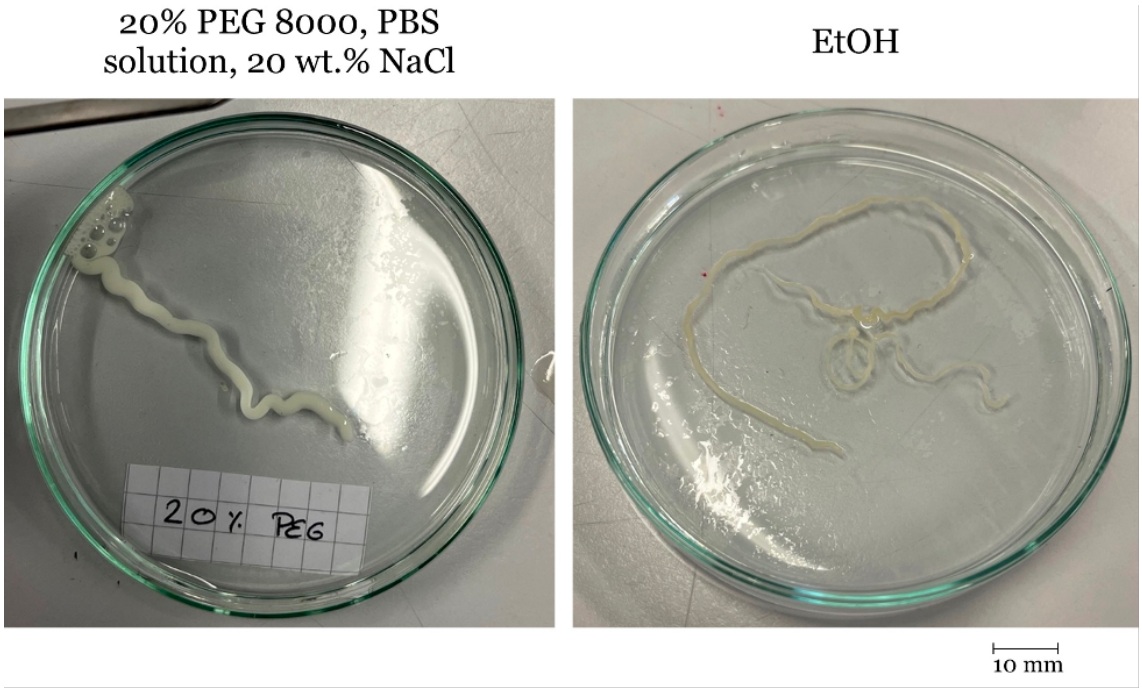

Figure 4.5: *20% gel-4VBC dope fibres spun into coagulation baths containing 20% PEG 8000, PBS solution and 20 wt.% NaCl; and EtOH.*

4.5.4 Plasticisers

This methodology was also employed to trial dope containing different molecular weights (MW) of PEG (8000 and 400). PEG was explored as a potential plasticiser to improve fibre flexibility and handleability and was selected due to its compatibility with PSG as shown in Rickman et al. [307]. PEG 8000 was initially investigated as it was the molecular weight (MW) investigated as a potential coagulant in work published by Rickman et al. [307]. In its powder form, this MW significantly increased the viscosity of the dope to the extent that it was extremely difficult to expel from the syringe. A lower MW of the plasticiser (PEG 400) was investigated to improve fibre plasticity, without increasing dope viscosity. The PEG was in a liquid state after a short period of heating, and so could be easily amalgamated with the gel-4VBC/I2959 dope as previously specified. Both dopes were manually pipetted into a coagulation bath containing EtOH held at 2°C. **Figure 4.6** presents WS fibres containing 5% w/v (a) PEG 400 and (b) 8000 respectively after a 3-minute incubation in the EtOH coagulation bath. The rate of coagulation was considerably slower in the dope containing PEG 8000 than in the lower MW.

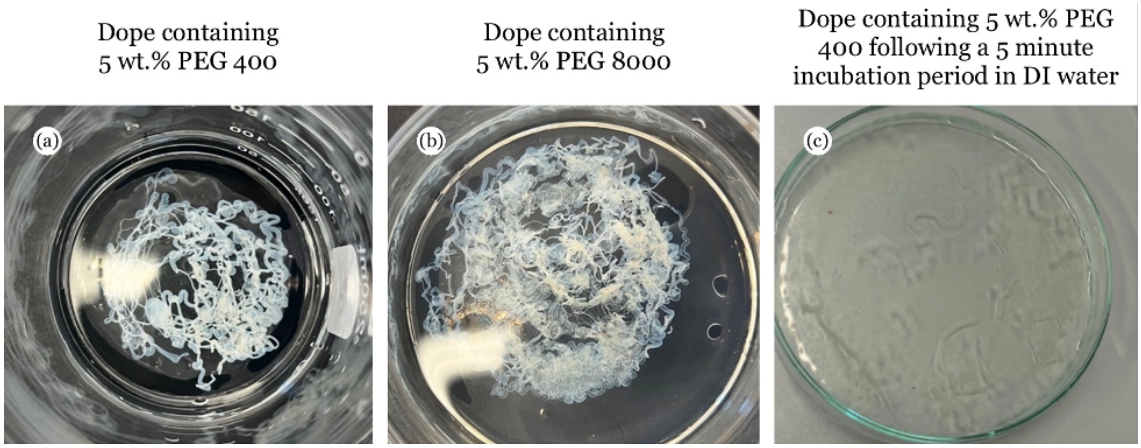

Figure 4.6: *WS fibres containing (a) 5 wt.% PEG 400 and (b) 5 wt.% PEG 800, and spun into a coagulation solution of EtOH held over ice, and (c) 5 wt.% PEG 400 following submersion in DI water for a period of 5 minutes.*

Regardless of the MW of PEG, the fibres displayed irregular morphologies. This irregularity in fibre morphologies is attributed to the merging of fibres on top of each other during the WS process. This prevented untangling if fibre bundles without the risk of fi-

bre damage or breakage, as well as surface buckling and collapse of the fibre structure. This could lead to variations in the appearance and properties of the fibres. Some of the fibres exhibited flattened, ribbon-like morphologies, indicating that the dope solvent (the solvent used in the fibre-forming gelatin solution) rapidly diffused out of the fibres, leading to this specific morphology.

Both samples (fibre/ribbon bundles) were cured for 30 minutes. It was assumed that these fibres would remain intact when placed in an aqueous bath (as I2959 has previously been demonstrated (**Section 4.4**) to improve wet stability of gel-4VBC dopes and fibres). PEG's high solubility in water, however, meant that fibres dissolved rapidly when placed into a water bath (room temperature). Pictured in **Figure 4.6c** is the outcome of placing fibres spun with a dope containing 5% w/v PEG 400.

4.5.5 Discussion on Drop Tests and Chemical Compatibility

Through these initial optimisation studies, several key decisions have been made to enhance the efficacy of the process. Dope optimisation studies have led to the selection of a 20% gel-4VBC dope solution, which is notably enhanced using a 50 mM AcOH solvent in cooler ambient temperatures. Furthermore, to ensure precise control over the coagulation process, an EtOH coagulation bath maintained at 2°C within an ice bath has been chosen. This low-temperature environment is expected to promote the efficient solidification and formation of fibres, ultimately contributing to the formation of fibres with a quicker rate of coagulation, in comparison to earlier literature. Regarding earlier work by Rickman et al. [307], the long coagulation time (incubation for 60 minutes, followed by a further 60-minute incubation in a wash bath) limits the scaled-up production of these fibres. In addition, the incubation period limits the maximum length of fibre that can be spun at one time, as fibre length and morphology will be largely governed by the physical dimensions of the coagulation bath container.

4.6 Optimisation of Gel-4VBC Fibres and Lab-Scale Wet Spinning Rig

The following section focuses on the optimisation of the WS rig. Following early chemical optimisation, the dope used was a 20 wt.% gel-4VBC polymer dissolved in 50 mM AcOH, and the coagulation bath was EtOH held at 2°C in an ice bath. Optimisation of the physical WS set-up is imperative the production of high-quality fibres, as well as ensuring uniformity and reproducibility. This plays into this project's focus of improving fibre production productivity in attempt to determine feasibility of scaled-up gel-4VBC fibre spinning. The following experiments look to fulfill **Objective 3**, to determine the feasibility of manufacturing UV-cured Gel-4VBC filament fibres through WS methodologies at a laboratory-scale.

4.6.1 Needle gauge

The needle gauge, or the diameter of the needle used in WS, is an important parameter that can significantly impact the process and the properties of the resulting fibres. Fibres were spun using 16G, 18G and 21G luer lock needles fixed to a 24 ml syringe, and pumped at 0.6 ml/min. Without tensile testing, fibres spun with the narrower gauge needle (21G) exhibited good handleability and flexibility in comparison to the larger gauges. Fibres spun using a 16G lumen required a longer coagulation period and were brittle when handled. This is likely due to uneven coagulation through the fibre's cross section due to the larger circumference. From this optimisation, a 21G needle was selected for further use in the optimisation of the rig. The reduction in needle hole size (from 16G to 21G) resulted in significant differences in fibre mechanical properties, which can be attributed to the reduced internal diameter of the extrusion nozzle, leading to higher internal die pressure and increased shear forces on the extruded dope. These factors likely contributed to greater molecular chain alignment and a reduction in fibre diameter. Die swelling (also referred to as the Barus effect) is characterised by a change in the elastic modulus (stiffness) when a liquid long-chain polymeric material is subjected to a sustained or static deformation, such as during extrusion from a WS nozzle (needle) [283][263][246].

Die swelling, known as the Barus effect, manifests when a liquid long-chain polymer like a polypeptide solution is compelled through a narrow passage, exemplified by a needle. While within the syringe, the molecular chains adopt a spherical configuration, however as it passes through the smaller internal diameter of the needle, flow rate accelerates, causing the chains to disentangle due to the shear stress. Subsequently, as the polymer exits the needle, the flow rate decelerates, and the chains re-establish their spherical organisation, leading to a swelling of the polymer solution. This results in the production of fibres with diameters slightly larger than that of the needle's internal cross-section. The diameter of the needle can impact the rate at which the spinning solution is extruded.

4.6.2 Pumping Speed

A larger needle gauge may allow for a higher flow rate, potentially leading to faster production. However, this must be balanced with other factors such as the quality and uniformity of the fibres. Following selection of a 21G needle, a compatible pumping speed was investigated. The dope pumping speed directly influences the rate at which the polymer solution is extruded or pumped through the needle. The ability to control the flow rate is crucial for ensuring uniform fibre properties and dimensions. Through spinning trials, significant back pressure of the dope on the syringe was found to occur at pumping speeds over 2:00 ml/min, resulting in inefficient fibre formation, and significant dope wastage. From this finding, slower pumping speeds, between 0.3 and 1.5 ml/min, were trialled (**Table 3.6**). A successful pumping speed would be represented by a continuous dope flow into the coagulation bath without the formation air bubbles, or gaps in flow.

Ultimately a pump speed of 1.2ml/min was selected as this facilitated the production of continuous filament fibres within the coagulation bath. The speed selected was significantly higher that previously reported in literature [307]. As mentioned in **Chapter 3**, the increased polymer wt.% (20 wt.% gel-4VBC) from the 15 wt.% originally stated in Rickman et al. [307]. While increasing the amount of polymer dissolved into the dope during wet spinning has a significant impact on the flow speed through the needle; as the increased viscosity generally results in higher resistance to flow, and therefore slower extrusion rate. However, many polymer solutions (such as gelatin) exhibit shear thinning

behavior, where the viscosity decreases as the shear rate increases; partially offsetting the effects of higher viscosity and allow for higher flow speeds at elevated polymer concentrations [334][447](Shirvan et al., 2022; Zhang et al., 2024)

Evidence from multiple sources in literature have confirmed that gelatin-based dopes, including native gelatin and Gel-MA, exhibit shear thinning behaviors during WS and other extrusion methodologies [286][211][307]. This shear thinning allows the dopes to flow more easily through the narrow nozzle or spinneret at higher shear rates, as the flow properties of gelatin solutions are not linearly proportional to the applied shear force [148]. While the literature does not specifically refer to 4VBC-functionalised-gelatin, we can infer that the gel-4VBC used in these studies, would exhibit similar properties.

4.6.3 Rotational Drawing

Due to lack of equipment (specifically an automated drawing component), it became very difficult to produce WS fibres of a decent quality when using a conventional (CWS) bath set up (as shown in **Figure 2.7**). To overcome this, a RWS process was adopted (illustrated in **Figure 2.8**). In this methodology, the syringe was placed vertically into a rotating coagulation. Rationale behind this method was that the effect of rotation on the dope would aid in aligning the polymer fibres along the fibre's length (in the longitudinal direction), assisting in improving phase separation and fibre formation, as well as in achieving a more uniform fibre morphology. Long fibres (**Figure 4.7a**) were spun continuously into a rotating coagulation bath and compared to a fibre spun using a conventional bath set up (**Figure 4.7c**); this fibre was spun until it the fibre naturally broke from the needle (due to constraints imposed by coagulation bath dimensions). Both RWS and CWS were spun under the same parameters (needle gauge, pumping speed, coagulation bath temperature, dope composition, temperature); and all samples were produced on the same day so to ensure comparable ambient conditions.

As is evident from **Figure 4.7**, a far higher yield of fibre could be attained using a RWS set-up in a single continuous spin. This is likely due to the slight draw-effect produced by the forces of the coagulation solution's rotational motion. No further drawing of either fibre was carried out so to best examine the effects of RWS-induced-drawing.

SEM imaging (**Figure 4.8**) was taken of the fibre samples presented in **Figure 4.7b** and **Figure 4.7c** to compare surface qualities. Visually, **Figure 4.8a** (CWS) exhibits a slightly rougher surface texture, as opposed to **Figure 4.8b** (RWS), where fibres, while more varied in degree of surface grooving, are smoother. A key reason for the variation in surface grooving in **Figure 4.8a** could be slight variations in fluid movement during rotation. It was hypothesised that similar fibre attributes could be produced through apparatus mechanisms that produce a slight draw of the fibre as it initially enters the coagulation bath.

Regarding scalability, it is difficult to predict how RWS could be adapted to facilitate mass production of fibres, without increasing the time spent in the coagulation bath. One suggestion could be by inducing some sort of movement of the coagulation fluid, as within the methodology presented in this body of research, it was the physical movement of the ethanol (in a circular motion) that applied a slight draw to the fibres. Here, distinct differences in fibre morphology at the same SEM-zoom are visible.

4.6.4 Spin Duration (Fibre Bundles)

An estimated total continuous fibre length (prior to drawing) of 47.75m could be spun from a filled syringe containing 24 ml dope. To calculate this, a uniform cylindrical fibre length with a diameter of 0.8 mm (corresponding to the internal diameter of the 21G needle) was assumed, and a constant flow rate of 0.6 ml/min was applied. At this flow rate, the total time to spin this quantity of dope was estimated to be 40 minutes. Taking

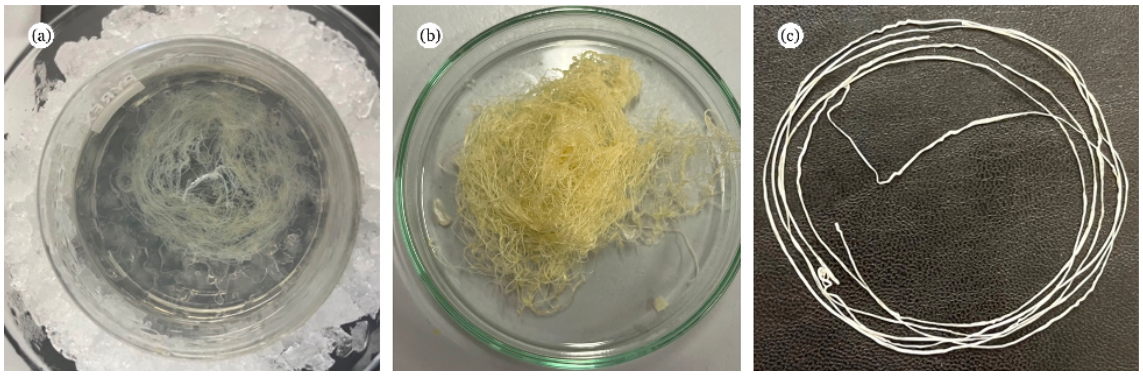

Figure 4.7: *(a) RWS fibre bundle during the coagulation phase; (b) dry RWS fibre bundle following a 30-minute cure period; and (c) CWS fibre, wound around a test tube and left to dry.*

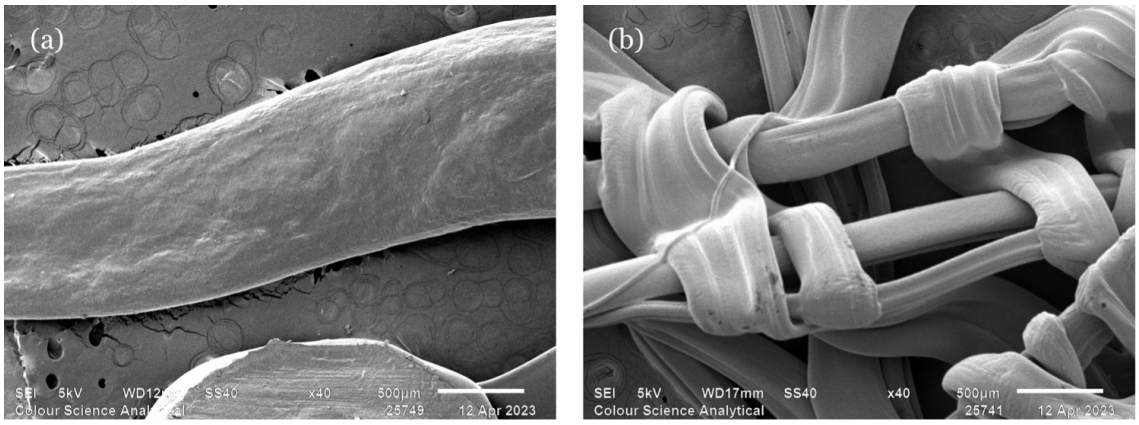

Figure 4.8: *SEM photographs at X40 zoom of (a) WS fibre (non-rotary), and (b) RWS fibre bundle spun on ice. Both samples were spun using 21G needle.*

these findings, it could be estimated that in a 60-minute period, a total potential fibre length of 71.62m could be produced with the same diameter.

From a materials perspective, to produce this length of fibre, the quantities of polymer and dope solvent would be 7.2 ml and 28.8 ml, respectively in order to produce the 36ml dope required to spin for a full hour. When taking drawing processes into account, total length of fibre produced in a 60-minute period will increase in accordance with the draw speed. A fibre length of 71.62 m, drawn with an extension of 50%, will give a total potential fibre length of 107.43m that could be spun in a 60-minute period. While these equations do not consider other extenuating factors (such as rotary speed, potential Barus effect), these do give a good indication of the potential of scaled up gel-4VBC production.

4.6.5 Effect of Heat Difference Between Dope and Coagulation Solution

This project clearly demonstrated that when working with a thermally sensitive polymer like gelatin, ambient temperature significantly affects various aspects of the experiments. Gelatin has a relatively low gelation temperature, which is close to room temperature, and one issue that arose was that of needle blockage, cause by the liquid dope congealing when removed from the hot plate (following the dissolution step). When a gelatin solution is heated and then allowed to cool, it undergoes a phase transition as it

approaches its gelation temperature, where molecules lose kinetic energy, allowing them to form a solid network structure. During this process, the individual gelatin molecules reorganise and entangle, forming a 3D polymer chain network, resulting in the congealing of the solution. This became an issue during the colder months when the ambient temperature (within the laboratory) was decreased. This was overcome through the previously mentioned electric heating sleeve (purchased from Science Warehouse) used to hold the syringe (containing gel dope) at a consistent temperature (65°C) during the WS process.

Prior to this the effect of cold coagulation bath was investigated on the RWS of gel-4VBC. Fibre bundles spun on ice, shown in **Figure 4.7** and **Figure 4.8** were compared to fibre bundles spun at room temperature (**Figure 4.9**). As before, samples depicted in **Figure 4.8** and **4.9** were spun on the same day to maintain similar ambient conditions. As is evident, while some fibres are visible, the bundle in **Figure 4.9** failed to fully form and appear to have melted into one another (to a degree). Individual fibres appear less cylindrical and flatter, and a large solid ring of coagulated dope is visible around the outer edge of the SEM image. The SEM images indicate that the rate of coagulation is significantly impacted by the temperature of the coagulation bath. The conclusion that the rate of coagulation increases as coagulation bath temperature decreases was drawn from these findings. The author notes that spinnability was highly affected by ambient temperature, and spinning over ice allowed for a degree of controllability on the external environment in which this laboratory work was carried out. It would be of benefit to spin these fibres in a temperature/humidity-controlled environment, however due to constraints, could not be facilitated through this body of research.

The benefits of maintaining the dope at a temperature above that of gelation, minimised needle blockage, and enabled a longer consistent spin duration. In addition, the increased dope temperature (combined with the decreased coagulation solution temperature), increased the thermal difference between object (dope/fibre) and environment (coagulation bath), which impacts the rate of cooling. As the temperature difference between the two components was increased, the speed at which the fibre cooled and solidifies (within the bath) did also.

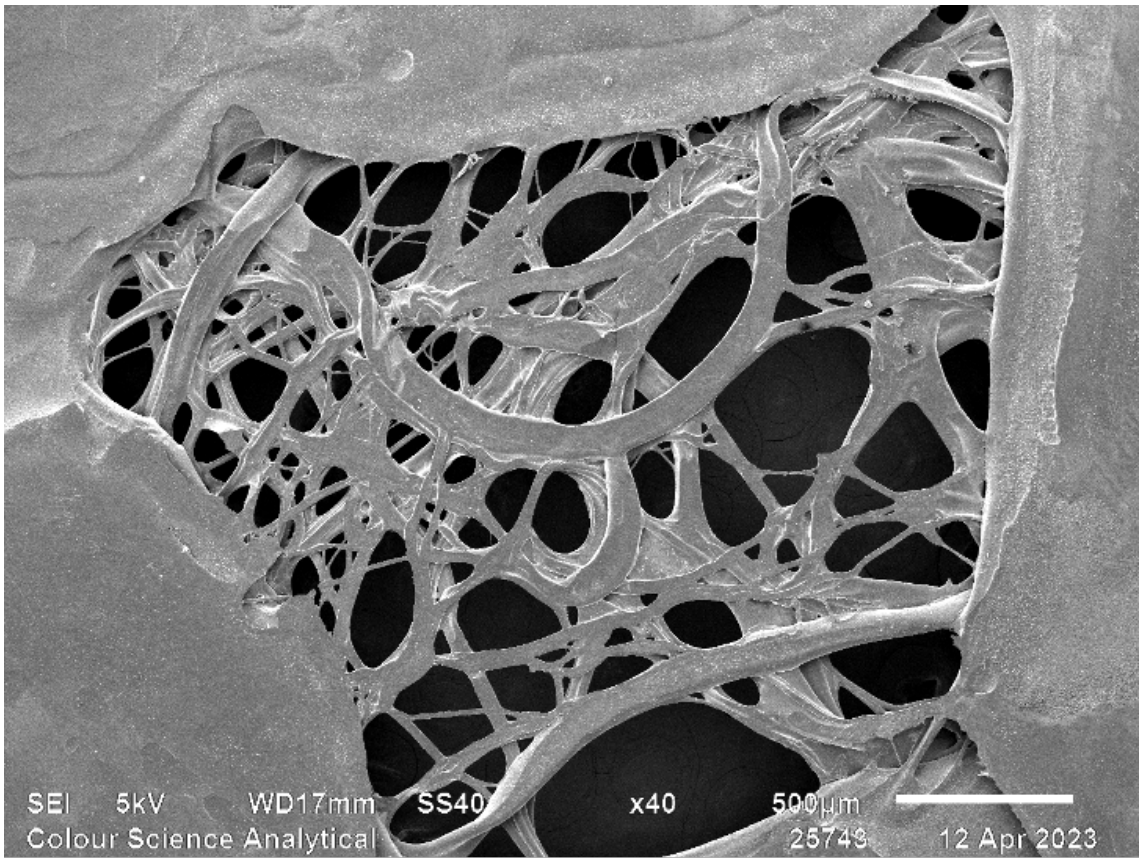

Figure 4.9: *SEM photographs at X40 zoom of Rotary WS fibre bundle spun at room temperature.*

4.6.6 Discussion on Rig Optimisation Processes

Through optimisation of the laboratory-scale spinning rig, several key decisions have been made to improve the effectiveness and productivity of the process. Firstly a 21 G needle was selected as the most effective needle gauge/internal diameter. It should be noted that this was the smallest diameter that the author could ascertain throughout this project. For this reason, it could be that an even smaller gauge (22 G +) could result in better fibres, opening some scope for further research. The heating sleeve (enabling the dope to be maintained at a temperature above that of gelation) was also found to be extremely successful in improving productivity and efficiency of the spinning process, while aiding in reducing frequency of fibre breakage through the reduction of needle blockage. A 0.6 ml/min pumping speed proved to provide a consistent dope flow through the needle and into the coagulation bath without causing air bubbles or gaps in the gel stream. In addition to this, the flow rate was too high to the point that excessive back pressure caused the syringe to leak or break.

The wet spinning methodologies have been successfully implemented at a laboratory scale to manufacture UV-cured Gel-4VBC filament fibers. This achievement showcases the feasibility of producing these specialised fibers using the WS techniques, opening up opportunities for further research and development in this area.

4.7 Drawing and Curing

The following experiments investigate the combined effect of fibre extension (drawing) and UV-curing duration on fibre morphology and mechanics. Fibre development in this section builds on the previous results discussed in this body of research by investigating the fourth step of the WS process; fibre collection and post-spin treatments. Short fibres (of roughly 100 μm) were spun using the WS conditions defined in **Section 4.4** and **4.5**. Once coagulated, fibres were transferred to an Instron 3365 (**Figure 4.10**) (Oral Biology, St James' Hospital, Leeds) and extended to a pre-determined length (prior to the fibre drying). The gauge length, referring to the distance between the clamping points was set to 50 mm (measured with digital calipers). This gave each WS fibre an initial length of 50 mm. The four drawing conditions were 25%, 50%, 75% and 100% of original length, giving final fibre lengths of 62.5mm, 75mm, 87.5mm, and 100mm, respectively. Once drawn, fibres were left to dry while still clamped in the Instron, so to prevent potential recoil or shrinkage of the fibre's length back to its original. Dry fibres were then transferred to a Chromato-Vue C-71 and irradiated at 365 nm for a pre-defined period (stated previously in **Table 3.7**).

Findings indicate that the drawing process can impact the molecular chain alignment and orientation, while the UV-crosslinking step can further stabilise the fiber structure and enhance its mechanical and thermal properties

4.7.1 Water Uptake and Fibre Swelling

WS fibres underwent UV-curing and were assessed regarding their ability to absorb liquid- so to examine fibre properties in a near-physiological environment. This property is especially relevant for applications in the medical field, such as that of tendon reconstruction, where wound exudate production can reach significant levels, and for tissue

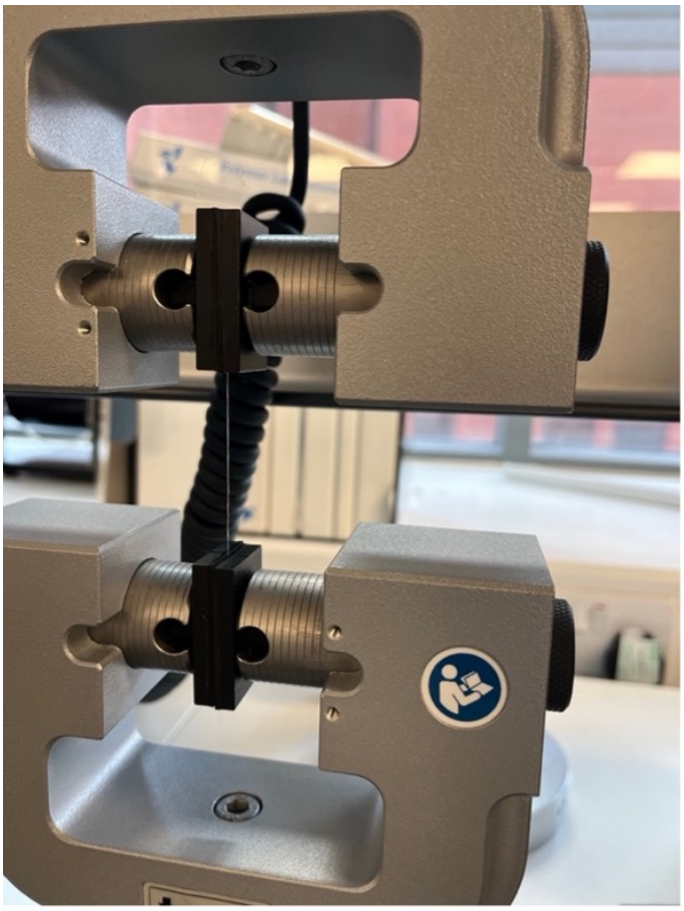

Figure 4.10: *Process of drawing fibres using the Instron 3365 to control and measure the rate of extension to a pre-defined limit.*

scaffolds where nutrient and waste exchange is influenced by the surrounding medium. The degree of swelling (indicative of water uptake) was calculated as a percentage increase in cross-sectional diameter (presented in **Table 4.5** and **Figure 4.11**). A general trend in that the degree of water uptake decreased as duration of UV-curing increased was concluded. Calculated as the mean increase in diameter from each curing condition. In fibres (regardless of draw length) cured for one minute, a mean % increase of 32% was calculated. When compared to fibres cured for 15 minutes, 30 minutes and 45 minutes, % increase values of 18.8%, 11.3%, and 6.9% respectively were obtained. These findings show a linear association between cure duration (crosslink network) and fibre swelling.

UV cross-linking can reduce gelatin swelling due to the formation of a crosslink network between gelatin polypeptide chains. During this chemical reaction, high-energy

Table 4.5: *Table showing the mean diameters of dry fibres versus the mean diameters of wet fibres with their resultant water uptake as indicated by the percentage increase in width.*

Sample	Mean dry diameter (m)	Wet dry diameter (m)	Water uptake (% increase)
25% D, 1 min C	212.6	246.8	35.3
50% D, 1 min C	179.0	206.3	32.9
75% D, 1 min C	138.0	158.7	32.2
100% D, 1 min C	112.5	127.0	27.6
25% D, 15 min C	217.8	244.8	26.3
50% D, 15 min C	187.7	207.0	21.7
75% D, 15 min C	146.7	158.5	16.7
100% D, 15 min C	118.3	124.3	10.4
25% D, 30 min C	234.7	253.3	16.5
50% D, 30 min C	170.7	180.4	11.8
75% D, 30 min C	160.8	168.5	9.9
100% D, 30 min C	125.5	129.8	7.1
25% D, 45 min C	218.7	228.2	8.9
50% D, 45 min C	195.4	201.0	5.8
75% D, 45 min C	153.4	157.9	5.9

UV light initiates a reaction that results in the formation of covalent bonds (crosslinks) between adjacent gelatin polymer chains. These cross-links create a network structure within the gelatin, enhancing the overall structural robustness of the gelatin network. In-turn, this reduces the permeability of WS fibres is diminished, reducing the ability of water molecules to penetrate and swell the fibre when exposed to aqueous environments.

4.7.2 Varying Extension

Tensile testing of drawn fibres revealed surprising results. Overall, mean strain for the four draw conditions; (regardless of cure duration or extension length) 25%, 50%, 75%, 100%, were 1.3, 1.2, 0.9, and 1.1 respectively. These findings indicate that the highest mean strain was found in fibres extended by 25%. This was a surprising finding, as

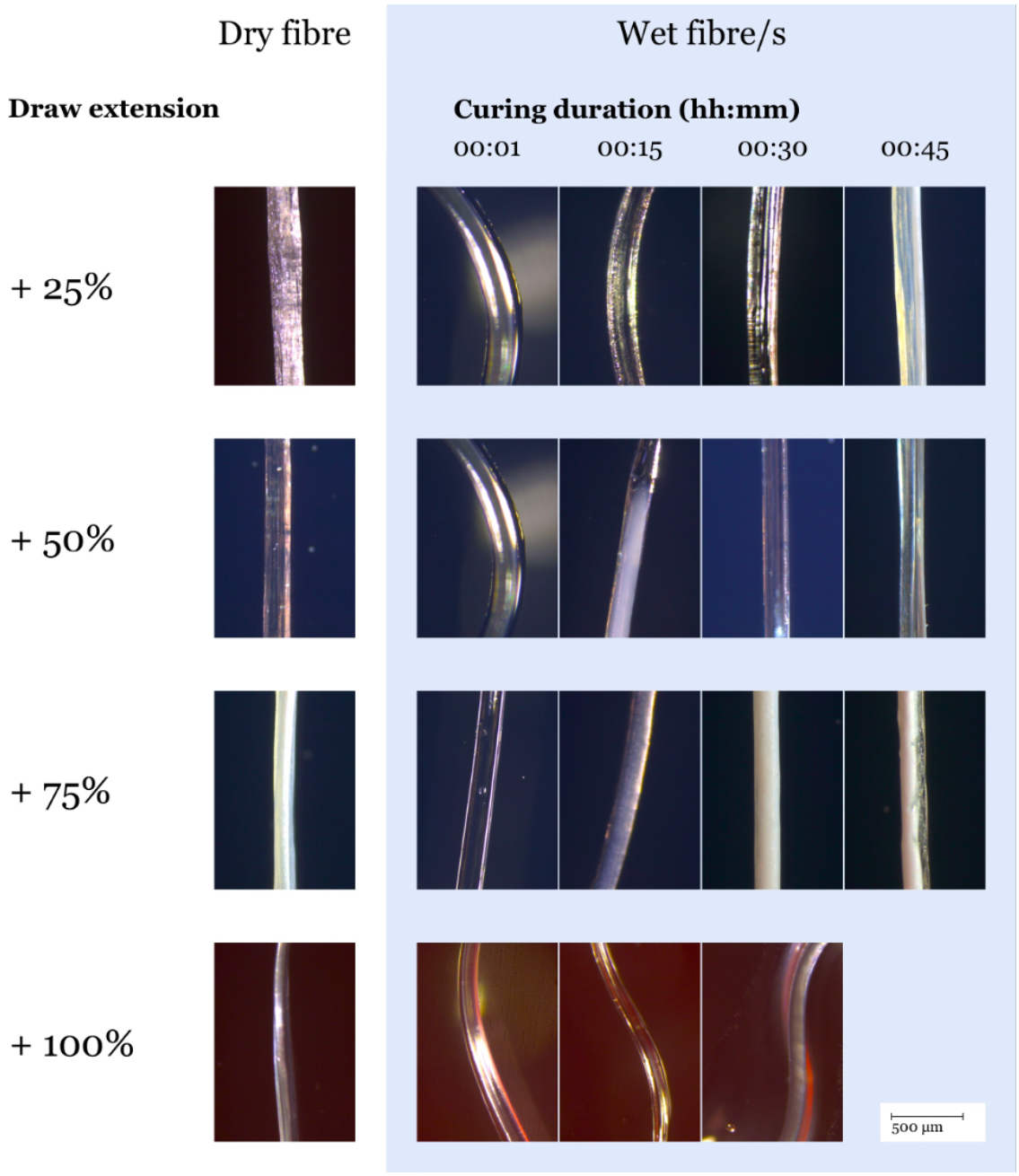

Figure 4.11: *Optical microscopy images showing comparisons between dry and wet fibres in the following conditions: (a) 25% draw, 30 minute cure; (b) 50% draw, 15 minute cure; (c) 100% draw, 30 minute cure; (d) 50% draw, 1 minute cure; (e) 75% draw, 15 minute cure; (f) 100% draw, 45 minute cure; (g) 100% draw, 15 minute cure; (h) 75% draw, 1 minute cure; (i) 25% draw, 45 minute cure; (j) 75% draw, 30 minute cure.*

much of the literature on drawing indicates that fibre tensile strength has a positive relationship (correlation) to draw extension [246]. Displacement measurements (at mechanical failure) and calculated strain values from tensile testing have been presented in **Table 4.6**. The process of increasing extension (from +12.5 mm to 50 mm), better

aligns the polypeptide chains, improving structure's crystallinity. Literature suggests that in materials with a degree of crystal alignment, strain can be more predictable and uniform; as the crystal alignment prevents dislocation movement, influencing the material's strength and hardness. A key example of this is Wu et al. [411] who described the manufacture of hierarchical and biodegradable WS silk fibroin scaffolds; employing a "double-drawing" procedure to enhance the fibre's mechanical properties; resulted in fibres that exhibited mechanical properties mechanically similar to those of the human ACL.

Additionally, in materials with lower crystal alignment, the strain might lead to more complex deformation patterns and variations in mechanical properties. Strain patterns did not follow expected trends. Looking at other published literature, a further increase in extension may be of benefit. The slight improvement in mean strain from 75% to 100% could potentially indicate that a longer extension length could theoretically better improve polymer alignment and consequently, strain. This would align to findings from Fukae et al. [115], how found a marked improvement in tensile strength when they drew their fibres by 6-times the original length. Overall, the change in length at mechanical failure (for all conditions) is varied and does not fully support (nor oppose) current published literature. One key reason for this may be due to inconsistencies of ambient conditions and slight variations during spinning due to this being a laboratory-based method (with less control-ability than an industrial WS process, for example).

4.7.3 Curing Duration

Mean wet cross-sectional area, applied load at mechanical failure and calculates stress values have been presented in **Table 4.8**. As a general trend, fibres cured for 30 minutes (regardless of extension) exhibited the highest overall stress values (29.35 N/mm2 mean stress), followed by those cured for 15 minutes (16.13 N/mm2 mean stress), and those cured for one minute in third (8.24 N/mm2 mean stress). Indicating a strong positive relationship between degree of polymerisation (UV-curing) and stress values. In addition, a linear relationship between stress and draw extension was also revealed. The highest overall load at breakpoint (and consequently, stress values) were observed across all cure-times in fibres extended by 75%, followed by the 100% draw condition. Due

Table 4.6: *Length (original) vs mean change in length of each fibre condition. Figures given to 1 decimal place.*

Sample	Original length L (mm)	Change in length at break L (mm)	Strain
25% D, 1 min C	20	17.5	1.2
50% D, 1 min C	20	18.3	1.1
75% D, 1 min C	20	21.1	1.0
100% D, 1 min C	20	17.0	1.2
25% D, 15 min C	20	39.8	1.2
50% D, 15 min C	20	42.9	1.1
75% D, 15 min C	20	46.3	0.8
100% D, 15 min C	20	42.3	1.0
25% D, 30 min C	20	19.8	1.0
50% D, 30 min C	20	22.9	0.9
75% D, 30 min C	20	30.4	0.7
100% D, 30 min C	20	20.3	1.0
25% D, 45 min C	20	15.7	1.7
50% D, 45 min C	20	17.8	1.5
75% D, 45 min C	20	16.7	1.2

to a significant decrease in mechanical property across fibres drawn by 50 and 75% and cured for 45 minutes, the final condition of fibres drawn by 100% and cured for 45 minutes was discounted.

Stress values were associated with the duration of curing. The process of UV-curing results in a reaction known as polymerisation, where individual monomeric units are intricately linked to produce larger polymer matrix, which defines the overall chain structure. Initiating cross-linking enhances dimensional stability, making the fibre more resistant to solvents, chemicals, and thermal stress. It also affects the fibre's tendency to swell or absorb moisture. The degree of crystallinity in the polymer structure influences thermal stability and mechanical strength. The polymerisation method and reagents impact the fibre's chemical reactivity, affecting its potential for bonding with other materials. Processability of the biopolymer solution during extrusion and fibre formation depends on polymerisation, which can influence the smoothness of the process.

4.7.4 Tensile Testing

An Instron 5544 tensile tester was used to conduct tensile break tests of wet fibres. An extension speed of 25 mm/min was set and the gauge length was set to 20 mm (in accordance with the (ISO 5079:2020 [368]). This method has been depicted in **Figure 4.12**. The relationship between stress and strain values in wet spun fibres plays a crucial role in understanding and characterising the mechanical behaviour of these materials. When subjected to an external force, the stress experienced by wet spun fibres is directly proportional to the applied force and inversely proportional to the cross-sectional area of the material. The stress-strain curve for wet spun fibres provides insights into their mechanical properties, including elasticity, toughness, and UTS. Variations in WS conditions, such as coagulation bath composition or spinning parameters, can significantly influence the stress-strain relationship, impacting the overall performance and utility of the fibres. A thorough analysis of stress and strain values thus contributes to the optimisation of WS processes, ensuring the development of fibres with desired mechanical characteristics for specific end uses.

Table 4.7: *Mean wet cross-sectional-area of fibres with applied load at break.*

Sample	Mean wet x-section (m^2)	Load at break (mN)	Load at break (N)	Stress '' (N/mm^2)
25% D, 1 min C	48161.1	100.5	0.100	2.075
50% D, 1 min C	33458.2	172.5	0.172	5.13
75% D, 1 min C	19783.9	287.1	0.287	14.49
100% D, 1 min C	12689.4	143.1	0.143	11.26
25% D, 15 min C	47255.7	129.5	0.130	2.75
50% D, 15 min C	33683.9	391.0	0.391	11.60
75% D, 15 min C	19770.8	663.0	0.663	33.48
100% D, 15 min C	12138.5	201.8	0.202	16.69
25% D, 30 min C	50544.8	341.9	0.342	6.77
50% D, 30 min C	25685.8	766.8	0.767	29.84
75% D, 30 min C	22358.9	1338.9	1.339	59.78
100% D, 30 min C	13287.9	249.8	0.250	21.01
25% D, 45 min C	40996.0	46.0	0.046	1.12
50% D, 45 min C	31729.2	55.0	0.055	1.74
75% D, 45 min C	19579.3	0.2	0.00023532	0.01

4.7.5 Discussion of Findings from Drawing and Curing Optimisation

The process of drawing and extension plays a pivotal role in shaping the properties and characteristics of WS biopolymer fibres. Findings indicated that up to 75% fibre extension, drawing significantly enhances fibre mechanical properties such as tensile strength owed to a more linear alignment of polymer chains along the fibre's axial length. Here are many benefits to fibre drawing both aesthetically and on the molecular scale. The effect of crystal alignment brought about by drawing leads to a reduction in fibre diameter (**Table 4.5**), resulting in finer fibres with increased flexibility, which improves fibre resistance to breakage and deformation. In addition, as the fibres undergo stretching and alignment, the molecular chains, are arranged in a semi-linear alignment along the fibre's axis, increasing the density and uniformity of H-bonds throughout the fibre. This

Figure 4.12: *Process images showing fibre extension during wet tensile testing of a fibre sample from the (a) 50% draw, 1 minute cure condition; and from the 75% draw, 15-minute cure condition (b) at full extension, and (c) mechanical failure/break, using the Instron 5544.*

aids in improving both thermal and chemical stability, while the orientation of functional groups impacts properties such as wettability and interactions with other materials. Visually, drawing results in the formation of a more uniform fibre smoother and more homogeneous surface texture (**Figure 4.8**). This feature enables control over shrinkage when exposed to wet conditions.

As fibres are subjected to stretching and alignment, the molecular chains within them are arranged in a semi-linear fashion along the fibre's axis. Furthermore, the process may have implications for the biodegradability of gelatin, a material inherently prone to biodegradation. However, the extent and specific conditions of drawing can influence this aspect. The adaptability of these effects is underscored by the flexibility of drawing conditions, which can be adjusted to meet the precise requirements of a wide range of applications, spanning industries such as food processing, pharmaceuticals, textiles, and medical devices.

4.7.6 Stress/Strain Curves

The stress-strain curve is a graphical representation of the relationship between stress and strain in a material subjected to mechanical loading, with its peak. The curves pre-

sented in **Figure 4.13** give an indication of mean ductility and toughness when exposed to increasing axial strain. During the plastic region, the fibre undergoes significant plastic deformation. The stress necessary to cause further deformation gradually increases. The fibre continues to deform (under axial load) plastically without a proportional increase in stress. The UTS, defined as the maximum stress the material can withstand; is where the fibre experiences localised necking, resulting in the cross-sectional area thinning. UTS was found to be the highest in the "75% draw, 30-minute cure" condition, followed by "50% draw, 30-minute cure" ad "75% draw, 15-minute cure" conditions. Eventually, the material fractures at the point of minimum cross-sectional area. General stress and swelling index values indicate strong correlation in the way of mechanical loading parameters; however, when coupled with more varied elastic potential and displacement limits (as indicated in both **Table 4.6** and **Figure 4.13**), general conclusions on the optimal draw and cure durations are more difficult to determine.

The mean elasticity modulus (EM) values for each fiber sample are presented in Table 9. These were calculated using **Equation 3.6**. By examining Figure 13 and the tabulated data, it can be deduced that the fiber category exhibiting the highest EM is the sample subjected to 75% draw ratio and a 30-minute curing process. General conclusions that can be made from these findings are as follows. This fibre condition also withstood the mean, highest load at breaking point (1.339 mN) Overall fibres that were cured for 30 minutes performed the strongest under mechanical loading, with the 75%, 50%, and 100% draw ratio fibres coming in the top five-highest EM-values. It can also be concluded that the most successful draw-ratio was the fibres that underwent a 75% draw, regardless of curing duration. This was followed by fibres drawn by 50%, and then 100%. In general, the samples cured for 45 minutes and/or underwent a 25% draw, performed the worst during mechanical loading. Regarding the long cure duration, the reduction on mechanical performance is likely due to "overcuring", which potentially leads to increased brittleness. While there is no available literature to compare these findings to, the negative effect of prolonged exposure to UV-light has been observed in collagen-based materials [86]. Additionally, the formation of a densely packed network of covalent bonds within the polymer structure, could limit the flexibility and handleability of the fibers: resulting in the structure to become brittle and less pliable.

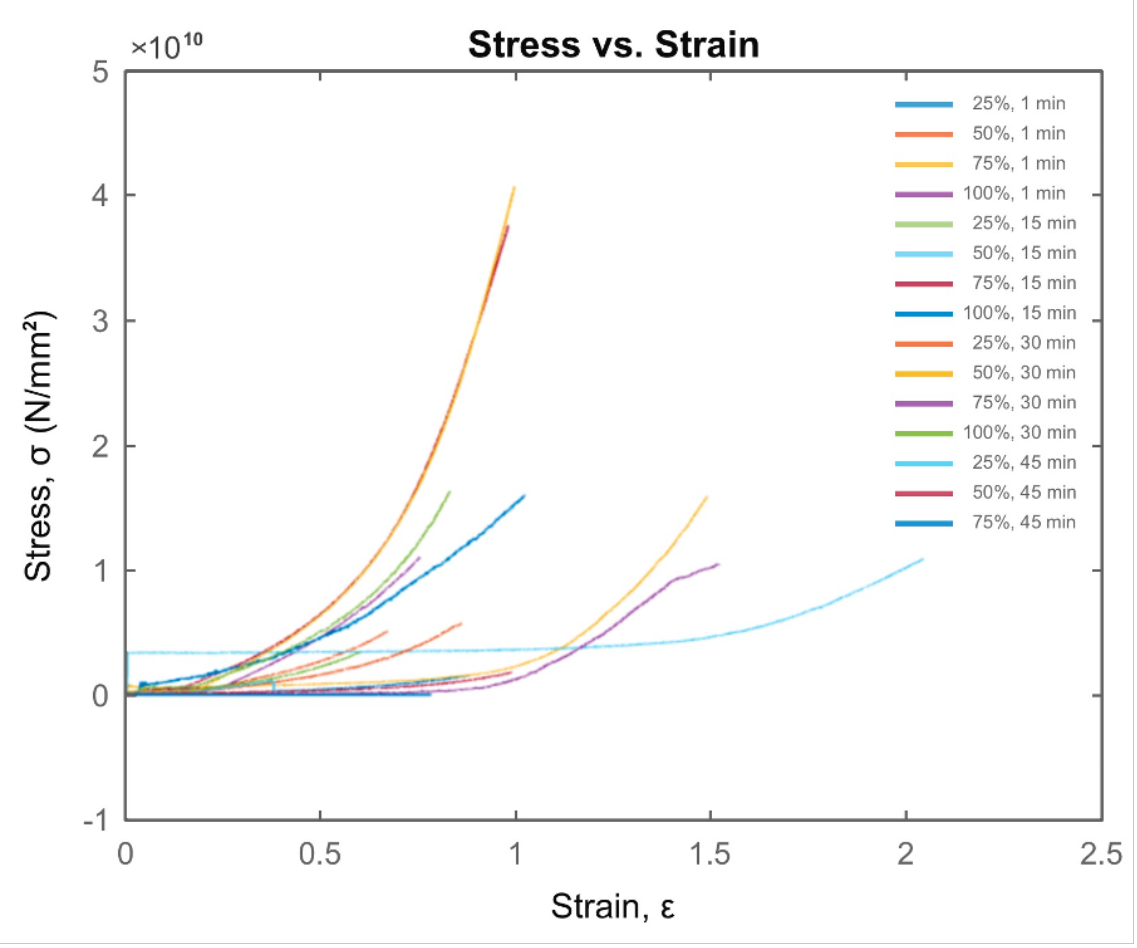

Figure 4.13: *Graph showing the stress/strain relationships of the fibre draw/cure conditions.*

4.8 Wetting and Heating Drawn and Cured Fibres

Regarding the manufacture of fibres, it was questioned whether findings from earlier dope characterisation studies (**Section 4.4** and **Figure 4.3**), would also be true for filament fibres produced through WS methodologies. Specifically, the effectiveness of combination crosslinking with both 4VBC and I2959 on fibres in a wet and warm environments was investigated on two RWS fibre bundles. Each bundle was spun in accordance with the parameters described in **Section 3.10**. No drawing of the fibres was conducted; however, each bundle was cured for 30 minutes. A 30-minute-cure-time was selected as this condition presented the most successful fibres across all draw-ratios. The first fibre bundle (shown in **Figure 4.14**), was saturated in a bath containing 200 ml DI water and incubated for 24 hours at 37°C.

Following this, the fibres were removed and inspected for any visual signs of degrada-

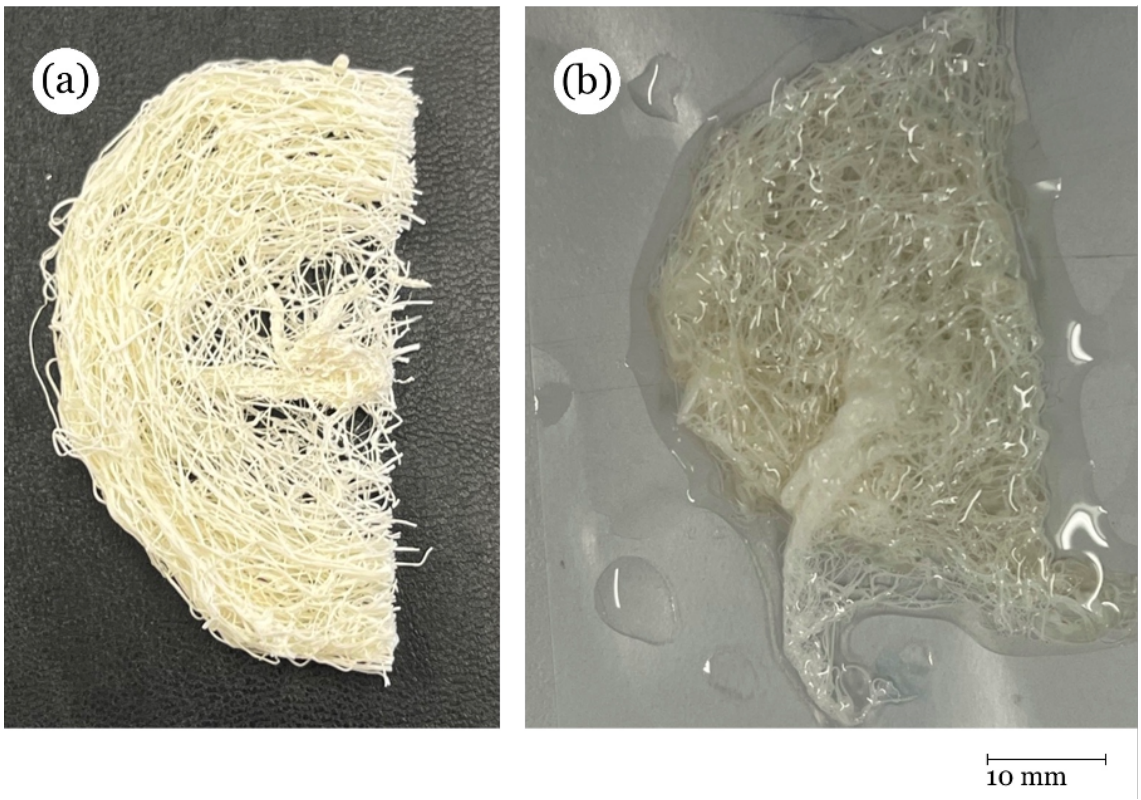

Figure 4.14: *Section of a RWS fibre bundle (cured for 30 minutes) (a) dry, and (b) after 24 hours incubated in DI water at 37°C.*

tion. Sample weights were taken both prior to and after incubation, with the findings presented in Table 4.8. An 8.8% increase in weight was observed after 24 hours of incubation, which aligns with previous swell measurements shown in Table 4.5 that indicated a degree of mass increase. Figure 4.15 displays the fibre sample following a one-month incubation period. During this time, room temperature water in the bath was topped up weekly to prevent total evaporation and dehydration of the sample. A slightly higher weight increase of 9.2% was measured, attributed to water uptake by the fibres. These findings suggest good wet and thermal stability, as the fibre bundles did not lose any mass through dissolution into the surrounding bath. It can be concluded from this experiment that a gelatin combination crosslinking of 4VBC and I2959 was sufficient to ensure the wet and thermal stability of RWS fibres under conditions that mimic the human body.

Table 4.8: *Mean elastic modulus values calculates for each sample, shown to 3DP.*

Sample	Elastic modulus, E
25% D, 1 min C	1.729
50% D, 1 min C	4.664
75% D, 1 min C	14.49
100% D, 1 min C	9.383
25% D, 15 min C	2.292
50% D, 15 min C	10.545
75% D, 15 min C	41.85
100% D, 15 min C	16.69
25% D, 30 min C	6.77
50% D, 30 min C	33.156
75% D, 30 min C	85.4
100% D, 30 min C	21.01
25% D, 45 min C	0.659
50% D, 45 min C	1.16
75% D, 45 min C	0.008

4.9 Chapter Conclusion

Table 4.10 presents the new chemical parameters for the dope and coagulation bath, as well as RWS and post-spin processes. These have been optimised from the original. Despite being in the early stages, the progress made so far has laid a solid foundation for achieving the key objectives related to the characterisation and utilisation of f-gelatin as a bioreceptive material and the production of UV-cured Gel-4VBC filament fibres through wet spinning methodologies at a laboratory-scale (**Objective 2**).

Building upon this foundation, a careful optimisation process has been undertaken for each critical phase of the WS process, with the aim of achieving the most successful and highest-quality gel-4VBC fibre production. Factors such as dope composition, coagulation bath formulation, spinning conditions, and post-spin treatments have been systematically evaluated and fine-tuned to ensure optimal fibre formation, morphology, and

Figure 4.15: *Photograph showing the wet stability of RWS fibre bundles (dry bundle shown previously in* ***Figure 26****) following a 1-month-incubation period in DI water at 37°C.*

properties. This precise optimisation approach has been instrumental in overcoming the challenges associated with the wet spinning of biopolymer-based materials and has enabled the production of Gel-4VBC fibres with desirable characteristics for potential applications in tissue engineering and regenerative medicine. The optimised parameters presented in **Table 4.10** represent the culmination of extensive experimentation and iterative refinement, incorporating insights from literature and empirical observations. By carefully controlling and optimising these critical parameters, the research has paved the way for the successful production of Gel-4VBC fibres with enhanced bioreceptivity, mechanical properties, and potential for integration with biological systems.

The optimal rotating speed for the laboratory RWS set-up employed in this project was not investigated due to certain limitations, due to a lack of appropriate equipment such as an automated turntable or similar apparatus to facilitate controlled and consistent rotation of the coagulation bath container. Instead, the rotation was manually performed by the author, which involved spinning the coagulation bath container within the ice bath, which proved successful in facilitating the RWS process but did not allow for precise measurement or control of the rotation speed. Consequently, it was not possible to

Table 4.9: *Sample weight before and after incubation in a 37°C water bath for 24 hours and one-month.*

Condition	Sample original weight (g)	Sample weight following incubation (g)
Incubation at 37°C for 24-hours	0.833	0.907
Incubation at 37°C for 1-month	1.051	1.242

quantitatively assess the spin speed in a reliable and reproducible manner, limiting the determination of an optimal rotating speed for the specific RWS set-up. Despite these limitations, investigating the optimal rotating speed could be an interesting avenue for future work. Potential approaches include incorporating an automated turntable or rotating mechanism, integrating rotational speed sensors, and conducting comparative studies between fibers produced at different controlled rotation speeds. Exploring the optimal rotating speed could potentially lead to improvements in fiber quality, reproducibility, and process control by addressing the limitations of the current manual rotation method and providing valuable insights into the role of spin speed in the wet spinning process and its impact on the resulting fiber properties.

Table 4.10: *Parameters table for the dope and coagulation bath.*

Dope component	**Quantity**	**Notes**
Gel-4VBC	20% w/v	Heated to 65 °C and stirred until dissolved at 650 rpm
AcOH	80% w/v	
I2959	2 wt.%	

Coagulation bath component	**Quantity**	**Notes**
EtOH	100% w/v	Held at 2°C; 10 s coagulation time

Extrusion component	**Feature**	**Notes**
Needle	21 G	Rotating bath
Dope extrusion	**0.6 ml/min**	**Dope held at 65°C prior to extrusion**

Post-spin treatment component	**Feature**	**Notes**
Draw ratio	75%	Increase in length from l_0
Cure duration	30 minutes	Irradiated at 365 nm

Chapter 5

Conclusion and Recommendations for Further Work

5.1 Conclusions from Research

This body of research aimed to assess the feasibility of scaled-up RWS manufacturing processes of novel F-gelatin-based filament fibres, crosslinked with 4VBC and a I2959 curing agent. Building on literature previously published by Rickman et al. [307], both chemical and process optimisation was conducted at each stage of the WS process in order to boost spin efficiency through the reduction of time taken to spin continuous fibres. Overall, this was achieved through the implementation of an alcohol-based coagulation bath and the control of spinning temperature at both the extrusion and coagulation stages. In addition, the supplementation of a UV-curing agent in the dope solution removed the need to a post-spin curing/wash bath, as had previously been required. The free radicals generated from I2959 are compatible with the amino groups present in gelatin, allowing for the crosslinking of gelatin and the formation of a stable hydrogel matrix. This approach demonstrated the potential for improved manufacture speed, as well as reducing the overall quantities of materials required to spin f-gelatin fibres (through the removal of supplementary baths). Processibility was further improved through UV-cure dissolvability studies which revealed I2959 could be integrated into the fibre at either the dissolution, coagulation, or supplementary bath stages; prompting an investigation into seeing whether the need for additional cure/wash stages could be re-

duces, so to minimise the number of materials required for gel-4VBC fibre manufacture. Ultimately, presenting the advantages of an experimental one-step WS and crosslinking production line, which reducing manufacturing time and addressing the challenge of transferring un-crosslinked fibres between baths and WS stages. In dissolving 2 wt.% I2959 into the dope and curing spun fibres once dry was found to be the most efficient option as this prevented over-coagulation of the fibres in a curing/coagulation solution.

Experiments employed a RWS laboratory set up to explore all parts of the WS process, including potential coagulants, the effect of temperature, and drawing/curing optimisation. Ultimately both EtOH and IPA proved to be successful coagulants for the gel-4VBC dope and were able to initiate a phase transition of the polymer solution within a matter of seconds, greatly reducing the speed of production from over 60-minutes [307], to less than a minute. Collagen and gelatin are soluble in aqueous solutions, so using a water-based coagulation bath can lead to dissolution of the extruded dope. Alcohols act as non-solvents, preventing the dope from dissolving and allowing fibre formation [241]. Alcohols like ethanol have a lower polarity compared to water, which causes rapid dehydration and solidification of the gelatin polymer dope when extruded into the coagulation bath. It was observed that in employing an alcohol-based bath to initiate the phase separation, a more homogenous fibre, with a greater potential for scaled-up production was made feasible. Drawing and curing optimisation of these fibres investigated the effects on stress/strain values, and swelling behaviours through optical microscopy and tensile testing (Instron 5544). Typically, fibres that underwent a longer duration of curing (30 and 45 minutes) experienced a greater stability in wet conditions, as opposed to fibres cured for only 1 minute. However these positive findings were mitigated by an increase in brittleness in the case of the ”45 minute cure” condition In addition, a positive correlation between UV-cure duration and axial load limits was observed, indicating a strong positive relationship between degree of polymerisation (UV-curing) and stress values. Unfortunately, strain values were varied and did not reveal any trends between fibre drawing/curing and overall displacement limits during tensile testing.

5.2 Recommendations for Further Work

Further exploration into WS gel-4VBC fibres could facilitate greater development of these novel filaments, as well as improve overall stress-strain relationships. As already discussed **(Section 4.9)**, the optimisation of rotation speed would be an interesting continuation of this project. Other areas of interest could be further controlling ambient conditions, such as temperature, humidity, and air flow, during the RWS process. Additionally, the impacts of drawing and post-processing techniques, especially on fibre properties, require additional investigation. Drawing and curing optimisation studies were carried out on short (5-10 mm) fibres due to a lack of access to a purpose-built drawing/fibre collection rig, which may limit the generalisation of findings to continuous fibres. Therefore, further development of continuous fibre production processes, including fibre drawing, collection, and post-processing techniques on longer lengths of fibre, is crucial for enabling the manufacturing of long, continuous Gel-4VBC fibres for various applications.

Finally, PEG was explored as a potential plasticiser to improve fibre handleability due to its use in previous research [307], and due to its availability to the author throughout this project. While it produced disappointing results, further research on more compatible plasticisers, such as sugars or polyols could be an area of potential further research.

5.2.1 Circular Bioeconomies Within Healthcare Materials

A CBE is a relatively new economic growth model that combines the principles of the circular economy (slowing, narrowing, and closing material resource loops) with the sustainable use of biological resources [257][361]. The expanding use of f-gelatin (such as gel-4VBC) could aid in the development of CBE within medical device development applications. The implementation of CBE within biomaterial and medical device applications presents a paradigm shift towards sustainable and regenerative practices in the healthcare sector; deviating from the more commonly used synthetic polymer plastics [255]. Gelatin (such as that explored in this paper) has the potential to play a crucial role in CBE, particularly in the sphere of medical devices [273][38]. Offering great versatility and biocompatibility, gelatin's biodegradability places the protein as an eco-friendly

choice, aligning with CBE principles focused on waste reduction and recycling. In addition, a shift toward CBE presents potential advantageous recycling routed for collagen and gelatin surplus resources, such as slaughterhouse waste [297][42], which can emphasise local and sustainable sourcing of gelatin from animal by-products, that would otherwise be incinerated [111][159].

5.2.2 Feasibility of Scaled-up Production

As discussed in **Section 4.6.3**, it was believed that the application of a slight draw of the fibre as it entered the coagulation bath, facilitated by the rotational component of the coagulation bath was fundamental in the production of good quality filament fibres. Looking to towards scaling up the rotation mechanism to accommodate larger bath volumes and higher production rates, may pose engineering challenges. The rotating components would need to be designed and constructed to withstand the increased loads and stresses associated with larger-scale operations. Therefore, maintaining uniform coagulation conditions may become more challenging as the production scale increases.

An alternative approach to the coagulation bath setup involves the use of a serpentine-type bath, where the neo-fibre passes through an extended cylindrical tube in a serpentine-like configuration, containing the coagulation fluid before being wound and collected. This design offers several advantages over conventional straight-path coagulation baths. Firstly, the longer path through the serpentine bath facilitates more efficient solvent exchange between the neo-fibre and the non-solvent in the coagulation bath, leading to improved fibre morphology and properties. Secondly, the cylindrical tube design provides a confined and controlled environment for the coagulation process, minimising disturbances and ensuring consistent coagulation conditions along the fibre path. Moreover, the serpentine path design for the coagulation bath could be further enhanced by introducing controlled movement of the coagulation solution. This can be achieved by flushing the coagulation fluid through the serpentine system at a predetermined flow rate. Such a dynamic coagulation environment would facilitate rapid coagulation and initial drawing of the fibres as they traverse the coagulation system. The combination of the serpentine path and controlled fluid flow would offer several advantages, including efficient solvent exchange, uniform coagulation conditions, and the ability to tailor the coagulation rate and initial drawing of the fibres by adjusting the flow rate and path

dimensions.

5.3 Applications of Optimised Fibres

5.3.1 Bioresceptive Attachment of Tendon and Muscle Fibres

Repairing ruptured tendons at the MTJ presents significant challenges due to the intermeshing of native tendon and muscle tissues that create a complex interface. **Figure 2.13c** depicts the complex interdigitation and interlocking of the tendon fibres and terminal muscle fibres (myocytes) within the MTJ. While advantageous in facilitating efficient force transition through a joint, this structure further complicates the reconstruction process: both on a cellular and surgical level, making successful repairs challenging to achieve. Tendons exhibit a slow healing process attributed to their hypocellular and hypo-vascular nature, resulting in limited cell presence and blood supply, which reduces both the rate and quality of healing. Moreover, the absence of a universally accepted standard for suture materials, techniques, and rehabilitation protocols adds complexity to tendon repair procedures.

5.3.2 Tendon Healing

Despite significant advancements in commercial benchmarks for flexor tendon surgery, the bio-imitation of natural tendon or muscle tissue is often overlooked in favor of rigid woven or braided textiles [395][29][136][296][28]. While these materials provide good mechanical strength to the joint system, the vast dissimilarity between tendon implants and native tissue often restricts natural movement and flexibility, and limits effective cell proliferation [416], impacting overall functionality post-reconstruction and hindering the healing process, potentially leading to suboptimal outcomes [177][386]. Considering the current challenges in reconstructing ruptured muscle-tendon junctions (MTJ), it could be inferred that the production of a biocompatible and bio-receptive scaffold material that enables fibre reintegration and supports fibre anchorage at the tendon-muscle interface could be beneficial in the repair of ruptured tendons, rather than conventional tendon reconstructive methods.

5.3.3 Warp Knitted Structures

To address the challenges associated with tendon repair procedures, the author to hypothesise the development of these fibres into warp knitted structures (**Figure 5.1a**), that exhibit a gradient quality along the length of the material; imitating a similar gradient to that observed along the length of the aformantioned MTJ. Differing from conventional weft knit structures **(Figure 5.1b)** Warp knits offer the advantage of creating fabrics with a vertical pattern, where each loop is formed from separate lengthwise yarns, allowing for precise control over the alignment and orientation of fibres. This capability enables the replication of the longitudinally aligned structure found in tendons and muscles, mimicking their natural arrangement for enhanced biomimicry. Additionally, warp knitted fabrics exhibit excellent dimensional stability and strength, making them ideal for applications requiring structural integrity and load-bearing capacity, similar to the requirements of tendon and muscle tissues. The controlled variation in density and alignment achievable through warp knitting allows for tailored characteristics that closely resemble the hierarchical organisation of natural tendon and muscle fibres, making warp knitted structures a preferred choice for biomimetic applications in tissue engineering and regenerative medicine. Warp knitting has proven attractive due to its ability to offer a versatile platform for producing complex medical textiles with tailored properties. It has been successfully implemented in a variety of *in vivo* biomedical applications, such as hernia repair meshes, artificial arteries, and as reinforcement scaffolds for organs, hearts, and bladders. The dynamic structure and adaptability of warp knitted textiles make them ideal for these complex medical textile applications, benefiting from controlled stretch, design versatility, and the ability to customise mechanical performance.

The dynamic structure and adaptability of warp knitted textiles make them well-suited for complex medical textile applications, such as artificial arteries, hernia repair meshes, hollow organ support and reinforcement, heart valves, tissue scaffolds, and cardiac support devices [446]. These applications benefit from the controlled stretch, design versatility, and the ability to customise the mechanical performance of the output fabric, which can be precisely managed through the warp knitting process. Warp knitted textiles have the ability to exhibit density gradients along their length, a quality that can be advantageous for certain applications. Creating a density gradient in warp knitted mate-

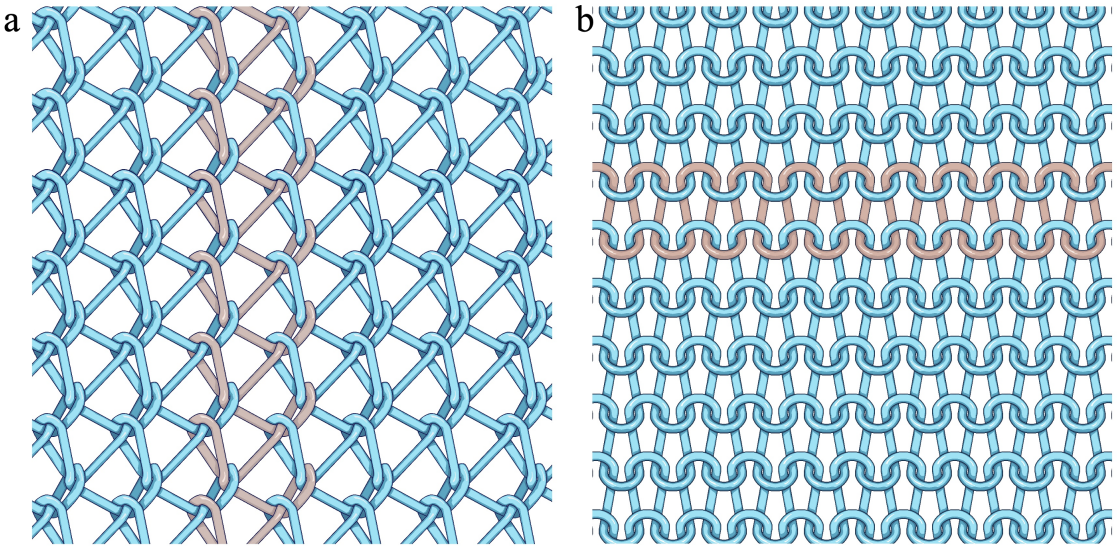

Figure 5.1: *Illustrations of (a) warp knit and (b) weft knit structures*

rials involves manipulating the fabric density across its structure by varying the number of yarns per unit area in specific sections. This can result in a gradient from low to high density, or vice versa. By adjusting the density of the warp knitted material, different mechanical and structural properties can be imparted to the fabric, influencing factors such as fabric thickness, tensile strength, bending properties, and overall performance. This controlled variation in density allows for tailored characteristics in the fabric, enhancing its functionality and suitability for specific applications.

The versatility of warp knitting technology allows for the design of textiles that mimic the longitudinal alignment and mechanical properties of tendons, offering a promising solution for enhancing tendon reconstruction outcomes. The unique suitability of biomimetic warp knits for tendon reconstruction lies in their ability to closely mimic the hierarchical structure and mechanical properties of natural tendons. By replicating the longitudinal alignment and controlled density gradients found in tendons, these warp knitted fabrics can provide tailored support for tendon repair. These biomimetic warp knitted materials offer a combination of structural mimicry and customised functionality, promoting cellular regrowth and tissue integration, which are crucial for effective tendon reconstruction. The ability to replicate the hierarchical organisation and mechanical properties of native tendons through controlled density gradients and longitudinal fibre alignment makes biomimetic warp knits a promising solution for enhancing tendon reconstruction outcomes and facilitating successful tissue repair.

References

[1] en-DE. N.D. URL: https://www.medi.de/en/diagnosis-treatment/ankle-pain/anatomy-achilles-tendon/.

[2] Census 2021. *National life tables – life expectancy in the UK - Office for National Statistics*. 2021. URL: https://www.ons.gov.uk/peoplepopulationandcommun birthsdeathsandmarriages/lifeexpectancies/bulletins/nationallifetablesunitedkingdom/2018to2020.

[3] Chemical Compound Deep Data Source 2022. *Structure Deep Data of 4-Vinylbenzyl chloride (C9H9Cl)*. en-US. URL: https://www.molinstincts.com/structure/.

[4] Sport England 2023. *Adults' activity levels in England bounce back to pre-pandemic levels — Sport England*. en. 2023. URL: https://www.sportengland.org/news/adults-activity-levels-england-bounce-back-pre-pandemic-levels.

[5] Nergis Abay et al. "Bone formation from porcine dental germ stem cells on surface modified polybutylene succinate scaffolds". In: *Stem Cells International* 2016 (2016).

[6] Shalimar Abdullah. "Usage of synthetic tendons in tendon reconstruction". In: *BMC Proceedings*. Vol. 9. Suppl 3. Springer. 2015, A68.

[7] Samson Afewerki et al. "Gelatin-polysaccharide composite scaffolds for 3D cell culture and tissue engineering: towards natural therapeutics". In: *Bioengineering & translational medicine* 4.1 (2019), pp. 96–115.

[8] Shabbir Ahammed et al. "Improvement of the water resistance and ductility of gelatin film by zein". In: *Food Hydrocolloids* 105 (2020), p. 105804.

[9] Abdul Latif Ahmad, Tunmise A Otitoju, and Boon S Ooi. "Hollow fiber (HF) membrane fabrication: A review on the effects of solution spinning conditions

on morphology and performance". In: *Journal of industrial and engineering chemistry* 70 (2019), pp. 35–50.

[10] J Ahmed. "Rheological properties of gelatin and advances in measurement". In: *Advances in food rheology and its applications*. Elsevier, 2017, pp. 377–404.

[11] Hyunchul Ahn et al. "Microstructure and mechanical properties of polyacrylonitrile precursor fiber with dry and wet drawing process". In: *Polymers* 13.10 (2021), p. 1613.

[12] Basheer Al-Shammari et al. "The effect of polymer concentration and temperature on the rheological behavior of metallocene linear low density polyethylene (mLLDPE) solutions". In: *Journal of King Saud University-Engineering Sciences* 23.1 (2011), pp. 9–14.

[13] Israel DL Albert, Tobin J Marks, and Mark A Ratner. "Rational design of molecules with large hyperpolarizabilities. Electric field, solvent polarity, and bond length alternation effects on merocyanine dye linear and nonlinear optical properties". In: *The Journal of Physical Chemistry* 100.23 (1996), pp. 9714–9725.

[14] Frank A Alexander Jr et al. "A parameter study for 3D-printing organized nanofibrous collagen scaffolds using direct-write electrospinning". In: *Materials* 12.24 (2019), p. 4131.

[15] Mohammad B Aljaber et al. "Influence of Gelatin Source and Bloom Number on Gelatin Methacryloyl Hydrogels Mechanical and Biological Properties for Muscle Regeneration". In: *Biomolecules* 13.5 (2023), p. 811.

[16] Laith Alrubaiy and Kathem K Al-Rubaiy. "Skin substitutes: a brief review of types and clinical applications". In: *Oman medical journal* 24.1 (2009), p. 4.

[17] Aayeena Altaf et al. "A comprehensive review of polysaccharide-based bionanocomposites for food packaging applications". In: *Discover Food* 2.1 (2022), p. 10.

[18] M Amirilargani et al. "Effects of coagulation bath temperature and polyvinylpyrrolidone content on flat sheet asymmetric polyethersulfone membranes". In: *Polymer Engineering & Science* 50.5 (2010), pp. 885–893.

[19] Jovito G Angeles, Heather Heminger, and Daniel P Mass. "Comparative biomechanical performances of 4-strand core suture repairs for zone II flexor tendon lacerations". In: *The Journal of hand surgery* 27.3 (2002), pp. 508–517.

[20] AA Apostolov et al. “Mechanical properties of native and crosslinked gelatins in a bending deformation”. In: *Journal of Applied Polymer Science* 76.14 (2000), pp. 2041–2048.

[21] M Tarik Arafat et al. “Biomimetic wet-stable fibres via wet spinning and diacid-based crosslinking of collagen triple helices”. In: *Polymer* 77 (2015), pp. 102–112.

[22] Fatih Arican et al. “Fabrication of gelatin nanofiber webs via centrifugal spinning for N95 respiratory filters”. In: *Bulletin of Materials Science* 45.2 (2022), p. 93.

[23] Jaweria Ashfaq et al. “Gelatin-and Papaya-Based Biodegradable and Edible Packaging Films to Counter Plastic Waste Generation”. In: *Materials* 15.3 (2022), p. 1046.

[24] Muhammad Aqeel Ashraf et al. “Green biocides, a promising technology: current and future applications to industry and industrial processes”. In: *Journal of the Science of Food and Agriculture* 94.3 (2014), pp. 388–403.

[25] Zhongxue Bai et al. “Versatile nano–micro collagen fiber-based wearable electronics for health monitoring and thermal management”. In: *Journal of Materials Chemistry A* 11.2 (2023), pp. 726–741.

[26] Nur Fateha Bakry, MIN Isa, and Norizah Mhd Sarbon. “Effect of sorbitol at different concentrations on the functional properties of gelatin/carboxymethyl cellulose (CMC)/chitosan composite films”. In: *International Food Research Journal* (2017).

[27] Preethi Balasubramanian et al. “Collagen in human tissues: structure, function, and biomedical implications from a tissue engineering perspective”. In: *Polymer Composites–Polyolefin Fractionation–Polymeric Peptidomimetics–Collagens* (2013), pp. 173–206.

[28] Michał Banaś et al. “Clinical assessment and comparison of ACL reconstruction using synthetic graft (Neoligaments versus FiberTape)”. In: *Advances in Clinical and Experimental Medicine* 30.5 (2021).

[29] John G Barber et al. “Braided nanofibrous scaffold for tendon and ligament tissue engineering”. In: *Tissue Engineering Part A* 19.11-12 (2013), pp. 1265–1274.

[30] Troels Barfred. “Achilles tendon rupture: aetiology and pathogenesis of subcutaneous rupture assessed on the basis of the literature and rupture experiments on rats”. In: *Acta Orthopaedica Scandinavica* 44.sup152 (1973), pp. 1–126.

[31] Kimberly A Barrie et al. “Effect of suture locking and suture caliber on fatigue strength of flexor tendon repairs”. In: *The Journal of hand surgery* 26.2 (2001), pp. 340–346.

[32] Kimberly A Barrie et al. “The role of multiple strands and locking sutures on gap formation of flexor tendon repairs during cyclical loading”. In: *The Journal of hand surgery* 25.4 (2000), pp. 714–720.

[33] Poulami Basu, U Narendra Kumar, and I Manjubala. “Wound healing materials–a perspective for skin tissue engineering”. In: *Current Science* (2017), pp. 2392–2404.

[34] Mohamed Basel Bazbouz, He Liang, and Giuseppe Tronci. “A UV-cured nanofibrous membrane of vinylbenzylated gelatin-poly (-caprolactone) dimethacrylate co-network by scalable free surface electrospinning”. In: *Materials Science and Engineering: C* 91 (2018), pp. 541–555.

[35] John M Beiner and Peter Jokl. “Muscle contusion injury and myositis ossificans traumatica”. In: *Clinical Orthopaedics and Related Research®* 403 (2002), S110–S119.

[36] Alvin Bacero Bello et al. “Engineering and functionalization of gelatin biomaterials: From cell culture to medical applications”. In: *Tissue Engineering Part B: Reviews* 26.2 (2020), pp. 164–180.

[37] Luis Beltran et al. “The proximal hamstring muscle–tendon–bone unit: A review of the normal anatomy, biomechanics, and pathophysiology”. In: *European journal of radiology* 81.12 (2012), pp. 3772–3779.

[38] Elyor Berdimurodov et al. “Green Electrospun Nanofibers for Biomedicine and Biotechnology”. In: *Technologies* 11.5 (2023), p. 150.

[39] Hugues Berry et al. “Gel–sol transition can describe the proteolysis of extracellular matrix gels”. In: *Biochimica et Biophysica Acta (BBA)-General Subjects* 1524.2-3 (2000), pp. 110–117.

[40] James L Beskin et al. “Surgical repair of Achilles tendon ruptures”. In: *The American journal of sports medicine* 15.1 (1987), pp. 1–8.

[41] Saurabh Bhatia et al. “A comparative study of the properties of gelatin (porcine and bovine)-based edible films loaded with spearmint essential oil”. In: *Biomimetics* 8.2 (2023), p. 172.

[42] Ankita Bhowmik et al. “Development of a Novel Helical-Ribbon Mixer Dryer for Conversion of Rural Slaughterhouse Wastes to an Organic Fertilizer and Implications in the Rural Circular Economy”. In: *Sustainability* 13.16 (2021), p. 9455.

[43] Maria Bikuna-Izagirre, Javier Aldazabal, and Jacobo Paredes. “Gelatin blends enhance performance of electrospun polymeric scaffolds in comparison to coating protocols”. In: *Polymers* 14.7 (2022), p. 1311.

[44] Helen L Birch, Chavaunne T Thorpe, and Adam P Rumian. “Specialisation of extracellular matrix for function in tendons and ligaments”. In: *Muscles, ligaments and tendons journal* 3.1 (2013), p. 12.

[45] Britani N Blackstone, Summer C Gallentine, and Heather M Powell. “Collagen-based electrospun materials for tissue engineering: A systematic review”. In: *Bioengineering* 8.3 (2021), p. 39.

[46] Gregory Bohn et al. “Ovine-based collagen matrix dressing: next-generation collagen dressing for wound care”. In: *Advances in wound care* 5.1 (2016), pp. 1–10.

[47] Pascal Boileau et al. “Arthroscopic repair of full-thickness tears of the supraspinatus: does the tendon really heal?” In: *JBJS* 87.6 (2005), pp. 1229–1240.

[48] S Bowald, C Busch, and I Eriksson. “Absorbable material in vascular prostheses: a new device.” In: *Acta Chirurgica Scandinavica* 146.6 (1980), pp. 391–395.

[49] Staffan Bowald, Christer Busch, and Ingvar Eriksson. “Arterial regeneration following polyglactin 910 suture mesh grafting”. In: *Surgery* 86.5 (1979), pp. 722–729.

[50] Laurent Bozec and Marianne Odlyha. “Thermal denaturation studies of collagen by microthermal analysis and atomic force microscopy”. In: *Biophysical journal* 101.1 (2011), pp. 228–236.

[51] Jef Brebels and Arn Mignon. “Polymer-based constructs for flexor tendon repair: a review”. In: *Polymers* 14.5 (2022), p. 867.

[52] Michael Brodie et al. “Biomechanical properties of Achilles tendon repair augmented with a bioadhesive-coated scaffold”. In: *Biomedical materials* 6.1 (2011), p. 015014.

[53] J Bruns et al. “Achilles tendon rupture: experimental results on spontaneous repair in a sheep-model”. In: *Knee Surgery, Sports Traumatology, Arthroscopy* 8.6 (2000), pp. 364–369.

[54] Leah Burrows. *A new spin on nanofibers*. 2016. URL: https://seas.harvard.edu/news/2016/10/new-spin-nanofibers.

[55] Laura Buttafoco et al. “Electrospinning of collagen and elastin for tissue engineering applications”. In: *Biomaterials* 27.5 (2006), pp. 724–734.

[56] Mari C Echave et al. “Gelatin as biomaterial for tissue engineering”. In: *Current pharmaceutical design* 23.24 (2017), pp. 3567–3584.

[57] Shaobo Cai et al. “Novel 3D electrospun scaffolds with fibers oriented randomly and evenly in three dimensions to closely mimic the unique architectures of extracellular matrices in soft tissues: fabrication and mechanism study”. In: *Langmuir* 29.7 (2013), pp. 2311–2318.

[58] Isabel Calejo et al. “A textile platform using continuous aligned and textured composite microfibers to engineer tendon-to-bone interface gradient scaffolds”. In: *Advanced Healthcare Materials* 8.15 (2019), p. 1900200.

[59] Chiara Emma Campiglio et al. “Cross-linking strategies for electrospun gelatin scaffolds”. In: *Materials* 12.15 (2019), p. 2476.

[60] Wayne Carver, Edie C Goldsmith, et al. “Regulation of tissue fibrosis by the biomechanical environment”. In: *BioMed research international* 2013 (2013).

[61] John F Cavallaro, Paul D Kemp, and Karl H Kraus. “Collagen fabrics as biomaterials”. In: *Biotechnology and bioengineering* 43.8 (1994), pp. 781–791.

[62] Jeffrey M Caves et al. “Fibrillogenesis in continuously spun synthetic collagen fiber”. In: *Journal of Biomedical Materials Research Part B: Applied Biomaterials: An Official Journal of The Society for Biomaterials, The Japanese Society for Biomaterials, and The Australian Society for Biomaterials and the Korean Society for Biomaterials* 93.1 (2010), pp. 24–38.

[63] Patricia Cazón et al. “Polysaccharide-based films and coatings for food packaging: A review”. In: *Food Hydrocolloids* 68 (2017), pp. 136–148.

[64] Nehar Celikkin et al. “Combining rotary wet-spinning biofabrication and electromechanical stimulation for the in vitro production of functional myo-substitutes”. In: *Biofabrication* 15.4 (2023), p. 045012.

[65] John M Centanni et al. *StrataGraft skin substitute is well-tolerated and is not acutely immunogenic in patients with traumatic wounds: results from a prospective, randomized, controlled dose escalation trial*. 2011.

[66] Jimmy J Chan et al. “Epidemiology of Achilles tendon injuries in collegiate level athletes in the United States”. In: *International Orthopaedics* 44 (2020), pp. 585–594.

[67] Daniel K Chang et al. “The basics of integra dermal regeneration template and its expanding clinical applications”. In: *Seminars in plastic surgery*. Vol. 33. 03. Thieme Medical Publishers. 2019, pp. 185–189.

[68] Thitirat Chaochai et al. “Preparation and properties of gelatin fibers fabricated by dry spinning”. In: *Fibers* 4.1 (2016), p. 2.

[69] Hongbo Chen et al. “Application of protein-based films and coatings for food packaging: A review”. In: *Polymers* 11.12 (2019), p. 2039.

[70] Yi-Ming Chen et al. “Supplementation of L-Arginine, L-Glutamine, Vitamin C, Vitamin E, folic acid, and green tea extract enhances serum nitric oxide content and antifatigue activity in mice”. In: *Evidence-Based Complementary and Alternative Medicine* 2020 (2020).

[71] Kiho Cho et al. “Dental resin composites: A review on materials to product realizations”. In: *Composites Part B: Engineering* 230 (2022), p. 109495.

[72] Sita T Clark et al. “Epidemiology of tendon and ligament injuries in Aotearoa/New Zealand between 2010 and 2016”. In: *Injury epidemiology* 7 (2020), pp. 1–10.

[73] Robert AE Clayton and Charles M Court-Brown. “The epidemiology of musculoskeletal tendinous and ligamentous injuries”. In: *Injury* 39.12 (2008), pp. 1338–1344.

[74] Daniela Coppola et al. “Marine collagen from alternative and sustainable sources: Extraction, processing and applications”. In: *Marine drugs* 18.4 (2020), p. 214.

[75] Francesca Corduas, Dimitrios A Lamprou, and Elena Mancuso. “Next-generation surgical meshes for drug delivery and tissue engineering applications: materials,

design and emerging manufacturing technologies". In: *Bio-Design and Manufacturing* 4 (2021), pp. 278–310.

[76] Carmelo Corsaro et al. "Hydrophilicity and hydrophobicity: Key aspects for biomedical and technological purposes". In: *Physica A: Statistical Mechanics and its Applications* 580 (2021), p. 126189.

[77] Matthew L Costa et al. "Plaster cast versus functional bracing for Achilles tendon rupture: the UKSTAR RCT." In: *Health Technology Assessment (Winchester, England)* 24.8 (2020), p. 1.

[78] Marco Costantini et al. "Co-axial wet-spinning in 3D bioprinting: state of the art and future perspective of microfluidic integration". In: *Biofabrication* 11.1 (2018), p. 012001.

[79] Alexander Croog et al. "Comparative biomechanic performances of locked cruciate four-strand flexor tendon repairs in an ex vivo porcine model". In: *The Journal of hand surgery* 32.2 (2007), pp. 225–232.

[80] Bing Cui et al. "Development and characterization of edible plant-based fibers using a wet-spinning technique". In: *Food Hydrocolloids* 133 (2022), p. 107965.

[81] Bing Cui et al. "Effect of salt on solution behavior of spinning medium and properties of meat analogue fibers". In: *Food Hydrocolloids* 139 (2023), p. 108540.

[82] Qing Cui et al. "Wet-spinning of biocompatible core–shell polyelectrolyte complex fibers for tissue engineering". In: *Advanced Materials Interfaces* 7.23 (2020), p. 2000849.

[83] Mathew H Cumming et al. "Intra-fibrillar citric acid crosslinking of marine collagen electrospun nanofibres". In: *International journal of biological macromolecules* 114 (2018), pp. 874–881.

[84] Sandra L Curwin. "Biomechanics of tendon and the effects of immobilization". In: *Foot and Ankle Clinics* 2.3 (1997), pp. 371–389.

[85] Stephanie Georgina Dakin et al. "Chronic inflammation is a feature of Achilles tendinopathy and rupture". In: *British journal of sports medicine* 52.6 (2018), pp. 359–367.

[86] Natalia Davidenko et al. "Optimisation of UV irradiation as a binding site conserving method for crosslinking collagen-based scaffolds". In: *Journal of Materials Science: Materials in Medicine* 27 (2016), pp. 1–17.

[87] Kelsey G DeFrates et al. “Protein-based fiber materials in medicine: A review”. In: *Nanomaterials* 8.7 (2018), p. 457.

[88] Peter A Delamere et al. “The Kelvin-Helmholtz Instability From the Perspective of Hybrid Simulations”. In: *Frontiers in Astronomy and Space Sciences* 8 (2021), p. 801824.

[89] Feng Deng et al. “Tendon-inspired fibers from liquid crystalline collagen as the pre-oriented bioink”. In: *International Journal of Biological Macromolecules* 185 (2021), pp. 739–749.

[90] Jianping Deng et al. “Using glycidyl methacrylate as cross-linking agent to prepare thermosensitive hydrogels by a novel one-step method”. In: *Journal of Polymer Science Part A: Polymer Chemistry* 46.6 (2008), pp. 2193–2201.

[91] Svetlana R Derkach et al. “Modified fish gelatin as an alternative to mammalian gelatin in modern food technologies”. In: *Polymers* 12.12 (2020), p. 3051.

[92] Carol DerSarkissian. *Ruptured Tendon: Symptoms, Causes, and Treatments*. en. URL: https://www.webmd.com/fitness-exercise/ruptured-tendon.

[93] CJ Doillon et al. “Collagen-based wound dressings: Control of the pore structure and morphology”. In: *Journal of biomedical materials research* 20.8 (1986), pp. 1219–1228.

[94] Eddy Dona, Mark P Gianoutsos, and William R Walsh. “Optimizing biomechanical performance of the 4-strand cruciate flexor tendon repair”. In: *The Journal of hand surgery* 29.4 (2004), pp. 571–580.

[95] Qinglin Dong et al. “Artificial ligament made from silk protein/Laponite hybrid fibers”. In: *Acta biomaterialia* 106 (2020), pp. 102–113.

[96] Mahmut Nedim Doral et al. “Functional anatomy of the Achilles tendon”. In: *Knee Surgery, Sports Traumatology, Arthroscopy* 18 (2010), pp. 638–643.

[97] Jean-Pierre Draye et al. “In vitro and in vivo biocompatibility of dextran dialdehyde cross-linked gelatin hydrogel films”. In: *Biomaterials* 19.18 (1998), pp. 1677–1687.

[98] Marzia Dulal et al. “Toward sustainable wearable electronic textiles”. In: *ACS nano* 16.12 (2022), pp. 19755–19788.

[99] Judyta Dulnik and Paweł Sajkiewicz. “Crosslinking of gelatin in bicomponent electrospun fibers”. In: *Materials* 14.12 (2021), p. 3391.

[100] Frédéric Dumur. “Recent advances on water-soluble photoinitiators of polymerization”. In: *European Polymer Journal* 189 (2023), p. 111942.

[101] Christopher J Dy et al. “Complications after flexor tendon repair: a systematic review and meta-analysis”. In: *The Journal of hand surgery* 37.3 (2012), pp. 543–551.

[102] Thomas Ebbinghaus, Gregor Lang, and Thomas Scheibel. “Biomimetic polymer fibers—function by design”. In: *Bioinspiration & Biomimetics* 18.4 (2023), p. 041003.

[103] Farah Fahma et al. “Potential Application of Nanocellulose for Filaments Production: A Review”. In: *Journal of Nanostructures* 10.3 (2020), pp. 553–563.

[104] Saeed Farzamfar et al. “Taurine-loaded poly (ε-caprolactone)/gelatin electrospun mat as a potential wound dressing material: In vitro and in vivo evaluation”. In: *Journal of Bioactive and Compatible Polymers* 33.3 (2018), pp. 282–294.

[105] Victor J Ferrans et al. “Pathology of bioprosthetic cardiac valves”. In: *Human Pathology* 18.6 (1987), pp. 586–595.

[106] Charles K Field and Morris D Kerstein. “Overview of wound healing in a moist environment”. In: *The American journal of surgery* 167.1 (1994), S2–S6.

[107] Nina Filip et al. “Biomaterials in orthopedic devices: current issues and future perspectives”. In: *Coatings* 12.10 (2022), p. 1544.

[108] Aurelien Forget et al. “Facile preparation of tissue engineering scaffolds with pore size gradients using the muesli effect and their application to cell spheroid encapsulation”. In: *Journal of Biomedical Materials Research Part B: Applied Biomaterials* 108.6 (2020), pp. 2495–2504.

[109] Dale Forsdyke et al. “Psychosocial factors associated with outcomes of sports injury rehabilitation in competitive athletes: a mixed studies systematic review”. In: *British journal of sports medicine* 50.9 (2016), pp. 537–544.

[110] Piergiorgio Francia et al. “History, prevalence and assessment of limited joint mobility, from stiff hand syndrome to diabetic foot ulcer prevention: a narrative review of the literature”. In: *Current Diabetes Reviews* 14.5 (2018), pp. 411–426.

[111] Ingrid H Franke-Whittle and Heribert Insam. “Treatment alternatives of slaughterhouse wastes, and their effect on the inactivation of different pathogens: A review”. In: *Critical reviews in microbiology* 39.2 (2013), pp. 139–151.

[112] Christian Frantz, Kathleen M Stewart, and Valerie M Weaver. “The extracellular matrix at a glance”. In: *Journal of cell science* 123.24 (2010), pp. 4195–4200.

[113] A Frinault et al. “Preparation of casein films by a modified wet spinning process”. In: *Journal of Food Science* 62.4 (1997), pp. 744–747.

[114] Kyosuke Fujikawa et al. “Anterior cruciate ligament reconstruction with the Leeds-Keio artificial ligament”. In: *Journal of long-term effects of medical implants* 10.4 (2000).

[115] Ryohei Fukae, Asuka Maekawa, and Osamu Sangen. “Gel-spinning and drawing of gelatin”. In: *Polymer* 46.25 (2005), pp. 11193–11194.

[116] Ryohei Fukae and Takehiko Midorikawa. “Preparation of gelatin fiber by gel spinning and its mechanical properties”. In: *Journal of applied polymer science* 110.6 (2008), pp. 4011–4015.

[117] Benu George et al. “Bioinspired gelatin based sticky hydrogel for diverse surfaces in burn wound care”. In: *Scientific Reports* 12.1 (2022), p. 13735.

[118] Jeam Marcel Geremia et al. “The structural and mechanical properties of the Achilles tendon 2 years after surgical repair”. In: *Clinical Biomechanics* 30.5 (2015), pp. 485–492.

[119] Mehran Ghasemlou et al. “Characterization of edible emulsified films with low affinity to water based on kefiran and oleic acid”. In: *International journal of biological macromolecules* 49.3 (2011), pp. 378–384.

[120] Eric Giza et al. “Augmented tendon Achilles repair using a tissue reinforcement scaffold: a biomechanical study”. In: *Foot & Ankle International* 32.5 (2011), pp. 545–549.

[121] S Gogolewski and AJ Pennings. “High-modulus fibres of nylon-6 prepared by a dry-spinning method”. In: *Polymer* 26.9 (1985), pp. 1394–1400.

[122] MC Gómez-Guillén et al. “Fish gelatin: a renewable material for developing active biodegradable films”. In: *Trends in Food Science & Technology* 20.1 (2009), pp. 3–16.

[123] MC Gómez-Guillén et al. “Functional and bioactive properties of collagen and gelatin from alternative sources: A review”. In: *Food hydrocolloids* 25.8 (2011), pp. 1813–1827.

[124] Selestina Gorgieva and Vanja Kokol. “Collagen-vs. gelatine-based biomaterials and their biocompatibility: review and perspectives”. In: *Biomaterials applications for nanomedicine* 2 (2011), pp. 17–52.

[125] Howard P Greisler. “Arterial regeneration over absorbable prostheses”. In: *Archives of Surgery* 117.11 (1982), pp. 1425–1431.

[126] Howard P Greisler et al. “Derivation of neointima in vascular grafts.” In: *Circulation* 78.3 Pt 2 (1988), pp. I6–12.

[127] Roberto Guizzardi et al. “Gelatin-based hydrogels through homobifunctional triazolinediones targeting tyrosine residues”. In: *Molecules* 24.3 (2019), p. 589.

[128] David P Gwynne-Jones and Martyn Sims. “Epidemiology and outcomes of acute Achilles tendon rupture with operative or nonoperative treatment using an identical functional bracing protocol”. In: *Foot & Ankle International* 32.4 (2011), pp. 337–343.

[129] RMRN Hafidz et al. “Chemical and functional properties of bovine and porcine skin gelatin”. In: *International Food Research Journal* 18.2 (2011), pp. 787–791.

[130] MR Hait. “Microcrystalline collagen. A new hemostatic agent”. In: *American journal of surgery* 120.3 (1970), p. 330.

[131] Shanshan Han et al. “3D Electrospun nanofiber-based scaffolds: from preparations and properties to tissue regeneration applications”. In: *Stem cells international* 2021 (2021).

[132] ZA Nur Hanani, Yrjo H Roos, and Joseph P Kerry. “Use and application of gelatin as potential biodegradable packaging materials for food products”. In: *International journal of biological macromolecules* 71 (2014), pp. 94–102.

[133] ZA Nur Hanani et al. “Extrusion of gelatin-based composite films: Effects of processing temperature and pH of film forming solution on mechanical and barrier properties of manufactured films”. In: *Food Packaging and Shelf Life* 2.2 (2014), pp. 91–101.

[134] Meenu Hans et al. “Production of first-and second-generation ethanol for use in alcohol-based hand sanitizers and disinfectants in India”. In: *Biomass Conversion and Biorefinery* 13.9 (2023), pp. 7423–7440.

[135] Rhiannon Harries, Jared Torkington, and Keith Harding. “Advances in Acellular Extracellular Matrices (ECM) for Wound Healing”. In: *Skin Tissue Engineering and Regenerative Medicine* (2016), p. 125.

[136] Max Haverfield. “Tissue Fixation System (TFS) neoligament pelvic organ repair procedures-12 and 24 month results”. In: *Pelviperineology* 34.3 (2015), p. 70.

[137] Jinmeng He et al. “The structural and functional differences between three species of fish scale gelatin and pigskin gelatin”. In: *Foods* 11.24 (2022), p. 3960.

[138] Gregory William Hess. “Achilles tendon rupture: a review of etiology, population, anatomy, risk factors, and injury prevention”. In: *Foot & ankle specialist* 3.1 (2010), pp. 29–32.

[139] KM Hirpara et al. “A biomechanical analysis of multistrand repairs with the Silfverskiöld peripheral cross-stitch”. In: *The Journal of Bone & Joint Surgery British Volume* 89.10 (2007), pp. 1396–1401.

[140] Eva Hoch et al. “Stiff gelatin hydrogels can be photo-chemically synthesized from low viscous gelatin solutions using molecularly functionalized gelatin with a high degree of methacrylation”. In: *Journal of Materials Science: Materials in Medicine* 23 (2012), pp. 2607–2617.

[141] JP Hodde et al. “Vascular endothelial growth factor in porcine-derived extracellular matrix”. In: *Endothelium* 8.1 (2001), pp. 11–24.

[142] Agnieszka K Hołda and Ivo FJ Vankelecom. “Understanding and guiding the phase inversion process for synthesis of solvent resistant nanofiltration membranes”. In: *Journal of Applied Polymer Science* 132.27 (2015).

[143] Jiyoung Hong et al. “Cell-electrospinning and its application for tissue engineering”. In: *International journal of molecular sciences* 20.24 (2019), p. 6208.

[144] Carlo P Honrado and Craig S Murakami. “Wound healing and physiology of skin flaps”. In: *Facial Plastic Surgery Clinics* 13.2 (2005), pp. 203–214.

[145] NHS Lancashire Teaching Hospitals. *Achilles Tendon Rupture*. English. 2022. URL: https://www.lancsteachinghospitals.nhs.uk/media/.leaflets/64ad6026d55fd3.05861850.pdf.

[146] Joseph A Houghton et al. “Coloration in Flow: The Potential of In Situ Coloration of Casein Fibers to Mitigate Environmental Impact of Traditional Dyeing Methods”. In: *ACS Sustainable Chemistry & Engineering* (2024).

[147] Shirzad Houshian, Thomas Tscherning, and Per Riegels-Nielsen. “The epidemiology of Achilles tendon rupture in a Danish county”. In: *Injury* 29.9 (1998), pp. 651–654.

[148] H Huang and CM Sorensen. “Shear effects during the gelation of aqueous gelatin”. In: *Physical Review E* 53.5 (1996), p. 5075.

[149] Lvxing Huang et al. “Biomimetic scaffolds for tendon tissue regeneration”. In: *Biomimetics* 8.2 (2023), p. 246.

[150] Xuantao Huang et al. “Origin of critical nature and stability enhancement in collagen matrix based biomaterials: Comprehensive modification technologies”. In: *International Journal of Biological Macromolecules* 216 (2022), pp. 741–756.

[151] Yao Huang et al. “Novel fibers fabricated directly from chitin solution and their application as wound dressing”. In: *Journal of Materials Chemistry B* 2.22 (2014), pp. 3427–3432.

[152] Yifei Huang et al. “Anaylsis of birefringence during wound healing and remodeling following alkali burns in rabbit cornea”. In: *Experimental eye research* 73.4 (2001), pp. 521–532.

[153] Jon Hyde. *How Edible Food Packaging Could Reduce Plastic Waste*. en-GB. Mar. 2023. URL: https://www.gmal.co.uk/how-edible-food-packaging-could-reduce-plastic-waste/.

[154] S Ibrahim et al. “Characterization of glycidyl methacrylate–Crosslinked hyaluronan hydrogel scaffolds incorporating elastogenic hyaluronan oligomers”. In: *Acta biomaterialia* 7.2 (2011), pp. 653–665.

[155] Jamorin International. *Glycidyl Methacrylate (GMA)*. en-US. URL: https://jamorin.com/products/glycidyl-methacrylate-gma/.

[156] Mihail Ionescu, Zoran S Petrović, and Xianmei Wan. “Ethoxylated soybean polyols for polyurethanes”. In: *Journal of Polymers and the Environment* 15 (2007), pp. 237–243.

[157] Renato V Iozzo and Alan D Murdoch. “Proteoglycans of the extracellular environment: clues from the gene and protein side offer novel perspectives in molecular diversity and function”. In: *The FASEB Journal* 10.5 (1996), pp. 598–614.

[158] Ahmad Fausi Ismail, SM Ibrahim, and NSB Nasri. “Effects of dope extrusion rate on the morphology and gas separation performance of asymmetric polysulfone hollow fiber membranes for O2/N2 separation”. In: *Songklanakarin J. Sci. Technol* 24 (2002), pp. 833–842.

[159] Grzegorz Izydorczyk et al. “Valorization of poultry slaughterhouse waste for fertilizer purposes as an alternative for thermal utilization methods”. In: *Journal of Hazardous Materials* 424 (2022), p. 127328.

[160] Agata Jabłońska-Trypuć, Marzena Matejczyk, and Stanisław Rosochacki. “Matrix metalloproteinases (MMPs), the main extracellular matrix (ECM) enzymes in collagen degradation, as a target for anticancer drugs”. In: *Journal of enzyme inhibition and medicinal chemistry* 31.sup1 (2016), pp. 177–183.

[161] WNR Jami’An et al. “Effect of evaporation time on cellulose acetate membrane for gas separation”. In: *IOP Conference Series: Earth and Environmental Science*. Vol. 36. 1. IOP Publishing. 2016, p. 012008.

[162] Daniel Jandacka et al. “Do athletes alter their running mechanics after an Achilles tendon rupture?” In: *Journal of foot and ankle research* 10.1 (2017), p. 53.

[163] Hyun-Jun Jang et al. “Wound-healing effects of human dermal components with gelatin dressing”. In: *Journal of biomaterials applications* 32.6 (2018), pp. 716–724.

[164] Tero AH Järvinen et al. “Achilles tendon injuries”. In: *Current opinion in rheumatology* 13.2 (2001), pp. 150–155.

[165] Tero AH Järvinen et al. “Collagen fibres of the spontaneously ruptured human tendons display decreased thickness and crimp angle”. In: *Journal of orthopaedic research* 22.6 (2004), pp. 1303–1309.

[166] DH Jenkins and B McKibbin. “The role of flexible carbon-fibre implants as tendon and ligament substitutes in clinical practice. A preliminary report”. In: *The Journal of Bone & Joint Surgery British Volume* 62.4 (1980), pp. 497–499.

[167] Tiantian Jiao et al. “A benzene chain-based contribution method for prediction of physical properties of aromatic compounds”. In: *Fluid Phase Equilibria* 361 (2014), pp. 60–68.

[168] Toufic R Jildeh et al. “Infection and rerupture after surgical repair of Achilles tendons”. In: *Orthopaedic Journal of Sports Medicine* 6.5 (2018), p. 2325967118774302.

[169] Alberto Jiménez et al. “Effect of re-crystallization on tensile, optical and water vapour barrier properties of corn starch films containing fatty acids”. In: *Food Hydrocolloids* 26.1 (2012), pp. 302–310.

[170] Yanhong Jin et al. “Lignin-based high-performance fibers by textile spinning techniques”. In: *Materials* 14.12 (2021), p. 3378.

[171] Xin Jing et al. “Effect of the amide units in soft segment and urea units in hard segment on microstructures and physical properties of polyurethane elastomer”. In: *Polymer* 233 (2021), p. 124205.

[172] Don Johnson and JP Laboureau. “Cruciate Ligament reconstruction with synthetics”. In: *Posterior cruciate ligament injuries: a practical guide to management*. Springer, 2001, pp. 189–214.

[173] Anthony C Jones et al. “The correlation of pore morphology, interconnectivity and physical properties of 3D ceramic scaffolds with bone ingrowth”. In: *Biomaterials* 30.7 (2009), pp. 1440–1451.

[174] Johan PE Junker et al. “Clinical impact upon wound healing and inflammation in moist, wet, and dry environments”. In: *Advances in wound care* 2.7 (2013), pp. 348–356.

[175] Wichaya Kalaithong et al. “Novel poly (l-lactide-co-caprolactone)/gelatin porous scaffolds for use in articular cartilage tissue engineering: Comparison of electrospinning and wet spinning processing methods”. In: *Polymer Engineering & Science* 57.8 (2017), pp. 875–882.

[176] Min Gyeong Kang et al. “Nanogels derived from fish gelatin: Application to drug delivery system”. In: *Marine drugs* 17.4 (2019), p. 246.

[177] E Karamuk, J Mayer, and G Raeber. “Tissue engineered composite of a woven fabric scaffold with tendon cells, response on mechanical simulation in vitro”. In: *Composites science and technology* 64.6 (2004), pp. 885–891.

[178] Hellmut G Karge and Wilhelm Nießen. “A new method for the study of diffusion and counter-diffusion in zeolites”. In: *Catalysis Today* 8.4 (1991), pp. 451–465.

[179] V Ketharanathan and BRUCE A CHRISTIE. “Glutaraldehyde tanned ovine collagen compared with polytetrafluoroethylene (Gore-tex) as a conduit for small calibre artery substitution; an experimental study in dogs”. In: *Australian and New Zealand Journal of Surgery* 51.6 (1981), pp. 556–561.

[180] Mohammad F Khan et al. “Structure–activity relationship study reveals the molecular basis for specific sensing of hydrophobic amino acids by the Campylobacter jejuni chemoreceptor Tlp3”. In: *Biomolecules* 10.5 (2020), p. 744.

[181] MY Khan et al. “Design of alkaline/surfactant/polymer (ASP) slug and its use in enhanced oil recovery”. In: *Petroleum Science and Technology* 27.17 (2009), pp. 1926–1942.

[182] Hyun Chan Kim et al. “Effect of wet spinning and stretching to enhance mechanical properties of cellulose nanofiber filament”. In: *International Journal of Precision Engineering and Manufacturing-Green Technology* 6 (2019), pp. 567–575.

[183] Ju Yeon Kim et al. “Design of a modified electrospinning for the in-situ fabrication of 3D cotton-like collagen fiber bundle mimetic scaffold”. In: *Materials Letters* 236 (2019), pp. 521–525.

[184] Suhee Kim et al. “Differential matrix metalloprotease (MMP) expression profiles found in aged gingiva”. In: *PloS one* 11.7 (2016), e0158777.

[185] Runa Kinitz et al. “The effect of age and intrinsic aerobic exercise capacity on the expression of inflammation and remodeling markers in rat Achilles tendons”. In: *International journal of molecular sciences* 23.1 (2021), p. 79.

[186] Michael Kjaer. “Role of extracellular matrix in adaptation of tendon and skeletal muscle to mechanical loading”. In: *Physiological reviews* 84.2 (2004), pp. 649–698.

[187] Kim Sarah Koeck et al. “Processing of continuous non-crosslinked collagen fibers for microtissue formation at the muscle-tendon Interface”. In: *Advanced Functional Materials* 32.15 (2022), p. 2112238.

[188] Julia Koehler, Ferdinand P Brandl, and Achim M Goepferich. “Hydrogel wound dressings for bioactive treatment of acute and chronic wounds”. In: *European Polymer Journal* 100 (2018), pp. 1–11.

[189] Margarita Koleva, Desislava Angelova, and Darina Zheleva. “METHODS FOR THE SYNTHESIS OF TiO2 NANOPARTICLES. PROPERTIES OF TEXTILE MATERIALS TREATED WITH TiO2 NANOPARTICLES”. In: *Journal of Chemical Technology and Metallurgy* 59.2 (2024), pp. 301–308.

[190] Paavo V Komi. “Relevance of in vivo force measurements to human biomechanics”. In: *Journal of biomechanics* 23 (1990), pp. 23–34.

[191] Nagavendra Kommineni et al. “Freeze-drying for the preservation of immunoengineering products”. In: *Iscience* 25.10 (2022).

[192] Jan Konasch et al. “Novel 3D printing concept for the fabrication of time-controlled drug delivery systems”. In: *Current Directions in Biomedical Engineering* 4.1 (2018), pp. 141–144.

[193] Thomas J Koob. “Biomimetic approaches to tendon repair”. In: *Comparative Biochemistry and Physiology Part A: Molecular & Integrative Physiology* 133.4 (2002), pp. 1171–1192.

[194] Nikos D Koromilas et al. “Synthesis and self-association in dilute aqueous solution of hydrophobically modified polycations and polyampholytes based on 4-vinylbenzyl chloride”. In: *European Polymer Journal* 54 (2014), pp. 39–51.

[195] G Kovalenko et al. “Electrospun Fibrous Materials Made of Collagen and Chitin Derivatives.” In: *Fibre Chemistry* 48.6 (2017).

[196] Toshihiro Kushibiki et al. “Photocrosslinked gelatin hydrogel improves wound healing and skin flap survival by the sustained release of basic fibroblast growth factor”. In: *Scientific reports* 11.1 (2021), p. 23094.

[197] Martti Kvist. “Achilles tendon injuries in athletes”. In: *Sports medicine* 18 (1994), pp. 173–201.

[198] Nicholas J Lemme et al. “Epidemiology of Achilles tendon ruptures in the United States: athletic and nonathletic injuries from 2012 to 2016”. In: *Orthopaedic journal of sports medicine* 6.11 (2018), p. 2325967118808238.

[199] Nicolas L’heureux et al. “A completely biological tissue-engineered human blood vessel”. In: *The FASEB Journal* 12.1 (1998), pp. 47–56.

[200] Hong-Yun Li, Ying-Hui Hua, et al. “Achilles tendinopathy: current concepts about the basic science and clinical treatments”. In: *BioMed research international* 2016 (2016).

[201] Xiaojing Li et al. “The chemistry and biology of collagen hybridization”. In: *Journal of the American Chemical Society* 145.20 (2023), pp. 10901–10916.

[202] Zhi Jie Li, Qian Qian Yang, and You Lang Zhou. “Basic research on tendon repair: strategies, evaluation, and development”. In: *Frontiers in medicine* 8 (2021), p. 664909.

[203] He Liang et al. “Monomer-induced customization of UV-cured atelocollagen hydrogel networks”. In: *Frontiers in chemistry* 6 (2018), p. 626.

[204] Xiao Tong Liang et al. “Effects of coagulation-bath temperature on the formation process of PVDF-g-PNIPAAm/poly (NIPAAm-co-AAc-L-Phe) membrane”. In: *Applied Mechanics and Materials* 713 (2015), pp. 2681–2684.

[205] Sio-Mei Lien, Wei-Te Li, and Ta-Jen Huang. “Genipin-crosslinked gelatin scaffolds for articular cartilage tissue engineering with a novel crosslinking method”. In: *Materials Science and Engineering: C* 28.1 (2008), pp. 36–43.

[206] Kai Bin Liew, Yvonne Tze Fung Tan, and Kok-Khiang Peh. “Effect of polymer, plasticizer and filler on orally disintegrating film”. In: *Drug development and industrial pharmacy* 40.1 (2014), pp. 110–119.

[207] Kanokrat Limpisophon, Munehiko Tanaka, and Kazufumi Osako. “Characterisation of gelatin–fatty acid emulsion films based on blue shark (Prionace glauca) skin gelatin”. In: *Food Chemistry* 122.4 (2010), pp. 1095–1101.

[208] Allen H Lin et al. “Collagen denaturation is initiated upon tissue yield in both positional and energy-storing tendons”. In: *Acta biomaterialia* 118 (2020), pp. 153–160.

[209] Shengjie Ling et al. “Polymorphic regenerated silk fibers assembled through bioinspired spinning”. In: *Nature communications* 8.1 (2017), p. 1387.

[210] Chia-Feng Liu et al. “What we should know before using tissue engineering techniques to repair injured tendons: a developmental biology perspective”. In: *Tissue Engineering Part B: Reviews* 17.3 (2011), pp. 165–176.

[211] Wanjun Liu et al. “Extrusion bioprinting of shear-thinning gelatin methacryloyl bioinks”. In: *Advanced healthcare materials* 6.12 (2017), p. 1601451.

[212] Anna V Lorimer and Patria A Hume. “Stiffness as a risk factor for Achilles tendon injury in running athletes”. In: *Sports Medicine* 46 (2016), pp. 1921–1938.

[213] M Loss et al. “Artificial skin, split-thickness autograft and cultured autologous keratinocytes combined to treat a severe burn injury of 93% of TBSA”. In: *Burns* 26.7 (2000), pp. 644–652.

[214] Candy Löwenberg et al. “Supramolecular Gelatin Networks Based on Inclusion Complexes”. In: *Macromolecular Bioscience* 20.10 (2020), p. 2000221.

[215] Ting Lu et al. “Bioactive scaffolds based on collagen filaments with tunable physico-chemical and biological features”. In: *Soft Matter* 16.18 (2020), pp. 4540–4548.

[216] Yanan Lu et al. “Application of gelatin in food packaging: A review”. In: *Polymers* 14.3 (2022), p. 436.

[217] Pauline Po Yee Lui et al. “Roles of oxidative stress in acute tendon injury and degenerative tendinopathy—a target for intervention”. In: *International Journal of Molecular Sciences* 23.7 (2022), p. 3571.

[218] Izeia Lukin et al. “Progress in gelatin as biomaterial for tissue engineering”. In: *Pharmaceutics* 14.6 (2022), p. 1177.

[219] AK Lynn, IV Yannas, and W Bonfield. “Antigenicity and immunogenicity of collagen”. In: *Journal of Biomedical Materials Research Part B: Applied Biomaterials: An Official Journal of The Society for Biomaterials, The Japanese Society for Biomaterials, and The Australian Society for Biomaterials and the Korean Society for Biomaterials* 71.2 (2004), pp. 343–354.

[220] Bing Ma et al. “Crosslinking strategies for preparation of extracellular matrix-derived cardiovascular scaffolds”. In: *Regenerative biomaterials* 1.1 (2014), pp. 81–89.

[221] Chao Ma et al. “Solvent-Free Plasticity and Programmable Mechanical Behaviors of Engineered Proteins”. In: *Advanced Materials* 32.10 (2020), p. 1907697.

[222] Nina KL Ma et al. “Collaboration of 3D context and extracellular matrix in the development of glioma stemness in a 3D model”. In: *Biomaterials* 78 (2016), pp. 62–73.

[223] Pengfei Ma et al. “Biomimetic gelatin/chitosan/polyvinyl alcohol/nano-hydroxyapatite scaffolds for bone tissue engineering”. In: *Materials & Design* 207 (2021), p. 109865.

[224] Jason J Madinya et al. “Surface Charge Density and Steric Repulsion in Polyelectrolyte–Surfactant Coacervation”. In: *Macromolecules* 56.11 (2023), pp. 3973–3988.

[225] JF Maempel et al. “The epidemiology of Achilles tendon re-rupture and associated risk factors: male gender, younger age and traditional immobilising rehabilitation are risk factors”. In: *Knee Surgery, Sports Traumatology, Arthroscopy* 30.7 (2022), pp. 2457–2469.

[226] Nicola Maffulli. “Current concepts review-rupture of the Achilles tendon”. In: *JBJS* 81.7 (1999), pp. 1019–36.

[227] Nicola Maffulli, Pankaj Sharma, and Karen L Luscombe. “Achilles tendinopathy: aetiology and management”. In: *Journal of the Royal Society of Medicine* 97.10 (2004), pp. 472–476.

[228] Nicola Maffulli, Alessio Giai Via, and Francesco Oliva. “Achilles injuries in the athlete: noninsertional”. In: *Operative Techniques in Sports Medicine* 22.4 (2014), pp. 321–330.

[229] B Martel et al. “Finishing of polyester fabrics with cyclodextrins and polycarboxylic acids as crosslinking agents”. In: *Journal of inclusion phenomena and macrocyclic chemistry* 44 (2002), pp. 443–446.

[230] James E Martin and D Adolf. “The sol-gel transition in chemical gels”. In: *Annual review of physical chemistry* 42.1 (1991), pp. 311–339.

[231] Paulo Eduardo Cavalcanti Martins Filho and Roberto Luiz Andrade Haiduke. “A Charge–Charge Flux–Dipole Flux Analysis of Simple Molecular Systems with Halogen Bonds”. In: *The Journal of Physical Chemistry A* 128.11 (2024), pp. 2058–2071.

[232] Michael L Mason and Clarence G Shearon. “The process of tendon repair: an experimental study of tendon suture and tendon graft”. In: *Archives of Surgery* 25.4 (1932), pp. 615–692.

[233] Shomita S Mathew-Steiner, Sashwati Roy, and Chandan K Sen. “Collagen in wound healing”. In: *Bioengineering* 8.5 (2021), p. 63.

[234] Shojiro Matsuda et al. “Bioadhesion of gelatin films crosslinked with glutaraldehyde”. In: *Journal of Biomedical Materials Research: An Official Journal of The Society for Biomaterials, The Japanese Society for Biomaterials, and The Australian Society for Biomaterials* 45.1 (1999), pp. 20–27.

[235] Hideo Matsumoto and Kyosuke Fujikawa. “Leeds-Keio artificial ligament: a new concept for the anterior cruciate ligament reconstruction of the knee”. In: *The Keio journal of medicine* 50.3 (2001), pp. 161–166.

[236] DN Matveev, KA Kutuzov, and VP Vasilevsky. “Effect of draw ratio on the morphology of polysulfone hollow fiber membranes”. In: *Membranes and Membrane Technologies* 2 (2020), pp. 351–356.

[237] Massimiliano Mauri et al. “Crosslinking of an ethylene-glycidyl methacrylate copolymer with amine click chemistry”. In: *Polymer* 111 (2017), pp. 27–35.

[238] Logan S McCarty and George M Whitesides. “Electrostatic charging due to separation of ions at interfaces: contact electrification of ionic electrets”. In: *Angewandte Chemie International Edition* 47.12 (2008), pp. 2188–2207.

[239] Jagan Singh Meena et al. “Electronic textiles: New age of wearable technology for healthcare and fitness solutions”. In: *Materials Today Bio* 19 (2023), p. 100565.

[240] Usha Meena. “Engineering Photo Cross-linked Norbornene Based Hydrogel and Its Application”. PhD thesis. Indian Institute of Science Education and Research Kolkata, 2018.

[241] M Meyer, H Baltzer, and K Schwikal. “Collagen fibres by thermoplastic and wet spinning”. In: *Materials Science and Engineering: C* 30.8 (2010), pp. 1266–1271.

[242] Takehiko Midorikawa et al. “Structure and physical properties of gelatin fibers prepared by gel-spinning in ethylene glycol”. In: *Journal of Applied Polymer Science* 125.S2 (2012), E332–E338.

[243] Kim S Midwood, Leyla Valenick Williams, and Jean E Schwarzbauer. “Tissue repair and the dynamics of the extracellular matrix”. In: *The international journal of biochemistry & cell biology* 36.6 (2004), pp. 1031–1037.

[244] Oleg V Mikhailov. “Gelatin as it is: history and modernity”. In: *International Journal of Molecular Sciences* 24.4 (2023), p. 3583.

[245] P-Y Mikus et al. “Deformation mechanisms of plasticized starch materials”. In: *Carbohydrate polymers* 114 (2014), pp. 450–457.

[246] Jiri Militky. “The chemistry, manufacture and tensile behaviour of polyester fibers”. In: *Handbook of tensile properties of textile and technical fibres*. Elsevier, 2009, pp. 223–314.

[247] Hamideh Mirbaha et al. “The impact of shear and elongational forces on structural formation of polyacrylonitrile/carbon nanotubes composite fibers during wet spinning process”. In: *Materials* 12.17 (2019), p. 2797.

[248] BS Mody et al. “The ABC carbon and polyester prosthetic ligament for ACL-deficient knees. Early results in 31 cases”. In: *The Journal of Bone & Joint Surgery British Volume* 75.5 (1993), pp. 818–821.

[249] Eva Möller, Lars Weidenhielm, and Suzanne Werner. “Outcome and knee-related quality of life after anterior cruciate ligament reconstruction: a long-term follow-up”. In: *Knee surgery, sports traumatology, arthroscopy* 17.7 (2009), pp. 786–794.

[250] M Möller et al. “Acute rupture of tendo Achillis: a prospective, randomised study of comparison between surgical and non-surgical treatment”. In: *The Journal of Bone & Joint Surgery British Volume* 83.6 (2001), pp. 843–848.

[251] Nelson Monteiro et al. “Photopolymerization of cell-laden gelatin methacryloyl hydrogels using a dental curing light for regenerative dentistry”. In: *Dental materials* 34.3 (2018), pp. 389–399.

[252] Bingnan Mu et al. “Spinnability and rheological properties of globular soy protein solution”. In: *Food hydrocolloids* 90 (2019), pp. 443–451.

[253] Naila A Mugheirbi et al. “Phase behavior of drug-hydroxypropyl methylcellulose amorphous solid dispersions produced from various solvent systems: Mechanistic understanding of the role of polymer using experimental and theoretical methods”. In: *Molecular pharmaceutics* 15.8 (2018), pp. 3236–3251.

[254] Indraneil Mukherjee and MaryAnn Rosolen. “Thermal transitions of gelatin evaluated using DSC sample pans of various seal integrities”. In: *Journal of Thermal Analysis and Calorimetry* 114 (2013), pp. 1161–1166.

[255] Abigail Muscat et al. “Principles, drivers and opportunities of a circular bioeconomy”. In: *Nature Food* 2.8 (2021), pp. 561–566.

[256] Delina Muscat et al. “Comparative study of film forming behaviour of low and high amylose starches using glycerol and xylitol as plasticizers”. In: *Journal of Food Engineering* 109.2 (2012), pp. 189–201.

[257] Dillirani Nagarajan, Duu-Jong Lee, and Jo-Shu Chang. “Circular bioeconomy: an introduction”. In: *Biomass, Biofuels, Biochemicals*. Elsevier, 2021, pp. 3–23.

[258] Majid Naghibzadeh et al. “Application of electrospun gelatin nanofibers in tissue engineering”. In: *Biointerface Research in Applied Chemistry* 8.1 (2018), pp. 3048–3052.

[259] Ruth Naomi et al. “Natural-based biomaterial for skin wound healing (Gelatin vs. collagen): Expert review”. In: *Polymers* 13.14 (2021), p. 2319.

[260] Sindi P Ndlovu et al. “Gelatin-based hybrid scaffolds: promising wound dressings”. In: *Polymers* 13.17 (2021), p. 2959.

[261] Arnold G Nelson and Jouko Kokkonen. *Stretching anatomy*. Human Kinetics Publishers, 2020.

[262] Shane J Nho et al. “Anatomic reduction and next-generation fixation constructs for arthroscopic repair of crescent, L-shaped, and U-shaped rotator cuff tears”. In: *Arthroscopy: The Journal of Arthroscopic & Related Surgery* 25.5 (2009), pp. 553–559.

[263] T Nishimura and T Kataoka. “Die swell of filled polymer melts”. In: *Rheologica acta* 23 (1984), pp. 401–407.

[264] E Nomura, M Inoue, and H Sugiura. “Ultrastructural study of the extra-articular Leeds-Keio ligament prosthesis”. In: *Journal of clinical pathology* 58.6 (2005), pp. 665–666.

[265] Mahdi Nouri et al. “Fabrication and characterization of drug-loaded wet spun polycaprolactone fibers”. In: *The Journal of The Textile Institute* 112.3 (2021), pp. 462–469.

[266] Kristo Nuutila and Elof Eriksson. “Moist wound healing with commonly available dressings”. In: *Advances in wound care* 10.12 (2021), pp. 685–698.

[267] T Nyyssönen, P Lüthje, and H Kröger. “The increasing incidence and difference in sex distribution of Achilles tendon rupture in Finland in 1987–1999”. In: *Scandinavian Journal of Surgery* 97.3 (2008), pp. 272–275.

[268] Yasushi Okamoto and Kuniomi Saeki. “Phase transition of collagen and gelatin”. In: *Kolloid-Zeitschrift und Zeitschrift für Polymere* 194 (1964), pp. 124–135.

[269] Melik Oksuz and H Yildirim Erbil. “Wet-spun graphene filaments: effect of temperature of coagulation bath and type of reducing agents on mechanical & electrical properties”. In: *RSC advances* 8.31 (2018), pp. 17443–17452.

[270] Nicklas Olsson et al. “Predictors of clinical outcome after acute Achilles tendon ruptures”. In: *The American journal of sports medicine* 42.6 (2014), pp. 1448–1455.

[271] Nicklas Olsson et al. “Stable surgical repair with accelerated rehabilitation versus nonsurgical treatment for acute Achilles tendon ruptures: a randomized controlled study”. In: *The American journal of sports medicine* 41.12 (2013), pp. 2867–2876.

[272] Ahmad Oryan et al. “Chemical crosslinking of biopolymeric scaffolds: Current knowledge and future directions of crosslinked engineered bone scaffolds”. In: *International journal of biological macromolecules* 107 (2018), pp. 678–688.

[273] Caio G Otoni et al. “The food–materials nexus: next generation bioplastics and advanced materials from agri-food residues”. In: *Advanced Materials* 33.43 (2021), p. 2102520.

[274] William K Ovalie. “The human muscle-tendon junction: A morphological study during normal growth and at maturity”. In: *Anatomy and embryology* 176 (1987), pp. 281–294.

[275] Ari Pajala et al. “Rerupture and deep infection following treatment of total Achilles tendon rupture”. In: *JBJS* 84.11 (2002), pp. 2016–2021.

[276] Saikat Pal and Rajib Kumar Mitra. “Investigation on the effect of nonpolar amino acids as macromolecular crowders on the stability of globular proteins”. In: *Chemical Thermodynamics and Thermal Analysis* 6 (2022), p. 100044.

[277] Giovanni Papa et al. “Five years of experience using a dermal substitute: indications, histologic studies, and first results using a new single-layer tool”. In: *Dermatologic surgery* 37.11 (2011), pp. 1631–1637.

[278] AM Pardes et al. “Aging leads to inferior Achilles tendon mechanics and altered ankle function in rodents”. In: *Journal of biomechanics* 60 (2017), pp. 30–38.

[279] Selene G Parekh et al. “Epidemiology and outcomes of Achilles tendon ruptures in the National Football League”. In: *Foot & ankle specialist* 2.6 (2009), pp. 283–286.

[280] Jin-Young Park et al. “Arthroscopic repair of large U-shaped rotator cuff tears without margin convergence versus repair of crescent-or L-shaped tears”. In: *The American Journal of Sports Medicine* 42.1 (2014), pp. 103–111.

[281] Seung-Hwan Park et al. “Treatment of acute Achilles tendon rupture”. In: *Clinics in orthopedic surgery* 12.1 (2020), p. 1.

[282] Concepcion Parrado et al. “Environmental stressors on skin aging. Mechanistic insights”. In: *Frontiers in pharmacology* 10 (2019), p. 759.

[283] DR Paul. “A study of spinnability in the wet-spinning of acrylic fibers”. In: *Journal of Applied Polymer Science* 12.10 (1968), pp. 2273–2298.

[284] Ying Pei et al. “Effectively promoting wound healing with cellulose/gelatin sponges constructed directly from a cellulose solution”. In: *Journal of Materials Chemistry B* 3.38 (2015), pp. 7518–7528.

[285] Tim S Peltz et al. “Influence of locking stitch size in a four-strand cross-locked cruciate flexor tendon repair”. In: *The Journal of hand surgery* 36.3 (2011), pp. 450–455.

[286] Gong-qiu Peng et al. “Effect of dope extrusion rate on the formation and characterization of polyacrylonitrile nascent fibers during wet-spinning”. In: *Polymer bulletin* 62 (2009), pp. 657–666.

[287] Zhiqing Peng et al. “Flexible wearable pressure sensor based on collagen fiber material”. In: *Micromachines* 13.5 (2022), p. 694.

[288] David M Phillips et al. “Regenerated silk fiber wet spinning from an ionic liquid solution”. In: *Journal of Materials Chemistry* 15.39 (2005), pp. 4206–4208.

[289] Judith Piermaria et al. “Kefiran films plasticized with sugars and polyols: water vapor barrier and mechanical properties in relation to their microstructure analyzed by ATR/FT-IR spectroscopy”. In: *Food Hydrocolloids* 25.5 (2011), pp. 1261–1269.

[290] George D Pins et al. “Effects of static axial strain on the tensile properties and failure mechanisms of self-assembled collagen fibers”. In: *Journal of Applied Polymer Science* 63.11 (1997), pp. 1429–1440.

[291] Heather M Powell and Steven T Boyce. “EDC cross-linking improves skin substitute strength and stability”. In: *Biomaterials* 27.34 (2006), pp. 5821–5827.

[292] Dario Puppi and Federica Chiellini. “Wet-spinning of biomedical polymers: from single-fibre production to additive manufacturing of three-dimensional scaffolds”. In: *Polymer International* 66.12 (2017), pp. 1690–1696.

[293] Peter P Purslow. “Contribution of collagen and connective tissue to cooked meat toughness; some paradigms reviewed”. In: *Meat science* 144 (2018), pp. 127–134.

[294] Xiuying Qiao, Zhongzhu Tang, and Kang Sun. “Plasticization of corn starch by polyol mixtures”. In: *Carbohydrate Polymers* 83.2 (2011), pp. 659–664.

[295] Yi Qin et al. “The thermal gelation behavior and performance evaluation of high molecular weight nonionic polyacrylamide and polyethyleneimine mixtures for in-depth water control in mature oilfields”. In: *Materials* 13.18 (2020), p. 4142.

[296] Harshini Ramakrishna et al. “Tissue engineering a tendon-bone junction with biodegradable braided scaffolds”. In: *Biomaterials Research* 23.1 (2019), p. 11.

[297] Jerome Ramirez et al. “Wastes to profit: a circular economy approach to value-addition in livestock industries”. In: *Animal Production Science* 61.6 (2021), pp. 541–550.

[298] John AM Ramshaw, Paul R Vaughan, and JEROME A WERKMEISTER. “Applications of collagen in medical devices”. In: *Biomedical Engineering: Applications, Basis and Communications* 13.01 (2001), pp. 14–26.

[299] John AM Ramshaw, Jerome A Werkmeister, and Veronica Glattauer. “Collagen-based biomaterials”. In: *Biotechnology and Genetic Engineering Reviews* 13.1 (1996), pp. 335–382.

[300] Jahangir A Rather et al. “A comprehensive review on gelatin: Understanding impact of the sources, extraction methods, and modifications on potential packaging applications”. In: *Food Packaging and Shelf Life* 34 (2022), p. 100945.

[301] Maria Grazia Raucci et al. “Bioactivation routes of gelatin-based scaffolds to enhance at nanoscale level bone tissue regeneration”. In: *Frontiers in bioengineering and biotechnology* 7 (2019), p. 27.

[302] Shelley Rawson, Sarah Cartmell, and Jason Wong. “Suture techniques for tendon repair; a comparative review”. In: *Muscles, ligaments and tendons journal* 3.3 (2013), p. 220.

[303] RR Ray, SC Jana, and G Nanda. “Immobilization of β-amylase from Bacillus megaterium B6 into gelatin film by cross-linking”. In: *Journal of applied bacteriology* 79.2 (1995), pp. 157–162.

[304] JM Reinke and H Sorg. “Wound repair and regeneration”. In: *European surgical research* 49.1 (2012), pp. 35–43.

[305] Darrell H Reneker and Alexander L Yarin. “Electrospinning jets and polymer nanofibers”. In: *Polymer* 49.10 (2008), pp. 2387–2425.

[306] Sylvie Ricard-Blum. “The collagen family”. In: *Cold Spring Harbor perspectives in biology* 3.1 (2011), a004978.

[307] Jessica Rickman et al. “Rotation-assisted wet-spinning of UV-cured gelatin fibres and nonwovens”. In: *Journal of materials science* 54.14 (2019), pp. 10529–10547.

[308] Chiara Rinoldi et al. “Tendon tissue engineering: effects of mechanical and biochemical stimulation on stem cell alignment on cell-laden hydrogel yarns”. In: *Advanced healthcare materials* 8.7 (2019), p. 1801218.

[309] Joana Rocha et al. “Wetspun polymeric fibrous systems as potential scaffolds for tendon and ligament repair, healing and regeneration”. In: *Pharmaceutics* 14.11 (2022), p. 2526.

[310] Meritaine da Rocha, Michele M de Souza, and Carlos Prentice. “Biodegradable films: An alternative food packaging”. In: *Food packaging and preservation*. Elsevier, 2018, pp. 307–342.

[311] Elisa Roldán et al. “Can we achieve biomimetic electrospun scaffolds with gelatin alone?” In: *Frontiers in Bioengineering and Biotechnology* 11 (2023).

[312] Elisabetta Rosellini et al. “Protein/polysaccharide-based scaffolds mimicking native extracellular matrix for cardiac tissue engineering applications”. In: *Journal of Biomedical Materials Research Part A* 106.3 (2018), pp. 769–781.

[313] Tania Rozario and Douglas W DeSimone. “The extracellular matrix in development and morphogenesis: a dynamic view”. In: *Developmental biology* 341.1 (2010), pp. 126–140.

[314] Sandra Ruiz-Alonso et al. “Tendon tissue engineering: Cells, growth factors, scaffolds and production techniques”. In: *Journal of Controlled Release* 333 (2021), pp. 448–486.

[315] Pim-on Rujitanaroj, Nuttaporn Pimpha, and Pitt Supaphol. “Wound-dressing materials with antibacterial activity from electrospun gelatin fiber mats containing silver nanoparticles”. In: *Polymer* 49.21 (2008), pp. 4723–4732.

[316] Mohammad Sadeghi and Behrouz Heidari. “Crosslinked graft copolymer of methacrylic acid and gelatin as a novel hydrogel with pH-responsiveness properties”. In: *Materials* 4.3 (2011), pp. 543–552.

[317] Nurul Saadah Said and Norizah Mhd Sarbon. “Physical and mechanical characteristics of gelatin-based films as a potential food packaging material: A review”. In: *Membranes* 12.5 (2022), p. 442.

[318] Takamasa Sakai et al. “Sol-gel transition behavior near critical concentration and connectivity”. In: *Polymer Journal* 48.5 (2016), pp. 629–634.

[319] Tarek Salem and Mohamed Salama. “Developing a new class of UV-curable polyurethane acrylate resins for coating applications”. In: *Egyptian Journal of Chemistry* 63.3 (2020), pp. 973–992.

[320] A Salih. “Kelvin–helmholtz instability”. In: *Indian Institute of Space Science and Technology, Thiruvananthapurm* (2010).

[321] MJ Sandow and MM McMahon. “Single-cross grasp six-strand repair for acute flexor tenorrhaphy: modified Savage technique”. In: *Atlas Hand Clin* 1.01 (1996), pp. 41–64.

[322] Liliana Schaefer and Roland M Schaefer. “Proteoglycans: from structural compounds to signaling molecules”. In: *Cell and tissue research* 339.1 (2010), pp. 237–246.

[323] Matthias Schäfer and Sabine Werner. “Cancer as an overhealing wound: an old hypothesis revisited”. In: *Nature reviews Molecular cell biology* 9.8 (2008), pp. 628–638.

[324] Jennifer L Schiefer et al. “Frequent application of the new gelatin-collagen nonwoven accelerates wound healing”. In: *Advances in skin & wound care* 29.2 (2016), pp. 73–78.

[325] ITJ Schroven et al. “Experience with the Leeds-Keio artificial ligament for anterior cruciate ligament reconstruction”. In: *Knee Surgery, Sports Traumatology, Arthroscopy* 2 (1994), pp. 214–218.

[326] Gregory S Schultz et al. “23 principles of wound healing”. In: *Mechanisms of vascular disease: a reference book for vascular specialists* (2011), p. 423.

[327] Maria A Schumacher, Kazunori Mizuno, and Hans Peter Bachinger. “The crystal structure of a collagen-like polypeptide with 3 (S)-hydroxyproline residues in the Xaa position forms a standard 7/2 collagen triple helix”. In: *Journal of biological chemistry* 281.37 (2006), pp. 27566–27574.

[328] Scott A Sell et al. “Electrospinning of collagen/biopolymers for regenerative medicine and cardiovascular tissue engineering”. In: *Advanced drug delivery reviews* 61.12 (2009), pp. 1007–1019.

[329] Özlem Şen and Mustafa Culha. “Boron nitride nanotubes included thermally cross-linked gelatin–glucose scaffolds show improved properties”. In: *Colloids and Surfaces B: Biointerfaces* 138 (2016), pp. 41–49.

[330] Sebnem Senol and Emel Akyol. “Synthesis and characterization of hydrogels based on poly (2-hydroxyethyl methacrylate) for drug delivery under UV irradiation”. In: *Journal of materials science* 53 (2018), pp. 14953–14963.

[331] Alan G Shamrock, Mark A Dreyer, and Matthew Varacallo. “Achilles tendon rupture”. In: *StatPearls [Internet]*. StatPearls publishing, 2023.

[332] DV Shepherd et al. “The process of EDC-NHS cross-linking of reconstituted collagen fibres increases collagen fibrillar order and alignment”. In: *APL materials* 3.1 (2015).

[333] Xuetao Shi et al. “Microfluidic spinning of cell-responsive grooved microfibers”. In: *Advanced Functional Materials* 25.15 (2015), pp. 2250–2259.

[334] Anahita Rohani Shirvan, Alireza Nouri, and Alessandra Sutti. “A perspective on the wet spinning process and its advancements in biomedical sciences”. In: *European Polymer Journal* 181 (2022), p. 111681.

[335] Ahmed Shoaib and Viren Mishra. “Surgical repair of symptomatic chronic Achilles tendon rupture using synthetic graft augmentation”. In: *Foot and Ankle Surgery* 23.3 (2017), pp. 179–182.

[336] Matthew D Shoulders and Ronald T Raines. “Collagen structure and stability”. In: *Annual review of biochemistry* 78 (2009), pp. 929–958.

[337] Manuel Vieira da Silva and Bruno Pereira. “Biomechanics of Lower Limb Injuries”. In: *Injuries and Health Problems in Football: What Everyone Should Know*. Springer, 2017, pp. 53–64.

[338] Pedro M Silva et al. “Management of operational parameters and novel spinneret configurations for the electrohydrodynamic processing of functional polymers”. In: *Macromolecular Materials and Engineering* 307.5 (2022), p. 2100858.

[339] Frederick H Silver, Joseph W Freeman, and Gurinder P Seehra. “Collagen self-assembly and the development of tendon mechanical properties”. In: *Journal of biomechanics* 36.10 (2003), pp. 1529–1553.

[340] Aparajita Singh et al. “Meta-analysis of randomized controlled trials on hydrocolloid occlusive dressing versus conventional gauze dressing in the healing of chronic wounds”. In: *Asian journal of surgery* 27.4 (2004), pp. 326–332.

[341] Valentina Siracusa et al. “Biodegradable polymers for food packaging: a review”. In: *Trends in food science & technology* 19.12 (2008), pp. 634–643.

[342] Manikandan Sivan et al. “Alternating current electrospinning: The impacts of various high-voltage signal shapes and frequencies on the spinnability and productivity of polycaprolactone nanofibers”. In: *Materials & Design* 213 (2022), p. 110308.

[343] Valentin Maximovich Slepukhin. *Network Dynamics: Biofilament and Neuronal Networks*. University of California, Los Angeles, 2021.

[344] PG Smith, HR Watling, and P Crew. “The effects of model organic compounds on gibbsite crystallization from alkaline aluminate solutions: polyols”. In: *Colloids and Surfaces A: Physicochemical and Engineering Aspects* 111.1-2 (1996), pp. 119–130.

[345] Payman Sobhanipour, Reza Cheraghi, and Alex A Volinsky. “Thermoporometry study of coagulation bath temperature effect on polyacrylonitrile fibers morphology”. In: *Thermochimica acta* 518.1-2 (2011), pp. 101–106.

[346] SportingTex. *Collagen Fabric— Wholesale Fabric Supplier— SPORTINGTEX®*. en-US. Jan. 2019. URL: https://www.sportingtex.com/collagen-fiber-fabric.

[347] Philipp R Stoessel et al. “Fibers mechanically similar to sheep wool obtained by wet spinning of gelatin and optional plasticizers”. In: *Macromolecular Materials and Engineering* 300.2 (2015), pp. 234–241.

[348] Julia Evangelou Strait. *Proteins critical to wound healing identified - The Source - Washington University in St. Louis*. en-US. Aug. 2014. URL: https://source.wustl.edu/2014/08/proteins-critical-to-wound-healing-identified/.

[349] Ian Streeter and Nora H de Leeuw. “A molecular dynamics study of the inter-protein interactions in collagen fibrils”. In: *Soft matter* 7.7 (2011), pp. 3373–3382.

[350] Andreas Stylianou. “Assessing collagen D-band periodicity with atomic force microscopy”. In: *Materials* 15.4 (2022), p. 1608.

[351] Yingchun Su et al. “3D electrospun synthetic extracellular matrix for tissue regeneration”. In: *Small Science* 1.7 (2021), p. 2100003.

[352] Yingchun Su et al. “A hierarchically ordered compacted coil scaffold for tissue regeneration”. In: *NPG Asia Materials* 12.1 (2020), p. 55.

[353] Amar A Suchak et al. “Postoperative rehabilitation protocols for Achilles tendon ruptures: a meta-analysis.” In: *Clinical Orthopaedics and Related Research (1976-2007)* 445 (2006), pp. 216–221.

[354] N Suderman, MIN Isa, and NM Sarbon. “The effect of plasticizers on the functional properties of biodegradable gelatin-based film: A review”. In: *Food bioscience* 24 (2018), pp. 111–119.

[355] Bo Sun. “The mechanics of fibrillar collagen extracellular matrix”. In: *Cell Reports Physical Science* 2.8 (2021).

[356] Qiang Sun, Yanfang Fu, and Weiqi Wang. “Temperature effects on hydrophobic interactions: Implications for protein unfolding”. In: *Chemical Physics* 559 (2022), p. 111550.

[357] Hsing-Wen Sung et al. “Evaluation of gelatin hydrogel crosslinked with various crosslinking agents as bioadhesives: in vitro study”. In: *Journal of Biomedical Materials Research: An Official Journal of The Society for Biomaterials, The Japanese Society for Biomaterials, and The Australian Society for Biomaterials and the Korean Society for Biomaterials* 46.4 (1999), pp. 520–530.

[358] Rene B Svensson et al. “Effect of aging and exercise on the tendon”. In: *Journal of Applied Physiology* 121.6 (2016), pp. 1353–1362.

[359] Anthony S Tadros, Brady K Huang, and Mini N Pathria. “Muscle-tendon-enthesis unit”. In: *Seminars in musculoskeletal radiology*. Vol. 22. 03. Thieme Medical Publishers. 2018, pp. 263–274.

[360] Takayuki Takei et al. “Hydrophobically-modified gelatin hydrogel as a carrier for charged hydrophilic drugs and hydrophobic drugs”. In: *International journal of biological macromolecules* 149 (2020), pp. 140–147.

[361] Eric CD Tan and Patrick Lamers. “Circular bioeconomy concepts—a perspective”. In: *Frontiers in sustainability* 2 (2021), p. 701509.

[362] Toshikazu Tanaka et al. “Tensile strength of a new suture for fixation of tendon grafts when using a weave technique”. In: *The Journal of hand surgery* 31.6 (2006), pp. 982–986.

[363] Jin Bo Tang et al. “Flexor tendon repair: recent changes and current methods”. In: *Journal of Hand Surgery (European Volume)* 47.1 (2022), pp. 31–39.

[364] Zhenhua Tang et al. “Highly stretchable core–sheath fibers via wet-spinning for wearable strain sensors”. In: *ACS applied materials & interfaces* 10.7 (2018), pp. 6624–6635.

[365] Domiziano Tarantino et al. “Achilles tendon rupture: mechanisms of injury, principles of rehabilitation and return to play”. In: *Journal of functional morphology and kinesiology* 5.4 (2020), p. 95.

[366] Selamu Temesgen et al. “Review on spinning of biopolymer fibers from starch”. In: *Polymers* 13.7 (2021), p. 1121.

[367] Zhao-lin Teng et al. “Epidemiological characteristics of patients operated for Achilles tendon rupture in Shanghai”. In: *Orthopaedic Surgery* 14.8 (2022), pp. 1649–1655.

[368] *Textile fibres-Determination of breaking force and elongation at break of individual fibres Fibres textiles-Détermination de la force de rupture et de l’allongement de rupture des fibres individuelles*. Standard. Beijing, China: International Organization for Standardization, Mar. 2020.

[369] Achilleas D Theocharis et al. “Extracellular matrix structure”. In: *Advanced drug delivery reviews* 97 (2016), pp. 4–27.

[370] Stavros Thomopoulos et al. “Mechanisms of tendon injury and repair”. In: *Journal of Orthopaedic Research* 33.6 (2015), pp. 832–839.

[371] Funda Tihminlioglu, İsa Doğan Atik, and Banu Özen. “Effect of corn-zein coating on the mechanical properties of polypropylene packaging films”. In: *Journal of applied polymer science* 119.1 (2011), pp. 235–241.

[372] Kevin D Tipton et al. “Postexercise net protein synthesis in human muscle from orally administered amino acids”. In: *American Journal of Physiology-Endocrinology And Metabolism* 276.4 (1999), E628–E634.

[373] Wiktoria Tomal and Joanna Ortyl. “Water-soluble photoinitiators in biomedical applications”. In: *Polymers* 12.5 (2020), p. 1073.

[374] K Tomihata et al. “Cross-linking and biodegradation of native and denatured collagen”. In: ACS Publications, 1994.

[375] Qunyi Tong, Qian Xiao, and Loong-Tak Lim. “Effects of glycerol, sorbitol, xylitol and fructose plasticisers on mechanical and moisture barrier properties of pullulan–alginate–carboxymethylcellulose blend films”. In: *International journal of food science & technology* 48.4 (2013), pp. 870–878.

[376] Giuseppe Tronci. “The application of collagen in advanced wound dressings”. In: *Advanced textiles for wound care*. Elsevier, 2019, pp. 363–389.

[377] Giuseppe Tronci, Stephen J Russell, and David J Wood. “Photo-active collagen systems with controlled triple helix architecture”. In: *Journal of materials chemistry B* 1.30 (2013), pp. 3705–3715.

[378] Giuseppe Tronci et al. “Multi-scale mechanical characterization of highly swollen photo-activated collagen hydrogels”. In: *Journal of the Royal Society Interface* 12.102 (2015), p. 20141079.

[379] Giuseppe Tronci et al. “Protease-sensitive atelocollagen hydrogels promote healing in a diabetic wound model”. In: *Journal of Materials Chemistry B* 4.45 (2016), pp. 7249–7258.

[380] Giuseppe Tronci et al. “Wet-spinnability and crosslinked fibre properties of two collagen polypeptides with varied molecular weight”. In: *International journal of biological macromolecules* 81 (2015), pp. 112–120.

[381] Kadriye Tuzlakoglu et al. “A new route to produce starch-based fiber mesh scaffolds by wet spinning and subsequent surface modification as a way to improve

cell attachment and proliferation". In: *Journal of Biomedical Materials Research Part A: An Official Journal of The Society for Biomaterials, The Japanese Society for Biomaterials, and The Australian Society for Biomaterials and the Korean Society for Biomaterials* 92.1 (2010), pp. 369–377.

[382] Bruce C Twaddle and Peter Poon. "Early motion for Achilles tendon ruptures: is surgery important? A randomized, prospective study". In: *The American journal of sports medicine* 35.12 (2007), pp. 2033–2038.

[383] Kezban Ulubayram et al. "Cytotoxicity evaluation of gelatin sponges prepared with different cross-linking agents". In: *Journal of Biomaterials Science, Polymer Edition* 13.11 (2002), pp. 1203–1219.

[384] In Chul Um et al. "Wet spinning of silk polymer: II. Effect of drawing on the structural characteristics and properties of filament". In: *International journal of biological macromolecules* 34.1-2 (2004), pp. 107–119.

[385] Muhammad Umar et al. "Wet-spun bi-component alginate based hydrogel fibers: Development and in-vitro evaluation as a potential moist wound care dressing". In: *International Journal of Biological Macromolecules* 168 (2021), pp. 601–610.

[386] Raju Vaishya et al. "Medical textiles in orthopedics: An overview". In: *Journal of clinical orthopaedics and trauma* 9 (2018), S26–S33.

[387] Kathy Van Den Houwe et al. "Migration of 17 photoinitiators from printing inks and cardboard into packaged food–results of a belgian market survey". In: *Packaging Technology and Science* 29.2 (2016), pp. 121–131.

[388] KW VanDusen and LM Larkin. "Muscle–tendon interface". In: *Regenerative engineering of musculoskeletal tissues and interfaces*. Elsevier, 2015, pp. 409–429.

[389] Surendra Kumar Verma et al. "Improved hemodialysis with hemocompatible polyethersulfone hollow fiber membranes: In vitro performance". In: *Journal of Biomedical Materials Research Part B: Applied Biomaterials* 106.3 (2018), pp. 1286–1298.

[390] Margaux Vigata et al. "Gelatin methacryloyl hydrogels control the localized delivery of albumin-bound paclitaxel". In: *Polymers* 12.2 (2020), p. 501.

[391] Claire B Vink and Jonathan R Woodward. “Effect of a weak magnetic field on the reaction between neutral free radicals in isotropic solution”. In: *Journal of the American Chemical Society* 126.51 (2004), pp. 16730–16731.

[392] Jacqueline van der Vis et al. “Functional outcome in patients who underwent distal biceps tendon repair”. In: *Archives of Orthopaedic and Trauma Surgery* 138 (2018), pp. 1541–1548.

[393] Arco C Van der Vlist et al. “Clinical risk factors for Achilles tendinopathy: a systematic review”. In: *British journal of sports medicine* 53.21 (2019), pp. 1352–1361.

[394] Marc P Vocht et al. “High-performance cellulosic filament fibers prepared via dry-jet wet spinning from ionic liquids”. In: *Cellulose* 28 (2021), pp. 3055–3067.

[395] Thomas J Vogl et al. “Reconstructed anterior cruciate ligaments using patellar tendon ligament grafts: diagnostic value of contrast-enhanced MRI in a 2-year follow-up regimen”. In: *European radiology* 11 (2001), pp. 1450–1456.

[396] Beat H Walpoth and Gary L Bowlin. “The daunting quest for a small diameter vascular graft”. In: *Expert Review of Medical Devices* 2.6 (2005), pp. 647–651.

[397] Chenguang Wang et al. “Global trends in research of achilles tendon injury/rupture: A bibliometric analysis, 2000–2021”. In: *Frontiers in surgery* 10 (2023), p. 1051429.

[398] Ling Wang et al. “Effects of non-solvents and electrolytes on the formation and properties of cellulose I filaments”. In: *Scientific Reports* 9.1 (2019), p. 16691.

[399] Shennan Wang, Kai Li, and Qi Zhou. “High strength and low swelling composite hydrogels from gelatin and delignified wood”. In: *Scientific reports* 10.1 (2020), p. 17842.

[400] Scott Watson et al. “Does the rotator cuff tear pattern influence clinical outcomes after surgical repair?” In: *Orthopaedic Journal of Sports Medicine* 6.3 (2018), p. 2325967118763107.

[401] Meng Wei et al. “Design of photoinitiator-functionalized hydrophilic nanogels with uniform size and excellent biocompatibility”. In: *Polymer Chemistry* 10.22 (2019), pp. 2812–2821.

[402] AC Weihermann et al. “Elastin structure and its involvement in skin photoageing”. In: *International journal of cosmetic science* 39.3 (2017), pp. 241–247.

[403] Manuela Weitkunat et al. “Tension and force-resistant attachment are essential for myofibrillogenesis in Drosophila flight muscle”. In: *Current Biology* 24.7 (2014), pp. 705–716.

[404] Sigmund A Wesolowski et al. “Arterial prosthetic materials”. In: *Annals of The New York Academy Of Sciences* 146.1 (1968), pp. 325–344.

[405] Sigmund A Wesolowski et al. “The compound prosthetic vascular graft: a pathologic survey”. In: *Surgery* 53.1 (1963), pp. 19–44.

[406] Olof Westin. “Achilles Tendon Ruptures Predictors; functional and economic impact”. In: (2018).

[407] Catherine J Williams et al. “A retrospective audit of the timescales involved in the diagnosis and management of suspected Achilles tendon ruptures at a single National Health Service trust: A quality service improvement and redesign project”. In: *Ultrasound* 30.2 (2022), pp. 117–125.

[408] Emilia I Wisotzki et al. “Tailoring the material properties of gelatin hydrogels by high energy electron irradiation”. In: *Journal of Materials Chemistry B* 2.27 (2014), pp. 4297–4309.

[409] Michael Wöltje et al. “Continuous Wet Spinning of Regenerated Silk Fibers from Spinning Dopes Containing 4% Fibroin Protein”. In: *International Journal of Molecular Sciences* 24.17 (2023), p. 13492.

[410] Fan Wu, Michael Nerlich, and Denitsa Docheva. “Tendon injuries: Basic science and new repair proposals”. In: *EFORT open reviews* 2.7 (2017), pp. 332–342.

[411] Hui Y Wu et al. “Wet-spun silk fibroin scaffold with hierarchical structure for ligament tissue engineering”. In: *Materials Letters* 135 (2014), pp. 63–66.

[412] Marlyn Wu, Kelly Cronin, and Jonathan S Crane. “Biochemistry, collagen synthesis”. In: (2018).

[413] Yahong Wu et al. “Complications in the management of acute Achilles tendon rupture: a systematic review and network meta-analysis of 2060 patients”. In: *The American journal of sports medicine* 47.9 (2019), pp. 2251–2260.

[414] YF Wu et al. “Biomechanical comparisons of four-strand tendon repairs with double-stranded sutures: effects of different locks and suture geometry”. In: *Journal of Hand Surgery (European Volume)* 36.1 (2011), pp. 34–39.

[415] Dane Wukich. *Achilles tendon injuries: Why do they take so long to heal? — Orthopaedics and Rehab — UT Southwestern Medical Center*. en-us. URL: http://utswmed.org/medblog/achilles-tendon-injuries-rehab/.

[416] Yu Xie et al. "A collagen/PLA hybrid scaffold supports tendon-derived cell growth for tendon repair and regeneration". In: *Journal of Biomedical Materials Research Part B: Applied Biomaterials* 110.12 (2022), pp. 2624–2635.

[417] Xiros. *Achilles Tendon Repair - AchilloCordPLUS System*. en-GB. N.D.a. URL: https://xiros.co.uk/product/achilles-tendon-repair-using-the-xiros-achillocordplus-system/.

[418] Xiros. *JewelACL - Anterior Cruciate Ligament Reconstruction*. en-GB. URL: https://xiros.co.uk/product/anterior-cruciate-ligament-reconstruction/.

[419] Xiros. *Patella stabilisation - Infinity-Lock Tape*. en-GB. URL: https://xiros.co.uk/product/medial-patellofemoral-ligament-reconstruction-using-infinity-lock-5-mm-tape/.

[420] Xiros. *Patella stabilisation - Infinity-Lock Tape*. en-GB. URL: https://xiros.co.uk/product/medial-patellofemoral-ligament-reconstruction-using-infinity-lock-5-mm-tape/.

[421] Xiros. *PatellarTape System - Patellar Tendon Reconstruction*. en-GB. URL: https://xiros.co.uk/product/patellar-tendon-reconstruction-using-xiros-patellartape-system/.

[422] Baoshan Xu et al. "Circumferentially oriented microfiber scaffold prepared by wet-spinning for tissue engineering of annulus fibrosus". In: *Rsc Advances* 5.53 (2015), pp. 42705–42713.

[423] Fei Xu et al. "Hydrogels for tissue engineering: addressing key design needs toward clinical translation". In: *Frontiers in bioengineering and biotechnology* 10 (2022), p. 849831.

[424] Zhen Xu and Chao Gao. "Graphene in macroscopic order: liquid crystals and wet-spun fibers". In: *Accounts of chemical research* 47.4 (2014), pp. 1267–1276.

[425] Lian Xue and Howard P Greisler. "Biomaterials in the development and future of vascular grafts". In: *Journal of vascular surgery* 37.2 (2003), pp. 472–480.

[426] Amit Yaari et al. “Wet spinning and drawing of human recombinant collagen”. In: *ACS Biomaterials Science & Engineering* 2.3 (2016), pp. 349–360.

[427] Naoya Yamaguchi and Holger Knaut. “Focal adhesion-mediated cell anchoring and migration: from in vitro to in vivo”. In: *Development* 149.10 (2022), dev200647.

[428] Takashi Yamashiki et al. “New class of cellulose fiber spun from the novel solution of cellulose by wet spinning method”. In: *Journal of applied polymer science* 44.4 (1992), pp. 691–698.

[429] Chen Y Yang et al. “Fabrication of porous gelatin microfibers using an aqueous wet spinning process”. In: *Artificial cells, blood substitutes, and biotechnology* 37.4 (2009), pp. 173–176.

[430] Dali Yang et al. “Controlling macrovoid formation in wet-spun polyaniline fibers”. In: *Smart Structures and Materials 2001: Electroactive Polymer Actuators and Devices*. Vol. 4329. SPIE. 2001, pp. 59–71.

[431] Gang Yang et al. “Assessment of the characteristics and biocompatibility of gelatin sponge scaffolds prepared by various crosslinking methods”. In: *Scientific reports* 8.1 (2018), p. 1616.

[432] Guang Yang, Benjamin B Rothrauff, and Rocky S Tuan. “Tendon and ligament regeneration and repair: clinical relevance and developmental paradigm”. In: *Birth defects research part C: embryo today: reviews* 99.3 (2013), pp. 203–222.

[433] X Yang et al. “Management of acute Achilles tendon ruptures: A review”. In: *Bone & joint research* 7.10 (2018), pp. 561–569.

[434] Yiqi Yang and Narendra Reddy. “Properties and potential medical applications of regenerated casein fibers crosslinked with citric acid”. In: *International journal of biological macromolecules* 51.1-2 (2012), pp. 37–44.

[435] Chun-Hsu Yao et al. “Preparation of networks of gelatin and genipin as degradable biomaterials”. In: *Materials Chemistry and Physics* 83.2-3 (2004), pp. 204–208.

[436] Ming-kung Yeh et al. “A novel cell support membrane for skin tissue engineering: Gelatin film cross-linked with 2-chloro-1-methylpyridinium iodide”. In: *Polymer* 52.4 (2011), pp. 996–1003.

[437] Kai Yi et al. “Diffusion coefficients of dimethyl sulphoxide (DMSO) and H2O in PAN wet spinning and its influence on morphology of nascent polyacrylonitrile (PAN) fiber”. In: *Journal of Engineered Fibers and Fabrics* 8.1 (2013), p. 155892501300800113.

[438] Senem Yilmazer, Duncan Schwaller, and Philippe J Mésini. “Beyond Sol-Gel: Molecular Gels with Different Transitions”. In: *Gels* 9.4 (2023), p. 273.

[439] Ashlyn T Young, Olivia C White, and Michael A Daniele. “Rheological properties of coordinated physical gelation and chemical crosslinking in gelatin methacryloyl (GelMA) hydrogels”. In: *Macromolecular bioscience* 20.12 (2020), p. 2000183.

[440] Jonathan S Young and Nicola Maffulli. “Etiology and epidemiology of achilles tendon problems”. In: *The Achilles Tendon* 15 (2007), pp. 39–49.

[441] Haydar U Zaman et al. “Physico-mechanical properties of wound dressing material and its biomedical application”. In: *Journal of the mechanical behavior of biomedical materials* 4.7 (2011), pp. 1369–1375.

[442] Samantha G Zambuto et al. “Evaluation of gelatin bloom strength on gelatin methacryloyl hydrogel properties”. In: *Journal of the Mechanical Behavior of Biomedical Materials* 154 (2024), p. 106509.

[443] Dimitrios I Zeugolis, Gordon R Paul, and Geoffrey Attenburrow. “Cross-linking of extruded collagen fibers—A biomimetic three-dimensional scaffold for tissue engineering applications”. In: *Journal of Biomedical Materials Research Part A: An Official Journal of The Society for Biomaterials, The Japanese Society for Biomaterials, and The Australian Society for Biomaterials and the Korean Society for Biomaterials* 89.4 (2009), pp. 895–908.

[444] Dimitrios I Zeugolis et al. “Electro-spinning of pure collagen nano-fibres–just an expensive way to make gelatin?” In: *Biomaterials* 29.15 (2008), pp. 2293–2305.

[445] Panpan Zhang et al. “Influence of coagulation bath temperature on the structure and dielectric properties of porous polyimide films in different solvent systems”. In: *ACS omega* 5.46 (2020), pp. 29889–29895.

[446] Xiaohui Zhang and Pibo Ma. “Application of knitting structure textiles in medical areas”. In: *Autex Research Journal* 18.2 (2018), pp. 181–191.

[447] Zihuan Zhang et al. “Engineering Strong Man-Made Cellulosic Fibers: A Review of Wet Spinning Process Based on Cellulose Nanofibrils”. In: *Nanoscale* (2024).

[448] Shiqi Zhou. “Effects of discreteness of surface charges on the effective electrostatic interactions”. In: *The Journal of Chemical Physics* 140.23 (2014).

[449] Yan Zhuang et al. “Effect of coagulation bath parameters on the morphology and absorption behavior of a skin–core filament based on biomedical polyurethane and native silk fibroin microparticles”. In: *Textile research journal* 90.3-4 (2020), pp. 460–468.